ADDIS ABABA UNIVERSITY

ADDIS ABABA INSTITUTE OF TECHNOLOGY

SCHOOL OF CIVIL AND ENVIRONMENTAL ENGINEERING

Size Effect on Shear Behavior of Reinforced Concrete Beams with Shear Reinforcement

A Thesis in Structural Engineering

By Mubarek Mudesir

November, 2019

Addis Ababa

A Thesis

Submitted in Partial Fulfillment of the Requirements for the Degree of Master of Science

The undersigned have examined the thesis entitled '**Size Effect on Shear Behavior of Reinforced Concrete Beams with Shear Reinforcement**' presented by **MUBAREK MUDESIR**, a candidate for the degree of **Master of Science** and hereby certify that it is worthy of acceptance.

Dr.-Ing. Adil Zakaria		21/11/2019
Advisor	Signature	Date
Dr. Esayas G/yohannes		NOV-21-2019
Internal Examiner	Signature	Date
Dr.-Ing. Girma Zerayohanes		21/11/2019
External Examiner	Signature	Date
Chair person	Signature	Date

UNDERTAKING

I certify that research work titled “Size Effect on Shear Behavior of Reinforced Concrete Beams with Shear Reinforcement” is my own work. The work has not been presented elsewhere for assessment. Where material has been used from other sources it has been properly acknowledged / referred.

Mubarek Mudesir

ABSTRACT

Past experimental researches showed that as the beam depth increases, there is a significant decrease on the shear stress capacity of reinforced concrete beams without shear reinforcement. This trend is called size effect. Since most beams contain at least minimum shear reinforcement as required by building codes, it is also important to study size effect on reinforced concrete beams with shear reinforcement. In this paper experimental and analytical investigations were made to study size effect on shear behavior of reinforced concrete beams with shear reinforcement. All parameters influencing shear capacity of beam were held constant except beam depth and shear reinforcement ratio. Six reinforced concrete beam specimens tested in laboratory and twelve beam specimens analyzed by VecTor2 nonlinear finite element software. Experimental results showed that for beams without shear reinforcement the shear stress capacity decreased by 9.3%, on the other hand, for beams which have shear reinforcement with ratio of 0.14% the shear stress capacity decreased by only 3.8%, when the beam height raised from 240mm to 360mm. Analytical results also showed that when depth of the specimen increased from 240mm to 1200mm, the shear stress capacity decreased by 58.2% for beam specimens without shear reinforcement and by 48.9% for beam specimens with 0.14% ratio of shear reinforcement. From both results it can be concluded that even if using shear reinforcement minimize size effect, they cannot eliminate size effect completely. The comparison made among experimental, code-based and analytical predictions showed that Eurocode 2 and ACI 318-19 shear provisions gave generally good estimates of shear capacity for al1 analyzed specimens. However, the ACI 318-14 shear provision overestimate shear capacity of reinforced concrete beams when depth of beams exceeds 800mm that is because it did not consider size effect, so that, the decision made by ACI committee to replace it by new equation in ACI 318-19 which consider effect of member depth is correct.

ACKNOWLEDGMENTS

First and foremost, I would like to express my sincere gratitude to my advisor, Dr. Ing. Adil Zakaria for giving me a chance to do my Thesis with him on such an interesting research topic. I also appreciate his expertise and continuous guidance he has given me throughout this study. The completion of this work would have not been possible without his invaluable support and knowledgeable advice.

I would like to extend my sincere gratitude to Dr. Esayas G/Youhannes who was instrumental in this thesis. He guided me along the entire course of the study and continually fueled my knowledge of structural engineering with his experience.

The experimental part of the thesis wouldn't have succeeded without the help of the staff at the Material Testing Laboratory of AAiT. The success of the experimental investigation was achieved with the priceless assistance of Binyam F., Wubet A., Demis, and Fikru B. I would like to take this opportunity to express all my gratitude for their professional expertise and kind support.

I want to express my appreciation to my friends here at the Addis Ababa Institute of Technology for their friendship, their suggestions on various aspects of my research, and their generous assistance during the tests.

Last, but not least, I would like to express my deepest love and gratitude to my family and to all those who have directly and indirectly helped me throughout my study.

TABLE OF CONTENTS

LIST OF TABLES

LIST OF FIGURES

LIST OF SYMBOLS

a = shear span

A_s = area of main flexural tension reinforcement

A_s' = area of main flexural compression reinforcement

A_v = area of transverse shear reinforcement

b_w= beam width

c = concrete cover thickness

d = beam effective depth

E_c = modulus of elasticity of concrete

Es = modulus of elasticity of reinforcement

f'_c = compressive strength of concrete

f_y = yield strength of steel reinforcement

f_u = ultimate strength of steel reinforcement

H = overall height of beam

L = beam length

S = spacing of shear reinforcement measured parallel to longitudinal axis of member

V_c = shear stress resistance provided by the concrete

V_s = shear stress resistance provided by shear reinforcement

V = shear force

Δ = deflection (downwards positive if vertical)

ρ = concrete density

ρ_l= longitudinal tension reinforcement ratio, equal to A_s/bd

ρ_v = transverse reinforcement ratio, equal to A_v/bs

ø = diameter of steel reinforcement

γ_c = partial factor for concrete

τ = shear stress

CHAPTER 1 INTRODUCTION

1.1 Background

The shear behavior of reinforced concrete structures remains an area of concern for structural engineers due to the lack of rational design equations in building codes. Even after many years of intensive research still we don't have a simple and analytically derived formula to predict the shear strength of reinforced concrete beams that has been generally adopted by most design codes. The shear design procedures of building codes such as Eurocode (EC2) and ACI 318-14 code, are semi- empirical methods which are based on statistical best fits of experimental data. That is the reason why the adopted shear design procedures vary from country to country. On the other hand, analytical methods for flexure which are based on the "plane sections remain plane" theory, have been established for many years and are capable of predicting not only the strength but also the load - deformation response of reinforced concrete members subjected to moment with very good accuracy.

Shear failure of reinforced concrete beams is a very complex phenomenon due to involvement of too many parameters. size effect is the least studied parameter because of the difficulties in preparing and testing large beams and such tests are generally expensive. The size effect essentially states that the shear stress to cause failure of a reinforced concrete member decreases as the effective depth increases (Kani, 1967). One explanation behind this occurrence is that deeper beams tend to have larger crack spacings and corresponding wider cracks that reduce the effectiveness of aggregate interlock capacity, the principal shear transfer mechanism in these members.

Research investigating the influence of beam size on the shear strength of reinforced concrete structures suggests that as the beam depth increases, there is a decrease in the shear strength of the section. These tests were conducted on specimens that did not contain transverse reinforcement to determine the shear strength provided by the concrete (V_c). Most sections, however, contains at least minimum transverse reinforcement as required by the building code. Therefore, the focus of this thesis is to investigate the effect of beam size on the shear behavior of reinforced concrete beams with shear reinforcement because they may also be affected by a size effect or may be using shear reinforcement eliminates the size effect.

1.2 Significance of the Study

Nowadays, the advances of modern construction technology enable large, complex structures to be built. The danger with these large-scale reinforced concrete structures is that they are more at risk of failures because of the so-called size effect in shear. Research has indicated that for reinforced concrete beams without shear reinforcement as the depth of a beam increases, a decrease in shear strength of the section can be expected. Most sections, however, contain at least minimum shear reinforcement as required by building design codes. Therefore, it is important to consider the effect of size on the shear behavior of reinforced concrete beams with shear reinforcement. Addition of shear reinforcement may enhance the shear capacity as well the ductility of such beams or the required minimum amount of shear reinforcement may not be enough to eliminate the size effect. The result of this thesis will allow an evaluation of the current Eurocode shear provisions and help identify their limitations. On the other hand, since relationships in ACI 318-14 for calculating the concrete contribution to shear resistance in reinforced concrete members have been replaced in ACI 318-19 by one general relationship that considers effects of member depth. This study will help to compare the applicability and accuracy of the new one-way reinforced concrete shear design provisions in ACI 318-19 with the older ACI 318-14.

1.3 Objective of the Study

1.3.1 General Objective:

The main aim of this thesis is to gain understanding about the effect of beam depth or size on the shear behavior of reinforced concrete beams with shear reinforcement as well as examining the accuracy of ACI and Eurocode formulas when determining shear capacity of reinforced concrete beams with shear reinforcement.

1.3.2 Specific Objectives:

- To study the effect of increasing depth on shear behavior and capacity of reinforced concrete beams with shear reinforcement.
- To investigate the effect of using shear reinforcement to mitigate size effect on reinforced concrete beams.
- To draw a comment by comparing the results obtain from experimental study, analytical simulation and values obtain with the formula of ACI-318-14, ACI-318-19 and Eurocode 2:2004 for shear capacity of reinforced concrete beams.

1.4 Scope of the Study

The primary focus of this thesis would be on how the size of reinforced concrete beams cross-section affect shear capacity of reinforced concrete beams with shear reinforcement. Therefore, other parameters influencing the shear capacity were held constant throughout the experiments. The only varying parameter was the height of the beams while the width, shear span-to-depth ratio, amount of longitudinal reinforcement ratio and concrete compressive strength were kept constant. This thesis included only normal beams designed intentionally to fail in shear. Deep beams, Pre-stressed beams and beams made of high-strength concrete were excluded from this thesis, since they have different shear mechanisms from normal strength concrete beams.

1.5 Methodology

The overall process of this study includes experimental program, analytical simulation using non-linear finite element modeling and Investigation on the accuracy of various international shear design procedures such as Eurocode (EC2) and ACI 318 code.

Totally six reinforced concrete beams with different depth constructed and tested in Material Testing Laboratory of AAiT. The preparation and testing of specimens was done in two phases, the first of which involved three beam specimens without transverse reinforcement, and the second also involved three beam specimens with 0.14% ratio of shear reinforcement.

After the experimental work completed, finite element analysis for different size of beam specimens using a nonlinear finite element analysis tool called Vector2 be done.

Finally, the experimental results were compared to the predictions from AC1 318-14, ACI 318-19 and the Eurocode (EC2): 2004 shear provisions as well as those from the non-linear finite element program approach (VecTor2) then based on that conclusions and recommendations are given.

1.6 Layout of the Thesis

This thesis is divided into six chapters and written based on "AAiT Guidelines for writing the Main Text of a Thesis". The following is a short description of each chapter.

Chapter 2 is literature review. It reviews previous works which have relatively similar objectives as this thesis and review the current understanding about effect of size on shear behavior of reinforced concrete beams in order to give a background. The chapter also includes brief explanations of shear provisions of design codes like ACI 318-14, ACI 318-19 and Eurocode 2: 2004, which were later examined with experimental results.

Chapter 3 describes details of the experimental program including design, construction, and instrumentation of reinforced concrete beam specimens. A total of six similar beams with different sizes were tested to examine size effect on shear behavior.

Chapter 4 discuss the nonlinear finite element study using vecTor2 software package which developed at University of Toronto. The concrete material models available in the software are first examined by comparing to the experimental results. The software model is then used to investigate the effect of size on shear behavior of reinforced concrete beams with and without shear reinforcement.

Chapter 5 covers the discussion and comparison of results from the experiment, the non-linear finite element simulations and shear provisions of design codes. Based on the results, the effect of size on shear behavior and capacity reinforced concrete beams is presented and discussed in detail. In addition, this chapter presents critical and extensive evaluation on ACI 318-14, ACI 318-19 and Eurocode 2: 2004 shear design models in predicting experimental results.

Chapter 6 presents the conclusion of the study and gives some recommendations for future research.

CHAPTER 2 LITRATURE REVIEW

2.1 General

In this section, previous research results are summarized about the topics related to this thesis. It must be noted first that members considered in this research have relatively large shear-span-to-depth ratios, a/d, so that they can be designed using sectional analysis. For shorter members compression struts form between the loading point and the supports and the shear is carried by arch action. The behavior of these short members can be dealt with based on the strut-and-tie model and hence this type of member, which has no significant size effect, is not treated in this thesis.

2.2 Shear Transfer Mechanisms

Shear is carried by three fundamental transfer mechanisms in a reinforced concrete member devoid of stirrups: shear in the compression zone, dowel action of longitudinal reinforcement, and aggregate interlock (See Figure 2.1) (Collins, 2006). Several tests and research have revealed that members without transverse reinforcement resists about 80% of total shear by the vertical component of aggregate interlock stresses integrated over the crack surface (V_{ci}) The remaining resistance is attributed to shear transmitted in the compression zone (V_{cz}), and dowel action (V_d). Presence of stirrups adds a supplementary element of shear resistance through the tensile straining of the transverse bars that cross a crack (Vs) (Phillip, T., 2016).

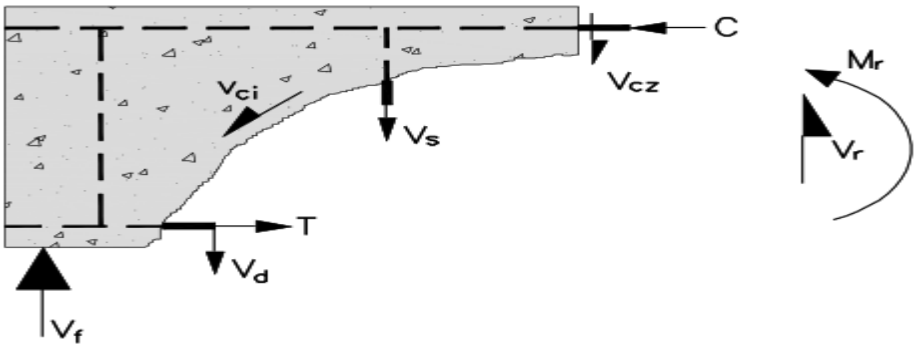

Figure 2-1: Shear transfer in reinforced concrete beam, taken from Phillip, T., 2016

2.2.1 Concrete Compression Zone

Mörsch demonstrated that shear is primarily transmitted in the web, as it was explicit that the extreme compressive fiber of a cross-section carries zero shear stress. Consequently, the uncracked compression zone constitutes only a small portion of the total shear resistance relative to contribution from the web (Collins, 2006).

2.2.2 Dowel Action

Dowel action of the longitudinal reinforcement creates a component of shear resistance due to the physical shearing of the bar across a crack. It can be an important mechanism in beams with short shear spans, specifically for capturing complete response and overall member ductility (Quach, 2016). For large, lightly reinforced specimens, dowel action is practically negligible due to the relative size of the bars to the overall specimen. There is also not enough slip to engage this particular mechanism in these deep shear-critical members prior to breakdown of aggregate interlock.

2.2.3 Aggregate Interlock

Mörsch's derivation of shear stresses infer that high shear in the flexural tension region were carried across the cracks. This interfacial shear transfer became the topic of study and further development by other researchers after Mörsch. Appropriately deemed "aggregate interlock," it comprises of the shearing mechanism of the aggregates and cement paste over a diagonal flexural-shear crack (Yoshida, 2000). Subsequent tests and literature indicate that aggregate interlock is the primary mechanism of shear transfer in large elements that do not contain stirrups, and thus, is an essential factor in the size effect phenomenon exhibited by reinforced concrete (ShenCa, 2001).

2.2.4 Shear Reinforcement

In addition to any shear carried by the stirrup itself, when an inclined crack crosses shear reinforcement, the steel may contribute significantly to the capacity of the member by increasing or maintaining the shear transferred by interface shear transfer, dowel action, and arch action. Thus, shear reinforcement restricts the widening of inclined cracks in beams and thus slows the decrease of interface shear transfer quite effectively. The addition of a small amount of shear reinforcement greatly improves the shear capacity and ductility of large members. Midspan deflections at failure for the specimens with minimum transverse reinforcement were three to four times larger than those for the specimen without transverse reinforcement (Yoshida, 2000).

2.3 The Size Effect in Shear

The size effect essentially states that the shear stress to cause failure of a reinforced concrete member decreases as the effective depth increases (Kani, 1967). One explanation behind this occurrence is that deeper beams tend to have larger crack spacings and corresponding wider cracks that reduce the effectiveness of aggregate interlock capacity, the principal shear transfer mechanism in these members. The shallower specimens were consistently able to resist higher shear stresses than the deeper ones (Ghannoum, 1998).

Ghannoum, 1998 constructed and tested twelve beam specimens in the Structures Laboratory of the Department of Civil Engineering at McGill University. The specimens were designed according to the modified compression field theory to fail in shear rather than bending. No transverse reinforcement was provided for any of the specimens. The shear span-to-depth ratio, a/d, of al1 specimens was kept constant at a/d=2.5, in order to produce a shear critical specimen (Kani 1966, 1967, 1979). AI1 of the beams were subjected to a two-point loading arrangement as shown in Figure 2.2.

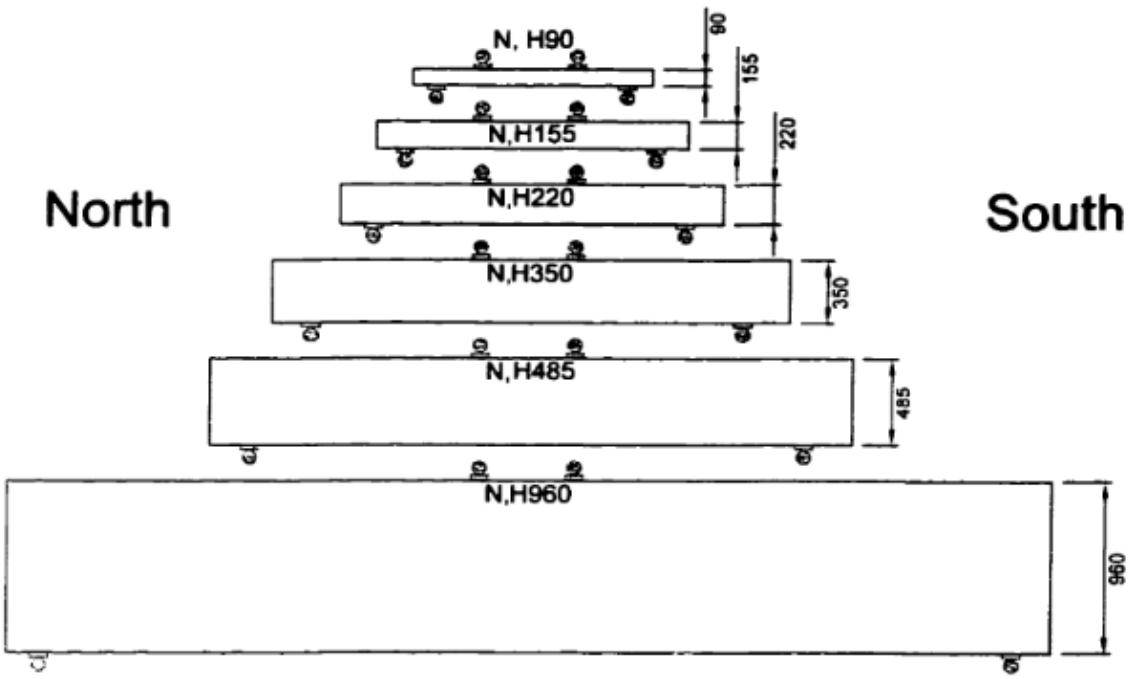

Figure 2-2: Specimen geometrical details (Ghannoum, 1998)

Ghannoum, (1998) conclude that the size effect on shear strength is evident. In both the normal and high-strength concrete. regardless of the steel ratio, the deeper members had lower shear stresses at failure than the shallower ones.

The cause of the size effect is mostly agreed among many researchers as being the wider cracks which form in larger members. Since beams usually have longitudinal reinforcement only at the top and the bottom, their capability to control crack distribution is very limited around the mid-depth of the beams.

From the observation of crack patterns in specimens he tested, Shioya, T. (1989) suggested that the spacing of diagonal cracks was approximately the effective depth of the specimens. Some other researchers assume the crack spacing to be half of the effective depth or 0.7(d - c) where c represents depth of compression zone. As can be seen, crack spacing is nearly always related to member depth. Since the crack width is estimated as a product of crack spacing and concrete strain, a larger crack spacing results in wider cracks. One of the consequences of wider cracks is a reduction of interface shear transfer, which is one of the mechanisms carrying shear in reinforced concrete members. For normal strength concrete, the interface shear transfer is known as "aggregate interlock" because along diagonal tension cracks aggregate particles protruding from the surfaces of the cracks resist the slip of the cracks. As the cracks become wider the resistance by the aggregate particles becomes smaller, consequently, the shear carried at failure decreases (Phillip, T., 2016).

Yoshida (2000) showed that even a single stirrup at the midspan of a beam can almost double shear strength and greatly increase ductility through attenuation of the size effect when compared to an unreinforced equivalent.

2.3.1 Parameters Related to Size Effect

2.3.1.1 Depth

Member size plays a significant role in determining the failure shear stress of member without web reinforcement. This effect means that the shear strength of members doesn't increase linearly as the member depth increases. In other words, for deeper members, the shear stress at failure is smaller than it is for smaller members. Extensive testing of reinforced concrete beams has revealed that crack patterns are geometrically consistent across specimens of varying cross-sectional dimensions (Collins, 2006). These tests illustrate that as the depth of a member is increased, both cracks spacing and crack widths will increase proportionally.

Walraven (1981) established that wider cracks translate to diminished aggregate interlocking capacity and hence lower shear strength. Additionally, deep beams demonstrated an evidently more brittle nature than small specimens of similar geometric scale; Sherwood's tests in 2008 revealed that shallower beams achieved more than twice the deformation capacity of their deep counterparts.

2.3.1.2 Aggregate Size

Aggregate interlock relies on the interfacial shear transfer on a crack, and as a result, it is heavily influenced by crack roughness. Irregularities on a crack surface arise from both the coarse aggregate and inherent unevenness of the fractured cement paste. As such, the coarse aggregate size, and implicitly the concrete strength, are responsible for the ability of a crack to transfer shear stresses. Increasing coarse aggregate size up to 25 mm improves shear resistance through the formation of rougher crack surfaces (ShenCao, 2001).

Bentz and Collins (2006) state that the effect of larger aggregate is more predominant in deeper beams, due to the fact that aggregate interlock governs the shear capacity of such members and aggregate is usually not scaled up with member depth. Beyond 25 mm, experimental results from Sherwood (2008) indicate unpredictable outcomes of shear strength, and thus aggregate larger than 25 mm should be taken as effectively 25 mm in size. Higher strength concrete has stronger cementitious paste that fractures a majority of the aggregate at the crack interface, creating more even crack planes. These smooth cracks have a severe reduction on shear stress transmissibility as the aggregate size will fundamentally be rendered useless. In such cases, ag should be taken as zero (Ghannoum, 1998).

2.3.1.3 Crack Control

Cracking is expected under service conditions for most, if not all, reinforced and partially prestressed concrete structures; it allows for the reinforcement to be passively engaged and enables more practical designs. Deep members without shear reinforcement tend to have wider and more largely spaced cracks within the web as there is no steel in this region to restrain crack growth through tension stiffening (See Figure 2.3). The lack of well distributed reinforcement consequentially reduces aggregate interlock capacity on account of wider crack widths over a larger portion of the crack (Phillip, T., 2016).

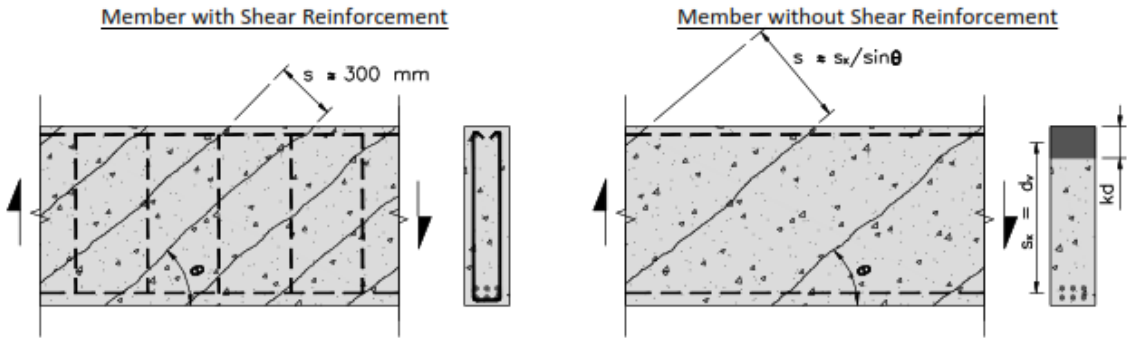

Figure 2-3: Influence of reinforcement on crack spacing, taken from Phillip, T., 2016

Crack control can be achieved by incorporating transverse reinforcement meeting the spacing requirements prescribed by codes or alternatively through the use of distributed flexural skin reinforcement. The latter specifically requires bars that can resist the increased demand at a crack caused by the lack of concrete tensile contribution at these interfaces (Bentz and Collins, 2006).

Research and testing by Sherwood (2008) highlight the inadequacy of using small bars to effectively control cracking because of the larger stresses they develop across the crack. Neglecting strain hardening, yielding of the bars by definition means that no additional load is required to continue elongating the reinforcement. Subsequently, straining of the member at a crack is further amplified at the onset of steel yielding, resulting in inadequate reserve capacity to impede crack width expansion. On that account, larger area bars will have better crack control characteristics as they are more apt to a lower degree of stress across a crack plane, provided they are well distributed over the cross-section.

2.3.1.4 Longitudinal Reinforcement

Bearing resemblance to the influence of crack control on shear capacity, primary longitudinal reinforcement also provides restraint to the widening of cracks. Although this is heavily constrained to the region within the local tension stiffened vicinity of the bar, the effect of larger reinforcement ratios results in smaller overall longitudinal strains and crack widths. Crack spacing at the mid-depth of beams are therefore less affected by the amount of longitudinal steel simply because of their distance away from the bars. As in the case of skin reinforcement, higher ratios of longitudinal steel serve to increase aggregate interlock capacity and enhance shear strength (ShenCao, 2001).

2.3.2 Previous Size Effect Investigations

Kani (1 966 and 1967) was amongst the first to investigate the effect of absolute member size on concrete shear strength after the dramatic warehouse shear failures of 1955 (Collins and Kuchma, 1997 and Collins and Mitchell, 1997). His work consisted of beams without web reinforcement with varying member depths, d, longitudinal steel percentages, ρ, and shear span-to-depth ratios, a/d. He determined that member depth and steel percentage had a great effect on shear strength and that there is a transition point at a/d=2.5 at which beams are shear critical (i.e. the value of the bending moment at failure was minimum) Figure 2.4 illustrates the results obtained by Kani.

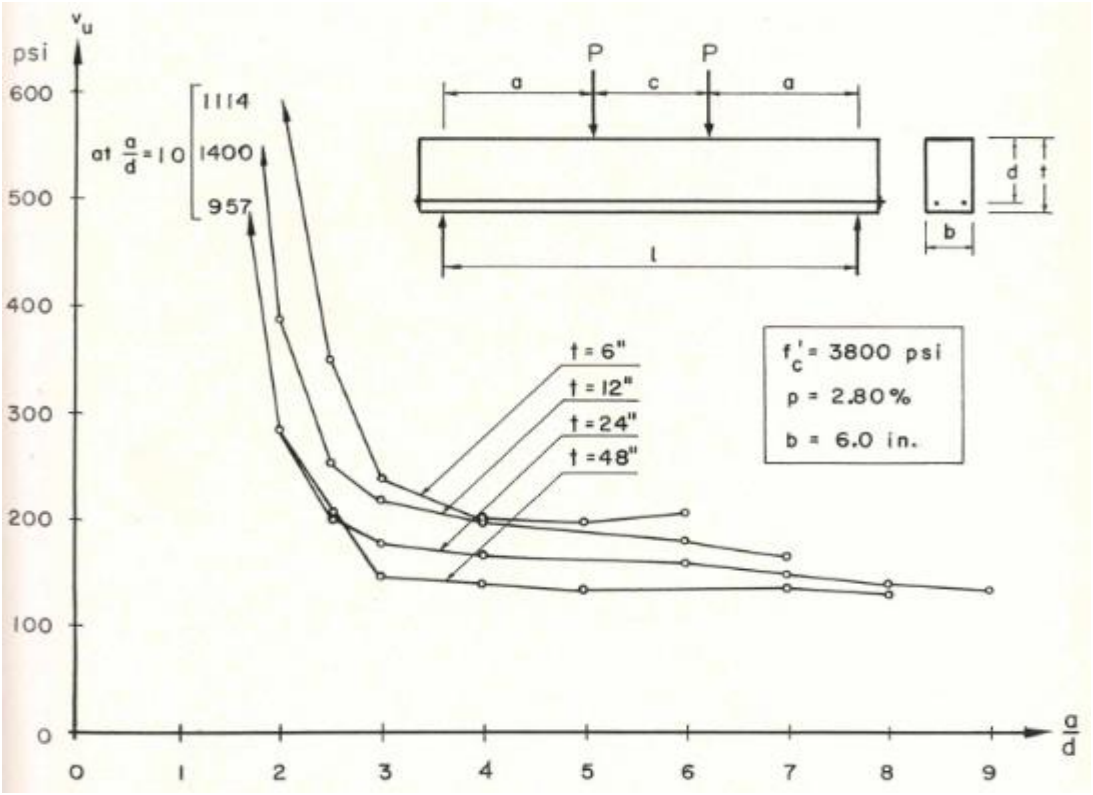

Figure 2-4: Shear stress at failure versus a/d for beams of various depths (Kani, 1967)

In addition. Kani found a clearly defined envelope bounded by limiting values of p and a/d. Inside this envelope diagonal shear failures are predicted to occur and outside of this envelope flexural failures are predicted to occur. These conclusions regarding the influence of both p and a/d were similar for al1 beam depths tested. Kani also looked at the effect of beam width and found no significant effect on shear strength. Kani's work was summarized in the textbook "Kani on Shear in Reinforced Concrete" (Kani et al. 1979)

Bazant and Kim (1984) derived a shear strength equation based on the theory of fracture mechanics. This equation accounts for the size effect phenomenon as well as the longitudinal steel ratio and incorporates the effect of aggregate size. This equation was calibrated using 296 previous tests obtained from the literature and was compared with the AC1 Code equations. It was noted after the comparison that the practice used in the AC1 Code of designing for diagonal shear crack initiation rather than ultimate strength does not yield a uniform safety margin when different beam sizes are considered. It was also found. according to the new equation. that for very large specimen depths the factor of safety in the AC1 Code almost disappears. However, no experimental evidence was available yet to confirm that fact as al1 the tests performed up to that time were on relatively small specimens. This equation was improved by Bazant and Sun (1987) to account for the maximum aggregate size distinctly from the size effect phenomenon and was extended to cover the influence of stirrups. This formula was calibrated using a larger set of test data consisting of 461 test results compiled from the literature.

Later on, Bazant and Kazemi (1991) performed tests on geometrically similar beams with a size range of 1:16 and having a constant a/d ratio of 3.0 and a constant longitudinal steel ratio, ρ. Beams tested varied in depth from 1 inch (25 mm) to 16 inches (406 mm). The main failure mode of the specimens tested was diagonal shear but the smallest specimen failed in flexure. This study confirmed the size effect phenomenon and helped corroborate the previously published formula. However, the deepest beam tested was relatively small and the authors concluded that for beams larger than 16 inches (406 mm) additional reductions in shear strength due to size effect were likely.

Kim and Park (1994) performed tests on beams with a higher than normal concrete strength (53.7 MPa). Test variables were longitudinal steel ratio, p, shear span-to-depth ratio, a/d, and effective depth. d. Beam heights varied from 170 mm to 1000 mm while the longitudinal steel ratio varied from 0.01 to 0.049 and dd varied from 1.5 to 6.0. Their findings were similar to Kani's from which it was concluded that the behavior of the higher strength concrete is similar to that of normal-strength concrete. However, since only one concrete strength was investigated no general conclusions could be made with respect to concrete strength and shear capacity.

Shioya (1989) conducted a number of tests on large-scale beams in which the influence of member depth and aggregate size on shear strength was investigated. In this study, lightly reinforced concrete beams containing no transverse reinforcement were tested under a uniformly distributed load. The beam depths in this experimental program ranged from 100 mm to 3000 mm. Shioya found that the shear stress at failure decreased as the member size increased and as the aggregate size decreased. It is interesting to note that the beams tested by Shioya contained about the same amount of longitudinal reinforcement as the roof beams of the Air Force warehouse which collapsed in 1955 (Collins and Kuchma, 1997 and Collins and Mitchell, 1997). The warehouse beams had an effective depth of 850 mm and failed at a shear stress of about 0.1 OK MPa. This shear stress level corresponds with the failure shear stress observed in beams having a depth of 1000 mm in the Shioya tests. It is important to mention that there was a tendency for reduced shear stresses at failure even with tests including 3000 mm deep beams.

Since Kani's early work in 1967 on reinforced concrete beams with different sizes, much research has been undertaken to investigate the influence of size on the behavior and shear strength of reinforced concrete beams. Figure 2-5 shows the experimental results of the beams tested by Taylor, Bazant and Kazemi and Kim and Park, and it can be seen that by increasing the member depth the shear strength reduces. In 2007, Bazant et al. explained that though shear reinforcement can reduce the size effect in RC beams, it cannot eliminate size effect completely.

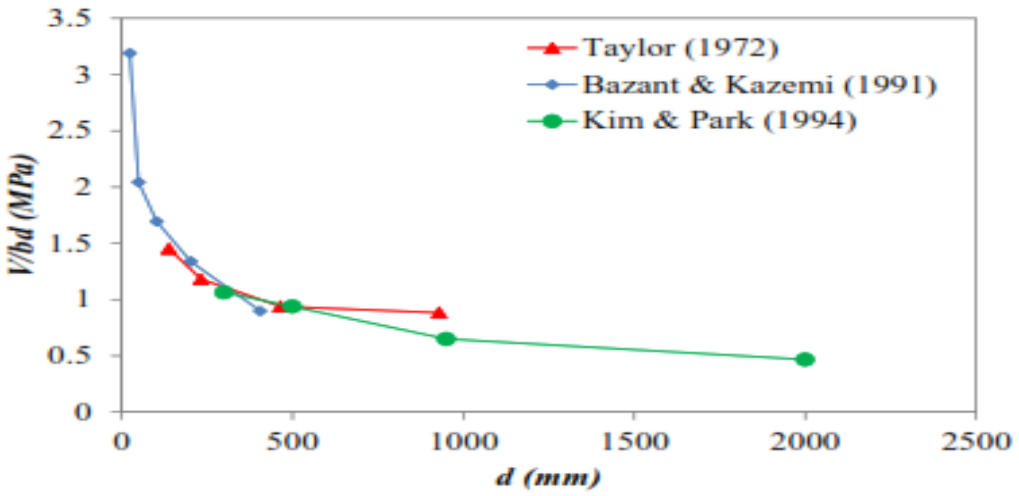

Figure 2-5: Effect of size of the beam on the shear strength, taken from Ismail, 2016.

2.3.3 The Toronto Size Effect Series

There exists a great amount of experimental work documenting the size effect in deep, reinforced concrete members lacking shear reinforcement dating back to 1967 when Kani first investigated beams just over 1 m deep. Some of the more recent research into this detrimental effect arose from University of Toronto, with specimens having an effective depth ranging from 1.5 m to 2.0 m being tested by Yoshida (2000), ShenCao (2001), and Sherwood (2008). Extensive experimental programs carried out in Toronto, including those by the aforementioned authors, have resulted in a large database of results termed the Toronto Size Effect Series (See Table 2.1).

Table 2-1: Toronto Size Effect Series (Phillip, T., 2016)

Name	f'_c [MPa]	a_g [mm]	ρ [%]	a/d	b_w [mm]	d [mm]	V_{exp} [kN]	V_{exp} [kN/m]	v_{exp} [MPa]	v_{MCFT} [MPa]	$\frac{v_{exp}}{v_{MCFT}}$
BN12	37.2	10	0.91	3.1	300	110	40	133	1.347	1.136	1.19
BN25	37.2	10	0.89	3.0	300	225	73	243	1.202	1.058	1.14
PLS300	44.8	14	0.65	3.1	175	264	-	-	-	1.037	-
S-10N1	41.9	10	0.83	2.9	122	280	36.6	300	1.190	1.048	1.14
S-10N2	41.9	10	0.83	2.9	122	280	38.3	314	1.246	1.048	1.19
BN50	37.2	10	0.81	3.0	300	450	132	440	1.086	1.026	1.06
BN100	37.2	10	0.76	2.9	300	925	192	640	0.769	0.721	1.07
L-10N1	38.4	10	0.83	2.9	300	1400	265	883	0.701	0.636	1.10
L-10N2	40.3	10	0.83	2.9	300	1400	242	807	0.640	0.647	0.99
YB2000/0	33.6	10	0.74	2.9	300	1890	255	850	0.500	0.510	0.98
PLS4000	40.0	14	0.66	3.1	250	3840	-	-	-	0.381	-

The Toronto Size Effect Series has provided convincing evidence that the size effect does in fact exist. Furthermore, these results offer valuable insight as to what causes it so that engineers may be more acquainted when designing large scale structures common in everyday infrastructure (Phillip, T., 2016).

A plot of the experimental results compared with American (ACI) and Canadian (CSA) code predictions excellently portrays the size effect (See Figure 2.6). It can be seen how the MCFT-based CSA predictions of shear strength accurately match the experimental results with nonlinear strength degradation. On the other hand, the empirically based ACI predicts a highly unconservative linear increase in shear resistance with depth, showing a complete disregard of the size effect (Phillip, T., 2016).

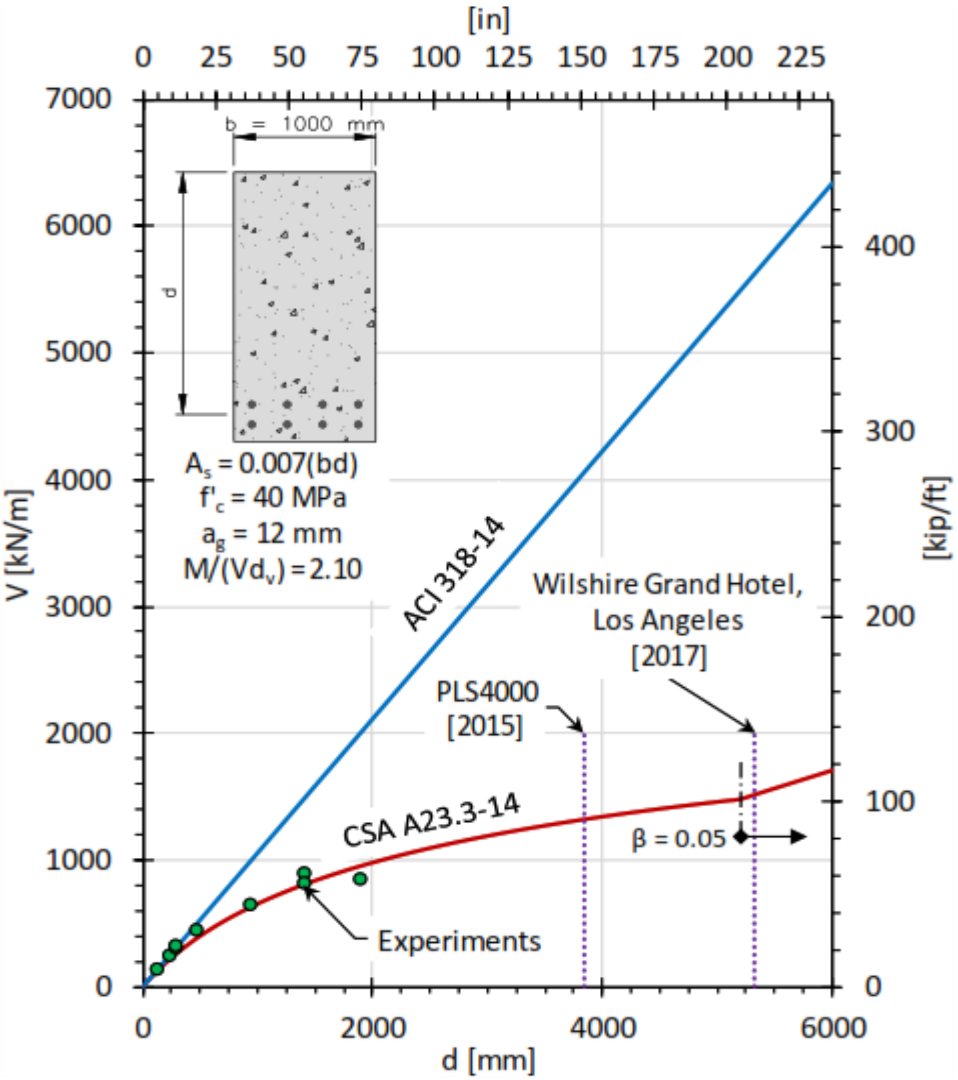

Figure 2-6: Size effect for beams without shear reinforcement (Phillip, T., 2016)

2.3.4 Deep beam

Reinforced concrete deep beams are structural members for which the load is applied at 'a' distance from the support so that a substantial proportion of the load is transferred directly to the support by arching action. Common structural applications of deep beams include transfer girders in buildings, bridges and offshore structures. According to ACI 318-14 "Deep beams are members that are loaded on one face and supported on the opposite face such that strut-like compression elements can develop between the loads and supports and that satisfy (a) or (b): (a) Clear span does not exceed four times the overall member depth h; (b) Concentrated loads exist within a distance 2h from the face of the support". On the other hand, Eurocode 2 (EC2) defines deep beams as all beams with span to depth ratio smaller than three.

2.4 International Shear Design Procedures

Many international codes of practice rely on purely empirical relations and/or plastic truss models that, by their nature, cannot result in a globally unified approach to shear design (Phillip, T., 2016). In this section, shear provisions in two codes are briefly reviewed. They are Eurocode 2 (2004), AC1(American Concrete Institute) 318-14 and ACI 318-19.

2.4.1 Eurocode 2 (2004)

Eurocode 2 (EC2) are the set of standards set out by the European Committee for Standardization regarding the design of concrete structures. Total shear resistance capacity of a beam is a sum of concrete contribution and shear reinforcement.

$$V_{Rd}=V_{Rd,c}+V_{Rd,s} \quad [KN] \qquad (2\text{-}1)$$

EC2, used empirical equations statistically fit through experimental data available when the provisions were created to formulate their expressions of shear resistance. While the resistance without transverse reinforcement is empirically derived, a variable angle truss model neglecting concrete tensile stresses is used to determine the shear resistance of a member with stirrups (Phillip, T.,2016). Eurocode 2 provides equation (2.2) to predict the ultimate shear strength of reinforced concrete beams without shear reinforcement.

$$V_{Rd,c} = [C_{Rd,c}k(100\rho_l f_{ck})^{1/3} + k_1\sigma_{cp}]b_w d \geq VRd_{,c,min} \quad [KN] \qquad (2\text{-}2)$$

$$V_{Rd,c,min} = [(0.035k^{1.5} \times f_{ck}^{0.5}) + k_1\sigma_{cp}]\, b_w d \quad [KN] \qquad (2\text{-}3)$$

Where:

$k = 1 + \sqrt{\frac{200}{d}}$ = size factor

ρ_l = longitudinal reinforcement ratio

f_{ck} = concrete strength

$C = \frac{0.18}{\gamma_c}$ = coefficient dependent on the loading case

d = effective beam height

b_w = beam width

Eurocode 2 actually does account for the size effect with their empirical k factor, although it is not strong enough for larger members (Phillip, T.,2016).

The EC2 shear design procedure for the members with shear reinforcement is based on the plasticity theory and the truss model. This model accounts for the effect of transverse steel reinforcement and strut inclination with respect to the member's neutral axis. (Phillip, T.,2016).

$$\mathbf{V_{Rd,s}} = \frac{A_{sw}}{s} \mathbf{z} f_{ywd} (\cot\theta + \cot\alpha) \sin\alpha \quad \textbf{[KN]} \qquad \textbf{(2-4)}$$

Where: $\mathbf{A_{sw}}$ = cross-sectional area of shear reinforcement,

S = spacing of shear reinforcement,

Z = lever arm (can be considered as 0.9d),

$\mathbf{f_{ywd}}$ = yield strength of the shear reinforcement,

θ = angle of the inclined struts, and

α = angle of the stirrups with respect to the axis of the member

It is also noted that the EC2 equation for concrete contribution erroneously implies that a member without longitudinal reinforcement (ρ_1 = 0) has zero shear resistance and is consequentially shear critical (assuming no axial load or prestressing, σ_{cp}=0). This is in fact fundamentally incorrect because it is obvious that the lack of flexural reinforcement would result in an immediate bending failure at the time of first cracking; shear failure cannot be triggered without the formation of flexural cracks. Accordingly, Eurocode 2 compensates for this by implementing the V_{Rd},c,min limit (Phillip, T.,2016).

2.4.2 ACI 318-14

AC1 318-14 predicts that the shear strength of a concrete member is provided by the concrete web and, if the member has shear reinforcement, by the shear reinforcement. The shear strength provided by concrete, Vc, is taken as the same value for beams with and without shear reinforcement and was derived empirically from many experimental data. The shear reinforcement contribution, Vs, is calculated based on the 45˚ truss analogy (Daniel A. et.al 2019). As a result, for non-prestressed concrete members with normal strength concrete and transverse reinforcement is as follows:

$$Vn = Vc + Vs \qquad \textbf{(2-5)}$$

Equation (2-6) given below is the SI unit version of the concrete contribution according to ACI 318-14.

$$\mathbf{V_c = (0.158\sqrt{f'_c} + 17.2\rho_w\frac{Vd}{M})b_w d \ [KN]} \qquad \textbf{(2-6)}$$

ACI fails to capture the realistic severity of shear capacity reduction stemming from the presence of moment. Furthermore, there is no factor accounting for the aforementioned size, and hence predicts no detriment in shear resistance for large-scale structures (Phillip, T.,2016).

Another downfall of the ACI code is that it is still based on the 45-degree truss model and hence neglects the flattening of the compressive struts that occurs towards shear failure. This can be seen from the omission of a principal angle of compression θ in the equation for the steel contribution. As a result, the steel contribution to shear resistance is fixed and the actual increase in web reinforcement straining, and intrinsically steel utilization, as crack inclinations flatten is not captured resulting in a conservative result in this regard (Phillip, T.,2016).

$$\mathbf{V_s = \frac{A_v f_{yt} d}{S}} \qquad \textbf{[KN]} \qquad \textbf{(2-7)}$$

2.4.3 ACI 318-19

Relationships in ACI 318-14 for calculating the concrete contribution to shear resistance (Vc) in reinforced concrete members (that is, non-prestressed) have been replaced in ACI318-19 by one general relationship that considers the combined effects of member depth, percentage of longitudinal reinforcement, and the effect of axial stress on predicted shear strength capacity (Daniel A. et.al 2019).

Table 2-2: ACI 318-19 one-way shear provisions for reinforced concrete members

Criteria	V_c		
$A_v \geq A_{v,\,min}$	Either of:	$[2\lambda\sqrt{f'c} + \frac{Nu}{6Ag}]b_w d$	(a)
		$[8\lambda(\rho)^{1/3}\sqrt{f'c} + \frac{Nu}{6Ag}]b_w d$	(b)
$A_v < A_{vmin}$	$[8\lambda\lambda_s(\rho)^{1/3}\sqrt{f'c} + \frac{Nu}{6Ag}]b_w d$		(c)

Notes: Axial load N_u is positive for compression and negative for tension: V_c shall not be taken less than zero; V_c shall not be taken greater than $5\lambda b_w d$; and $N_u/(6A_g)$ shall not be taken greater than $0.05f'_c$.

Table 2-3: Cases where $A_{v,\,min}$ is not required if $V_u \leq \Phi V_c$

Beam type	Condition ≤ ≥
Shallow beam	h ≤ 10 in.
Integral with slab	h ≤ greater of $2.5t_f$ or $0.5b_w$ and h ≤ 24 in.
Constructed with steel fiber-reinforced normal-weight concrete conforming to specific requirements and with $f'_c \leq$ 6000 psi	h ≤ 24 in. and $V_u \leq \phi 2\sqrt{f'c}\, b_w d$
One-way joint system	Conforming to specific requirements

Note: 1 in. = 25.4 mm; 1psi = 0.0069 MPa

$$\lambda_s = \sqrt{\frac{2}{1+\frac{d}{10}}} \qquad \textbf{(2-8)}$$

The size effect factor λ_s given in the above equation, which identifies that the reduction in shear strength with depth begins at 10 in. (254mm).

2.5 Introduction of Analysis Program

Among the many programs developed for the analysis of reinforced concrete structures VecTor2 © Analytical program was used for nonlinear finite element analysis of reinforced concrete beams in this research.

2.5.1 VecTor2

VecTor2 is a nonlinear finite element program for the analysis of two-dimensional reinforced concrete membrane structures. The program has been developed at University of Toronto since 1990, when its original version was known as TRIX. This development has coincided with experimental tests to corroborate the ability of VecTor2 to predict the load-deformation response of a variety of reinforced concrete structures exhibiting well-distributed cracking when subject to short-term static monotonic, cyclic and reverse cyclic loading. The theoretical bases of VecTor2 are the Modified Compression Field Theory (Vecchio and Collins, 1986) and the Disturbed Stress Field Model (Vecchio, 2000) – analytical models for predicting the response of reinforced concrete elements subject to in-plane normal and shear stresses (Vecchio, 2013).

VecTor2 (VT2) is a two-dimensional nonlinear finite element analysis (NLFEA) program used in combination with the preprocessor FormWorks© and the postprocessor Augustus©. The former allows simple model creation to be executed using an intuitive graphical user interface (GUI), while the latter is used to visually interpret analysis results (See Figure2-7) (Phillip, T.,2016).

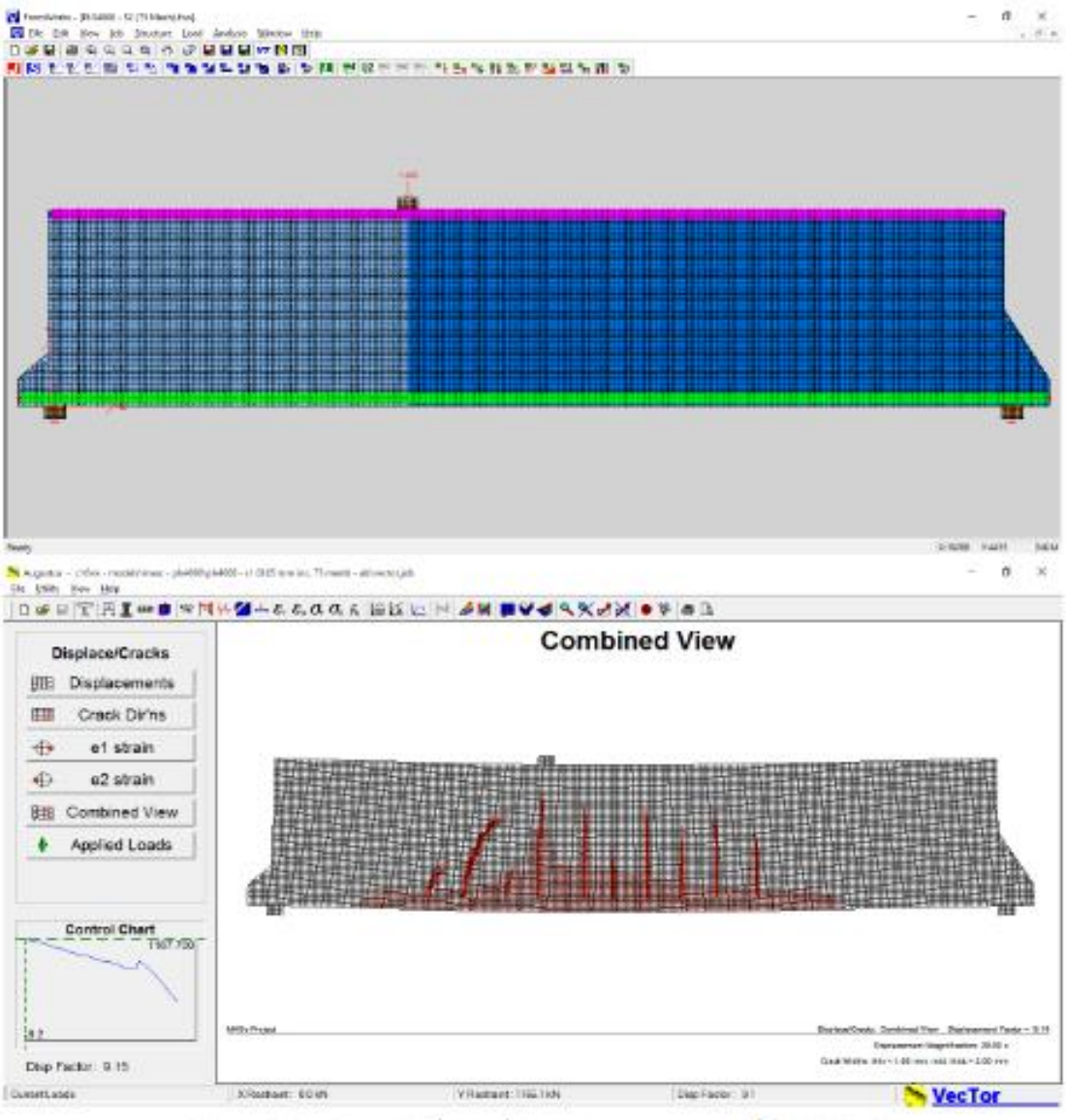

Figure 2-7: FormWorks and Augustus processors for VecTor2 (Phillip, T.,2016)

CHAPTER 3 EXPERIMENTAL PROGRAM

The experimental program for this thesis consisted of the design, construction, and testing of six reinforced concrete beam specimens. A summary of the experimental program will be outlined in this chapter with simplified diagrams and limited pictures of the test specimens and setup. In the following sections test specimens, materials used, specimen fabrication, testing setup and instrumentation will be discussed.

3.1 Design of Test Specimens

In this experimental program Six rectangular reinforced concrete beam specimens were constructed and tested in the Material Testing Laboratory of Addis Ababa University at AAiT. The specimens were designed to fail in shear rather than bending. All specimens were categorized in two groups based on their shear reinforcement usage. No transverse reinforcement was provided for three of the specimens while the other three specimens contained Ø6 stirrups at 200 mm spacing.

In order to maintain a maximum degree of uniformity among all tests every shear influencing parameters like beam width, concrete strength, longitudinal reinforcement ratios and shear span to depth ratio (a/d) were made similar in all specimens. The only varying parameter was height of the specimens which varied from 240 mm to 360 mm. All specimens had one layer of bottom steel with 2% longitudinal reinforcement ratio and the target concrete grade was C25. The longitudinal steel was evenly distributed along the width of the specimens leaving a 25 mm clear cover on each side and 25 mm bottom cover. All of the covers and the spacings of longitudinal reinforcement satisfied the requirements of the Eurocode 2.

The size of the specimens was determined considering the capacity of the laboratory testing machine and lifting equipment. A total of six specimens were divided into two series: beams without stirrup series (B) and beams with stirrups series (BS). Both series have similar geometry and steel reinforcement. Specimens were numbered according to their absolute height (in cm) as follows: B24, B30, B36, BS24, BS30, and BS36. The detail of each specimen in the two groups with their designations and other properties are given below in Table 3-1, Figure 3-1 and Figure 3-2.

Table 3-1: Properties of Reinforced concrete beam series specimens

Specimen	Beam-1 (B24)	Beam-2 (B30)	Beam-3 (B36)	Beam-4 (BS24)	Beam-5 (BS30)	Beam-6 (BS36)
Cross-sectional Dimensions						
Width, b_w(mm)	200	200	200	200	200	200
Height, H(mm)	240	300	360	240	300	360
Beam Dimensions						
Effective depth d (mm)	201	259	319	201	259	319
Shear span a (mm)	505	650	800	505	650	800
Shear span to depth ratio, a/d	2.51	2.51	2.51	2.51	2.51	2.51
Longitudinal reinforcement						
Top	2Ø10 157.1mm^2	2Ø10 157.1mm^2	2Ø10 157.1mm^2	2Ø10 157.1mm^2	2Ø10 157.1mm^2	2Ø10 157.1mm^2
Bottom	4Ø16 804.2mm^2	2Ø16&2Ø20 1,030.4mm^2	4Ø20 1,256.6mm^2	4Ø16 804.2mm^2	2Ø16&2Ø20 1,030.4mm^2	4Ø20 1,256.6mm^2
$\rho_{bottom,}$ (A_{st}/bd)	2.0%	1.99%	1.97%	2.0%	1.99%	1.97%
Transverse reinforcement						
Stirrup	No	No	No	Yes	Yes	Yes
Bar designation	-	-	-	Ø6 56.6mm^2	Ø6 56.6mm^2	Ø6 56.6mm^2
Spacing, S(mm)	-	-	-	200	200	200
Shear reinforcement ratio $\rho_{bottom,}$ A_v/bs	-	-	-	0.14%	0.14%	0.14%

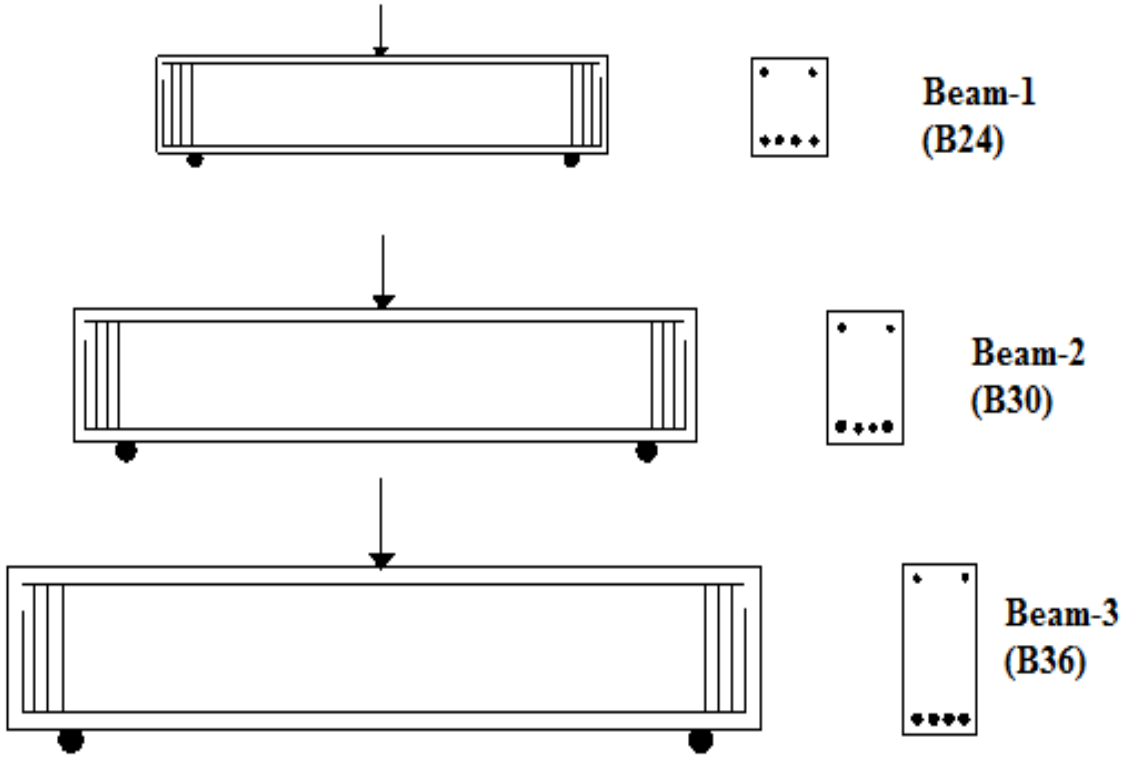

Figure 3-1: Geometric details of beams without shear reinforcement series

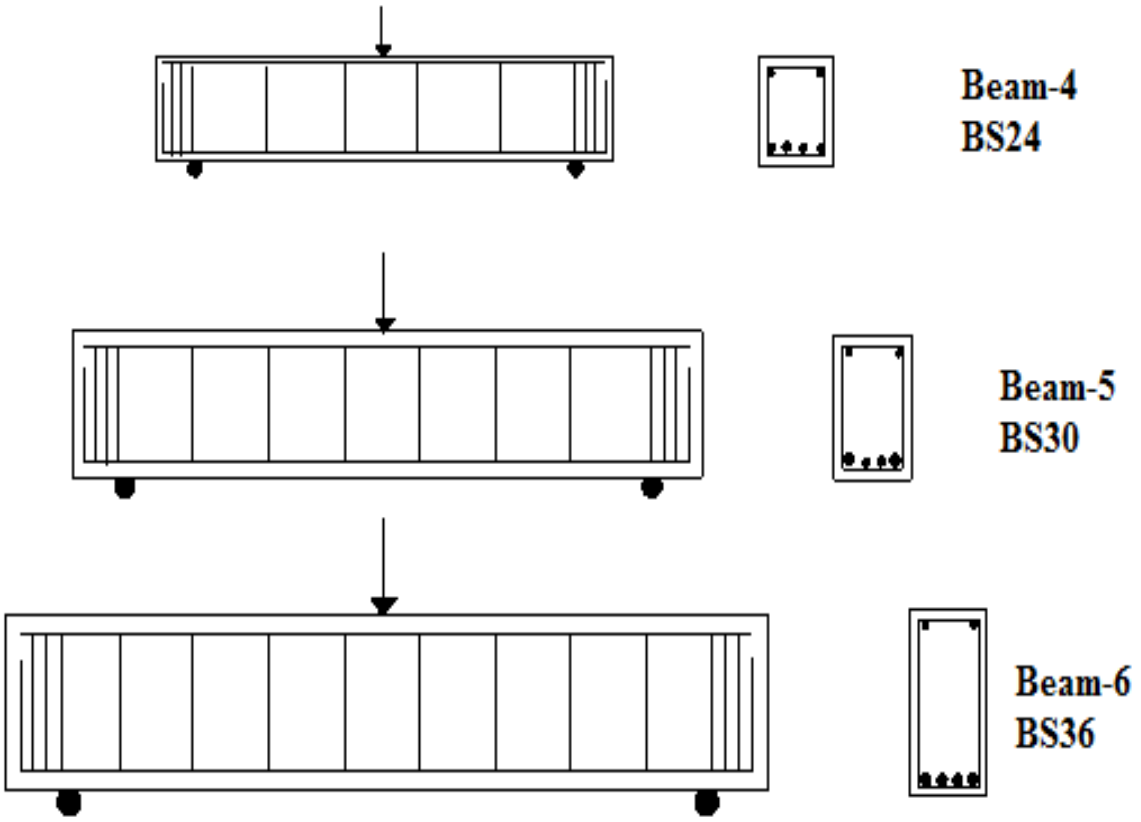

Figure 3-2: Geometric details of beams with shear reinforcement series

3.2 Material Properties

3.2.1 Concrete Properties

The concrete making materials used to construct the specimens were batched and mixed in the Material Testing Laboratory of Addis Ababa University at AAiT. Using ACI procedure concrete mix design was prepared with a targeted cylindrical compressive strength of 25 MPa. Using an ordinary Portland cement, aggregate with a maximum size of 19mm and 0.61 water to cement ratio concrete mix proportion were specified as shown in Table 3.2 below.

Table 3-2: Mix Design before adjustment

Cement type	Ordinary Portland Cement (OPC)
Maximum aggregate size (mm)	19
Mixing water (Kg/m)	205
Cement (Kg/m)	336.07
Fine aggregate (Kg/m)	806.6
Coarse aggregate (Kg/m^3)	997.33
Water to cement ratio(w/c)	0.61

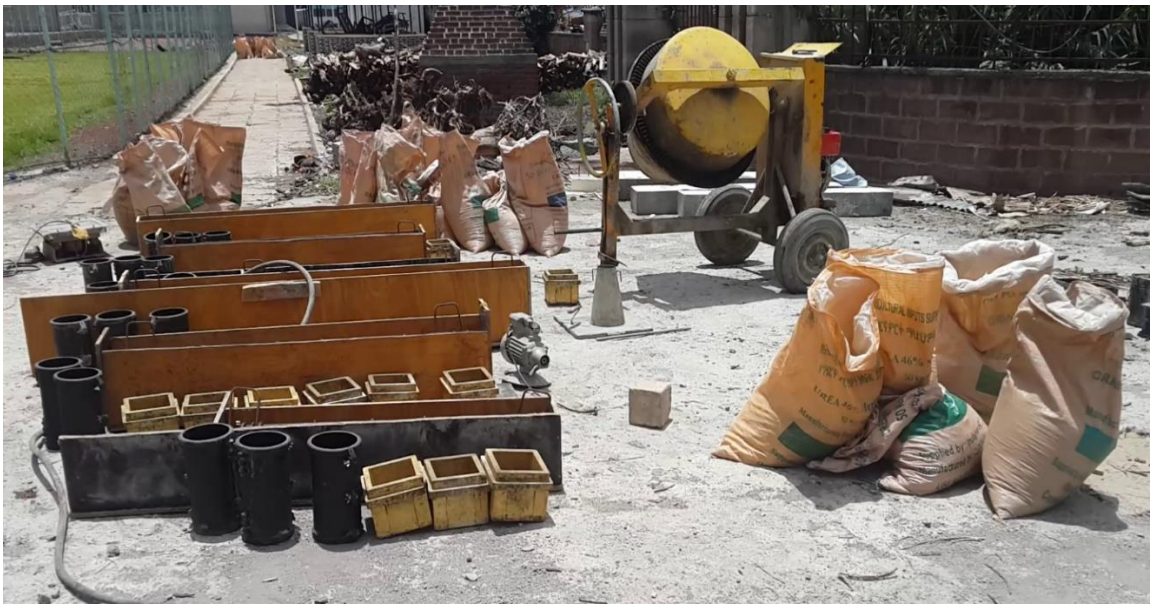

Figure 3-3: Batching and preparation of concrete ingredients before mixing

Six cube and three Cylinder samples were taken from each concrete mix for determining concrete properties of each specimen. The development of the compressive strength was observed by testing the cubes at the age of 28 days and at the beam testing date using a load-controlled test machine. The tensile strengths of the concrete at the age of the beam tests were obtained using cylinder splitting test machine. Cube compression and split-cylinder tests were conducted to determine the mean values of the concrete compressive strength f_c and the splitting tensile stress f_{sp}. Standard cubes 150x150x150mm were used for compression test and Standard cylinders, 150 mm in diameter and 300 mm long, were used for the split-cylinder tests.

Table 3-3: 28th day compressive strength of representative cube samples

Specimen	Compressive strength (MPa)			
	Cube 1	Cube 2	Cube 3	Average
Beam-1(B24)	30.79	31.41	26.74	29.65
Beam-2(B30)	33.03	32.44	33.74	33.07
Beam-3(B36)	28.31	34.30	23.19	28.6
Beam-4(BS24)	30.52	28.26	29.18	29.32
Beam-5(BS30)	28.55	31.43	32.09	30.69
Beam-6(BS36)	32.36	31.91	30.77	31.68

Figure 3-4: Compressive Strength testing machine

Table 3-4: Beam Test day compressive strength of cube samples

Specimen	Compressive strength (MPa)			
	Cube 1	Cube 2	Cube 3	Average
Beam-1(B24)	33.60	35.32	30.64	33.19
Beam-2(B30)	35.46	33.70	-	34.58
Beam-3(B36)	34.99	35.71	33.57	34.76
Beam-4(BS24)	34.83	33.26	32.54	33.54
Beam-5(BS30)	28.91	32.60	34.65	32.05
Beam-6(BS36)	29.79	35.26	34.05	33.03

Figure 3-5: Concrete split tensile strength test machine

Split tensile strength of the concrete is calculated by $f_t = \frac{2P}{\pi DL}$ (3-1)

Where: - P = Compressive load at failure

L = Length of cylinder

D = Diameter of cylinder

Table 3-5: Beam Test day Tensile strength of cylinder samples

Specimen	Tensile strength (MPa)			
	Cylinder 1	Cylinder 2	Cylinder 3	Average
Beam-1(B24)	1.83	1.75	1.79	1.79
Beam-2(B30)	1.72	1.76	1.81	1.76
Beam-3(B36)	1.74	1.47	1.58	1.60
Beam-4(BS24)	1.68	1.72	1.78	1.73
Beam-5(BS30)	1.56	1.87	1.64	1.69
Beam-6(BS36)	1.93	1.63	1.88	1.81

3.2.2 Reinforcing Steel Properties

Deformed bars with a diameter of 10mm, 16mm and 20mm were used for top and bottom longitudinal reinforcements. Additionally, for three specimens plain bar with a diameter of 6mm were used as shear reinforcement. A uniaxial tension tests were conducted on all samples from both longitudinal and shear reinforcement to determine their mechanical properties. Key properties of the various steel samples obtained from the tensile tests are reported in Table 3-6:

Table 3-6: Test results of reinforcement

Specimen No	Diameter		Yield load (KN)	Failure Load (KN)	Elongation (%)	Length (mm)
	D1, (mm)	D2, (mm)				
Ø 6-1	5.63	5.66	9.2	12.6	22.8	100
Ø 6-2	5.98	5.98	9.1	13.9	23.0	100
Ø 10-1	9.32	10.59	39.8	51.2	23.5	100
Ø 10-2	9.36	10.62	39.7	50.7	23.4	100
Ø 16-1	15.40	16.04	124.2	131.2	23.6	100
Ø 16-2	15.42	16.08	123.9	132.4	235	100
Ø 20-1	18.30	21.15	195.0	226.3	22.3	100
Ø 20-2	18.32	21.18	193.6	225.4	22.0	100

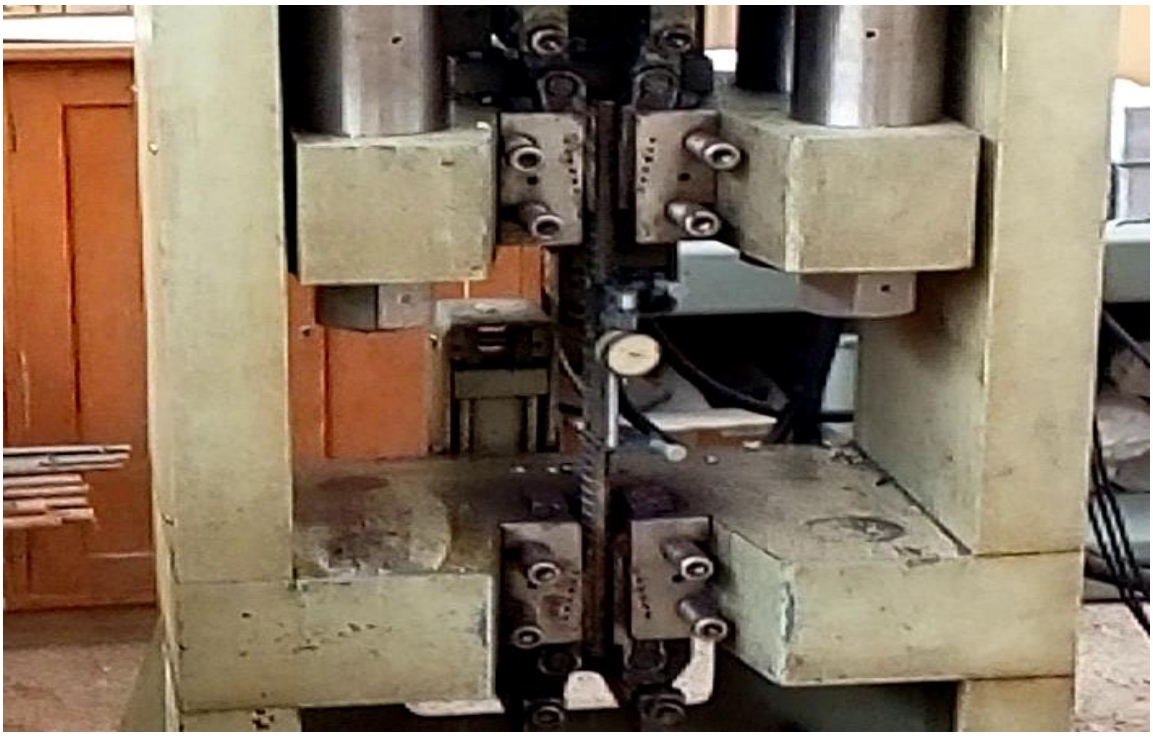

Figure 3-6: Universal Testing Machine testing tensile strength of reinforcement bar

Table 3-7: Mechanical properties of reinforcement from test result

Specimen	Average Diameter (mm)	Area (mm^2)	Yield load (KN)	Failure load (KN)	Yield stress (MPa)	Ultimate stress (MPa)
Ø6	5.64	24.98	9.15	13.25	366.29	530.42
Ø10	9.97	78.07	39.75	50.95	509.16	652.62
Ø16	15.74	194.58	124.05	131.8	637.53	677.36
Ø20	19.74	306.04	194.3	225.85	634.88	737.97

3.3 Specimen Fabrication

All testing specimens were constructed on the space prepared for this purpose by Materials Testing Laboratory of AAiT.

3.3.1 Preparation of the rebar

The reinforcement cages preparation was done by experienced personnel. First cutting of longitudinal rebars for each specimen was done based on the length of the beam then top and bottom rebars anchored by rectangular tie on both side of the beam outside of clear span. For beam series with stirrup additional stirrups used with 200mm spacing. Spacing of shear reinforcement and detailing provisions were closely monitored. All of the above-mentioned work for assemblage of reinforcement cage were done outside of the formwork.

Figure 3-7: Reinforcement cage preparation

3.3.2 Formwork Construction

The formwork panels are made up of specially coated plywood. The work begins by cutting the plywood into different size specimens based on the dimension of specimens. Then these segments of plywood assembled and stiffened at the mid span to avoid bulging of concrete during casting. After the formwork assembled, form releasing agent applied on the inner surface of the forms for easy stripping of formwork. Once the formwork was ready, the steel cage placed inside it. Concrete cover maintained by attaching 25mm dried mortar on all sides of reinforcement cage as shown in Figure 3-8.

Figure 3-8: Formwork preparation and concrete cover assembling

3.3.3 Concrete Casting

One day before casting day sand and aggregate needed for mixing was batched based on ACI mix design ratio for C25 concrete. Each and every mix of concrete cast one beam specimen, six cube samples and three Cylinder samples. Totally six mixes were done for all specimens. Concrete on beam specimens were compacted by using industrial concrete vibrator and table shake vibrator was used to consolidate concrete on cube and cylinder samples. Finishing of the top surface upon completion of the concrete placement was achieved by standard troweling.

Figure 3-9: concrete casting on beam specimens and representative samples

3.3.4 Curing of Specimens

In order to maintain equivalent curing conditions between the casted specimens and cylinders(cubes), the side forms were removed after 24 hours. The curing of the concrete was achieved by spreading wet burlaps on top of beam specimens, cubes and cylinders, which were then sprinkled regularly twice a day for one week since the casting and remained covered by plastic sheet to prevent moisture loss during the curing process.

Figure 3-10: Curing of concrete on beam specimens, cubes and cylinders

3.3.5 White Painting

Before testing date, the entire faces of all specimens were painted with white paint to make cracks visible and marking clear. It also helps to make cracks more visible in photographs. The beams were transported from casting area to laboratory by man power and positioned in the testing machine by using indoor crane.

Figure 3-11: Beam specimens painted white on both faces before test

3.4 Test Setup

All beam specimens were tested by applying concentrated load at the mid span. The loading was applied monotonically with load and deflection values being recorded at small increments of loading as shown in figure below.

Figure 3-12: Loading setup during testing of beam specimen

The specimens were supported on a pair of steel rollers at each support. These roller supports were installed on concrete members anchored to the strong floor. Plastic bags filled with gypsum were placed in between the roller support and beam to make a smooth contact surface, and also protected the beam from sliding. A concentrated load was applied at mid span using manually operated hydraulic jack. The load transfer from the testing machine to the specimens was through a loading plate that was leveled by gypsum on the top of the specimens. The loading plate was 3cm thick steel plate covering the entire width of the specimens over a length of 20cm. Two displacement measuring devices are used to measure mid span deflation of the beam one at the bottom centerline of the beam and the other on the back face of the beam but both of them are located at mid span location.

3.5 Instrumentation and Data Acquisition

The experimental program for this thesis incorporated different instrumentations to properly observe the behavior of all beam specimens. Additional measurements taken by camera was media capture in the form of high-quality pictures and video being recorded during all stages of testing.

3.5.1 Load Cell

Load cell is an instrument which placed between the top of beam specimens and bottom of hydraulic jack. Load cell assemblies used at the mid span loading location of the test. This load cell was connected to a data logger that recorded the data and displayed the applied force on the screen.

Figure 3-13: Loading cell used to read applied load

3.5.2 Hydraulic Jack

Hydraulic jack was used to applied the load on the top of testing beam specimen. The hydraulic jack used for loading had a maximum capacity of 300 KN (30 tons). Since the load was applied manually by using a hydraulic jack loading rate could not be kept constant. Because of that the loading rate varied randomly for each experiment. Measure are taken to make loading uniform as much as possible for all beam specimens. Therefore, the effect of increase in loading rate was somehow controlled but not consistently regulated like machine with an automatic actuator.

Figure 3-14: Manual hydraulic jack with maximum capacity of 300KN

3.5.3 Data logger

All of the instrumentations such as load cell and displacement transducers were connected to a data logger were connected to a data logger. This data logger displays the applied load and mid span deflections on its screen. The experimental data were recorded in excel format by the data logger and accessed through USB flash disk.

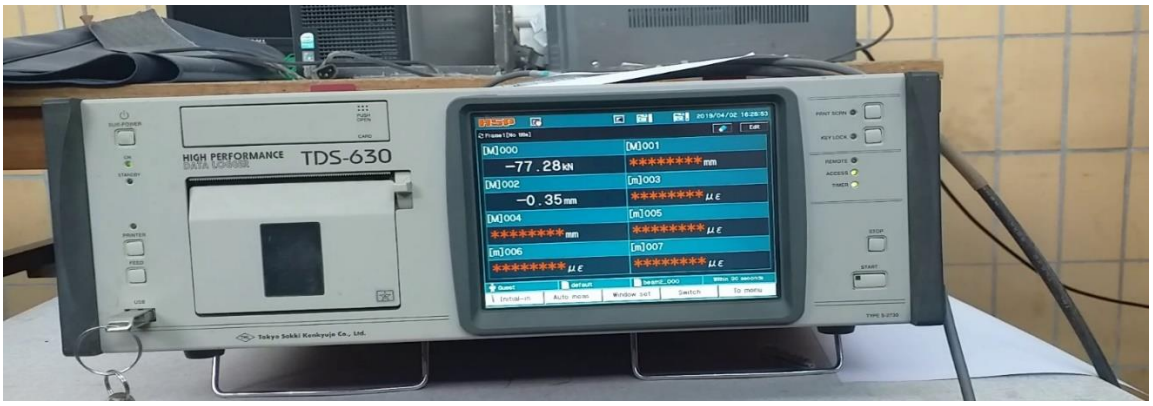

Figure 3-15: Data logger used to display the applied load and deflection

3.5.4 Displacement Measuring Instrument

Vertical displacements at mid span were measured using a Linear Variable Differential Transformers (LVDTs). These instruments were fixed to the bottom and back face of the specimen. Bottom displacement measuring instrument was held by magnetic mounts at mid span location. Displacement measuring instrument on the back face at mid span location was attached to a static horizontal rod. This rod was anchored to a beam on both ends by drilling at the axis of rotation.

Figure 3-16: Displacement measuring device installed at the back of the specimen

3.5.5 Media

High-definition video recording and photographs using a smart phone camera were taken continuously throughout the testing process.

CHAPTER 4 NONLINEAR FINITE ELEMENT ANALYSIS

4.1 General

This chapter describe in detail the aspects of analytical modeling demonstrated in this thesis. Since the experimental work is expensive and limited by the capacity of testing machine finite element analysis is also performed to investigate the effect of size on shear behavior of reinforced concrete beams with and without shear reinforcement. In addition to six beams tested in the experimental program another six reinforced concrete beams with relatively large depth are also modeled on finite element software. Nonlinear finite element analysis (NLFEA) programs permit more accurate assessment of structural performance (strength, post-peak behavior, failure mode, deflections and cracking) than can be achieved by linear elastic methods. Among the many NLFEA programs for the analysis of reinforced concrete structures VecTor2© was selected for this study.

4.2 The VecTor2 Program

VecTor2© (VT2) is a nonlinear finite element program for the analysis of two-dimensional reinforced concrete membrane structures. The program has been developed at University of Toronto since 1990, when its original version was known as TRIX©. This development has coincided with experimental tests to corroborate the ability of VecTor2 to predict the load -deformation response of a variety of reinforced concrete structures exhibiting well distributed cracking when subject to short term static monotonic, cyclic and reverse cyclic loading.

The theoretical bases of VecTor2 are the Modified Compression Field Theory (Vecchio and Collins, 1986) and the Disturbed Stress Field Model (Vecchio, 2000) – analytical models for predicting the response of reinforced concrete elements subject to in-plane normal and shear stresses. Originally, VecTor2 employed the constitutive relationships of the MCFT. Subsequent developments have incorporated alternative constitutive models for a variety of second-order effects including compression softening, tension stiffening, tension softening, and tension splitting.

4.3 Specimens

Total number of specimens that are used in the simulation are twelve, six of them are identical with the specimens used in the experimental program and the remaining six specimens are prepared for finite element simulation because of their large size. This is will help to get further information on the effect of size on the shear behavior of reinforced concrete beams with and without shear reinforcement. There are two groups of beam specimens depending on their shear reinforcement ratio. The first group has six beam specimens without shear reinforcement and the second hold the remaining six beams with 0.14% shear reinforcement ratio. Each beam specimen is identified with a label consisting of a series of letters and numbers as presented in tables below. The First letter B stands for beam and the number indicate depth of the beam in centimeter, letter S also used for beams which have shear reinforcement. The specimen's designation with their properties is provided in Table 4-1. Below.

Table 4-1: Specimen designation and their properties used in VecTor2

Specimen	Height (mm)	Width (mm)	Effective Depth, d (mm)	Shear Span, a (mm)	a/d	Shear reinforcement ratio, (ρ_w)	Bottom Steel Area (mm^2)
B24	240	200	201	505	2.51	-	804.25
B30	300	200	259	650	2.51	-	1030.44
B36	360	200	319	800	2.51	-	1256.64
B60	600	200	557	1400	2.51	-	2228.00
B90	900	200	855	2150	2.51	-	3420.00
B120	1200	200	1153	2900	2.51	-	4612.00
BS24	240	200	201	505	2.51	0.14%	804.25
BS30	300	200	259	650	2.51	0.14%	1030.44
BS36	360	200	319	800	2.51	0.14%	1256.64
BS60	600	200	557	1400	2.51	0.14%	2228.00
BS90	900	200	855	2150	2.51	0.14%	3420.00
BS120	1200	200	1153	2900	2.51	0.14%	4612.00

The specimens, as modelled in VecTor2, are displayed in the following diagrams. The reinforcement cage is modelled with different colors for longitudinal and shear reinforcements. Better clarification on the modeling process shall be discussed in following sections.

B24(without stirrup)

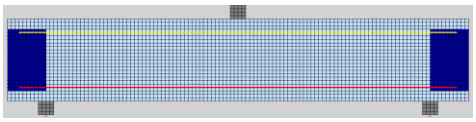

B30(without stirrup)

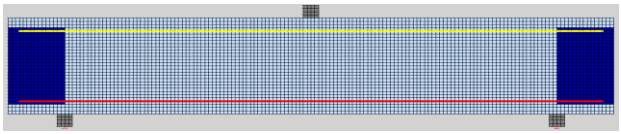

B36(without stirrup)

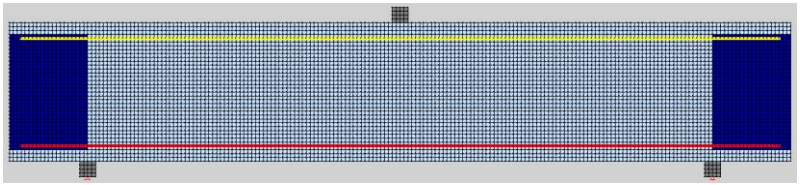

B60(without stirrup)

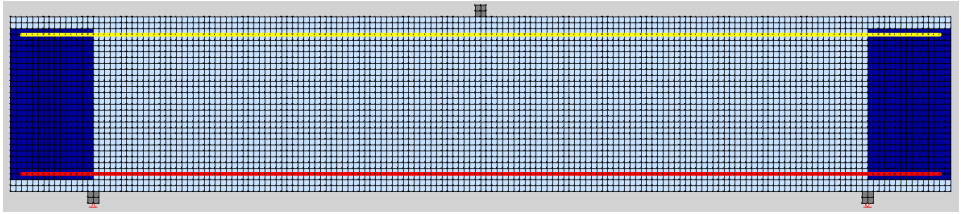

B90(without stirrup)

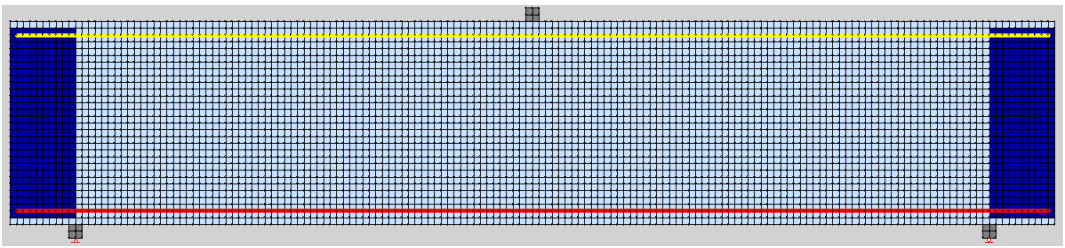

B120(without stirrup)

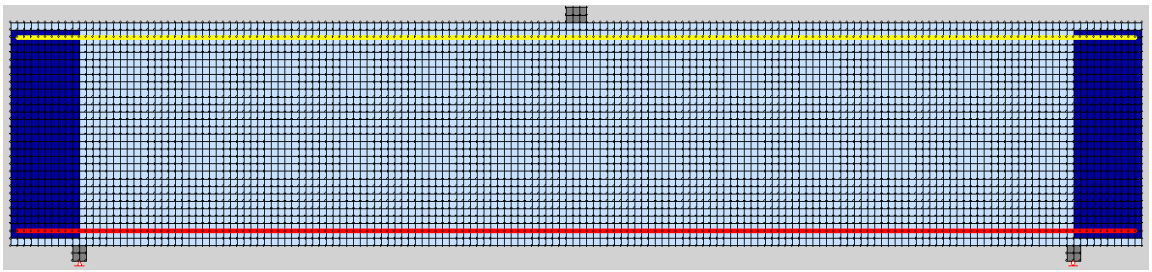

Figure 4-1: VT2 Model of beams without shear reinforcement series

BS24(with stirrup)

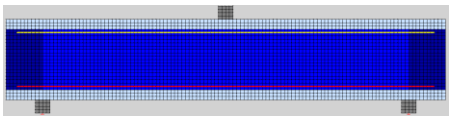

BS30(with stirrup)

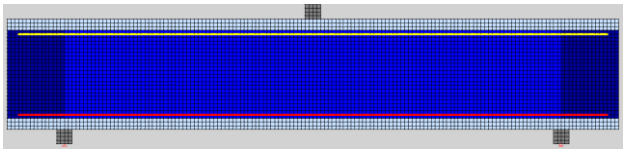

BS36(with stirrup)

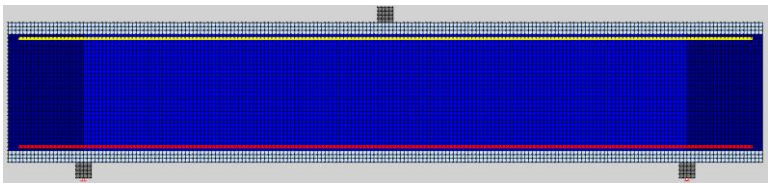

BS60(with stirrup)

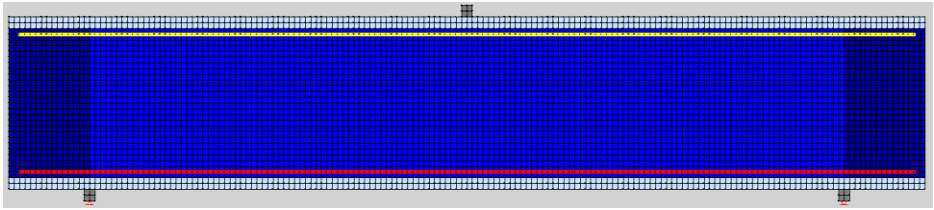

BS90(with stirrup)

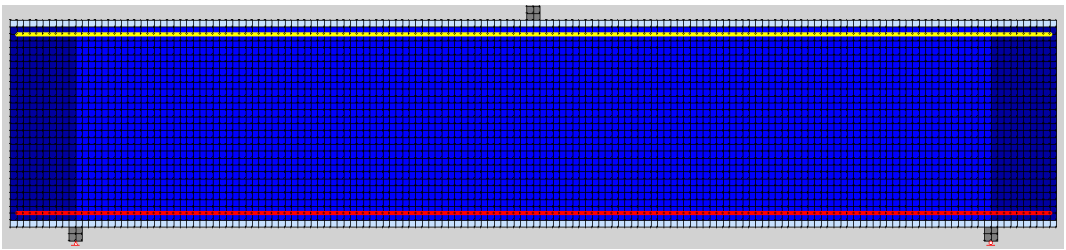

BS120(with stirrup)

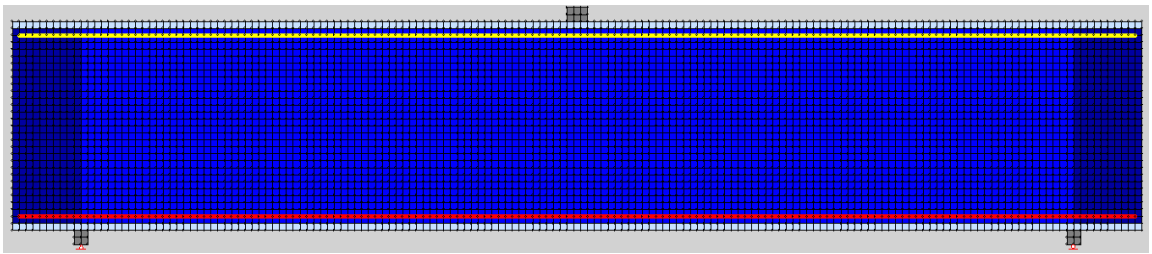

Figure 4-2: VT2 Model of beams with shear reinforcement series

4.4 Materials

The compressive and tensile strength of the concrete for six specimens up to 360mm depth were directly taken from the experimental program and for the remaining six specimens which have no experimental data average value is used. The cylindrical compressive strength of concrete is calculated from its 150mm cube sample experimental results according to Eurocode specification. The modulus of elasticity and other properties of concrete were left as the default values in the VecTor2 program; the program calculates appropriate values using the following formulas.

Initial Tangent Modulus, Ec $E_C = 5500\sqrt{f'c}$ MPa

Tensile strength, $f't$ $f't = 0.33\sqrt{f'c}$ $[MPa]$

Cylinder Strain at peak strength, $\epsilon'c$ $\epsilon'c = 1.8 + 0.0075 \times \sqrt{f'c}$ $[mm/m]$

Poisson's Ratio, υ $\upsilon = 0.15$

Thermal Expansion Coefficient, Cc Cc = 10x10-6 /°C

Density, ρ ρ = 2400 kg/m3

Table 4-2: Mechanical properties of concrete used in the VecTor2 model

Beam specimens	Cube *f'cu* (MPa)	Cylinder *f'cm* (MPa)	*f't* (MPa)	Ec (MPa)	ε'c (mm/m)
Beam-1(B24)	33.19	26.55	1.70	28339.68	1.8386
Beam-2(B30)	34.58	27.66	1.73	28926.03	1.8394
Beam-3(B36)	34.76	27.81	1.74	29004.35	1.8395
Beam-4(B60)	33.52	26.82	1.71	28483.42	1.8388
Beam-5(B90)	33.52	26.82	1.71	28483.42	1.8388
Beam-6(B120)	33.52	26.82	1.71	28483.42	1.8388
Beam-7(BS24)	33.54	26.83	1.71	28488.72	1.8388
Beam-8(BS30)	32.05	25.64	1.67	27849.77	1.8380
Beam-9(BS36)	33.03	26.42	1.70	28270.21	1.8385
Beam-10(BS60)	33.52	26.82	1.71	28483.42	1.8388
Beam-11(BS90)	33.52	26.82	1.71	28483.42	1.8388
Beam-12(BS120)	33.52	26.82	1.71	28483.42	1.8388

The mechanical behavior of different diameter longitudinal and transverse reinforcements was also taken from the tension tests conducted in the material testing laboratory of AAiT. These experimental results summarized in Table 5.3 were directly inserted in the VecTor2 analytical model.

Table 4-3: Mechanical properties of the steel bars

Diameter	Ø6, Transverse	Ø10, Top Longitudinal	Ø16, Bottom Longitudinal	Ø20, Bottom Longitudinal
Modules of elasticity (GPa)	200	200	200	200
Yield strength MPa	366.29	509.16	637.53	634.88
Ultimate strength MPa	530.42	652.62	677.36	737.97

4.5 Modeling

The finite element analysis models and assumptions used for the six experimentally tested beam specimens were also used for the scaled up six beam specimens. The stiffness matrix in VecTor2 suits is constructed from the determined values of the stress and the strain from the selected models. This necessitates an appropriate selection of constitutive models, particularly for the concrete.

In this modeling, it is decided to model the beam with four node rectangular elements for the concrete, and two node truss bar elements for the longitudinal reinforcing bars. In VecTor2 suits, it is possible to model reinforcements in discrete as well as smeared manner. Longitudinal reinforcement was modelled as discrete truss bars, while the transverse shear reinforcement was smeared over the respective spans for the different testing phases. since it is advisable to select the VecTor2 default models for the majority of analyses material and behavioral models used in this thesis are the VecTor2 default models.

The VecTor2 model was assumed to be represented by two-dimensional plane-stress behavior. A total of 30 elements were used over the specimen depth, corresponding to a very fine mesh size of 8mm up to 40 mm. A total of about 3620 rectangular elements and 232 truss elements are used in the model.

4.6 Support Condition and Loading

The beam specimens were simply supported by pin support on left side and roller support on the other sides with different clear distance between the supports. Load and support plates were modelled as steel in purely elastic state. The nonlinear finite element simulation program was planned to have a loading scenario controlled by displacement. To capture the post peak behavior of the beam specimens, a displacement-controlled analysis was performed by applying a downward displacement at the mid span with the width of the loading and supporting plate increasing proportionally with the member size. Self-weight was applied in a single load step through uniformly applied density assignments (ρ = 2400 kg/m^3) to all concrete elements. The point load was imposed as a nodal displacement at the mid span loading point in monotonic fashion with increments of 0.1 mm until failure.

CHAPTER 5 RESULT AND DISCUSSION

5.1 General

In this chapter, the test results are discussed. In addition, nonlinear finite element analysis was performed and the results are compared to the experimental results. The validity of the code provisions for shear strength is also investigated. In the discussion part effect of beam depth (size effect) on the failure shear stress of beams without shear reinforcement are discussed. Then the possible contribution of shear reinforcement to mitigate the size effect on the shear strength of reinforced concrete beams are discussed. Finally, the results of all beam specimens are compared with shear provisions of EC2, ACI-318-14 and ACI-318-19 for reinforced concrete slender beams to assess their accuracy.

5.2 Experimental Results

The shear forces shown in table 5.1 were calculated at the critical section for shear, which is d_v away from the applied load, considering the effect of the self-weight of the beam. The shear force due to the self-weight of the beam (V_d) was added to the half of the applied load to obtain the shear force at the critical section. This V_d is:

$$\mathbf{V_d = \gamma.h.b.\ (a\text{-}d_v) = \gamma.h.b.\ (a\text{-}0.9d) = 23.5\ kN/m^3\ .h.b.(a\text{-}0.9d)\quad [kN]} \qquad \mathbf{(5\text{-}1)}$$

Table 5-1: Experimental result for beams of B series and BS series

Specimen	H (mm)	D (mm)	b (mm)	a (mm)	ρ_{shear} (%)	$P_{Ultmate}$ (KN)	V_d (KN)	$V_{Ultimate}$ (KN)	Deflection at failure Δ_{Ult} (mm)
B24	240	201	200	505	-	129.55	0.366	65.14	1.29
B30	300	259	200	650	-	158.24	0.536	79.66	2.29
B36	360	319	200	800	-	186.58	0.805	94.10	3.00
BS24	240	201	200	505	0.14	169.32	0.366	85.03	2.26
BS30	300	259	200	650	0.14	210.08	0.536	105.58	2.86
BS36	360	319	200	800	0.14	259.36	0.805	130.48	4.36

5.2.1 Crack Patterns and Failure Modes

In all tested beams, flexural cracks developed first in the pure bending region, and then spread into the shear span. With further increase in the applied load diagonal cracks formed suddenly at mid-depth in the middle of the shear span. The diagonal cracks propagated initially towards the load and subsequently backwards towards the support. In most cases, a second major inclined crack developed parallel to the initial crack and together they induced failure. Photographs of each reinforced concrete beam specimens after they have been tested are attached below to show cracking pattern obtained at failure of the specimens.

5.2.1.1 Beam-1(B24)

In this beam designation B stands for beam and 24 stands for depth of the beam in centimeter unit which is 24 cm. since it has no shear reinforcement on the shear span the failure in this specimen was sudden after diagonal shear cracks appeared. First, the flexural cracks initiated then with further increase of load new flexural cracks formed in the shear span and curved toward the loading point. As shown in the photograph below Shear-Compression failure occurred after diagonal cracks propagated in the shear span causing high stresses to be developed in the compression zone above the tip of the cracks, which lead to brittle failure.

Figure 5-1: Specimen B24 beam without shear reinforcement after failure

5.2.1.2 Beam-2(B30)

Specimen designation of this beam B30 has the same meaning as the previous one and it has no shear reinforcement on the shear span. Diagonal crack was first observed in the east end of the beam at this time no such crack appeared in the west end, both ends has no shear reinforcement. With further increase of load the major diagonal crack on the east side propagated initially towards the load and subsequently backwards towards the support. Then just prior to failure a critical diagonal crack opened without warning. Failure of this beam specimen was in shear and in a brittle fashion with a major crack on the right side of loading point.

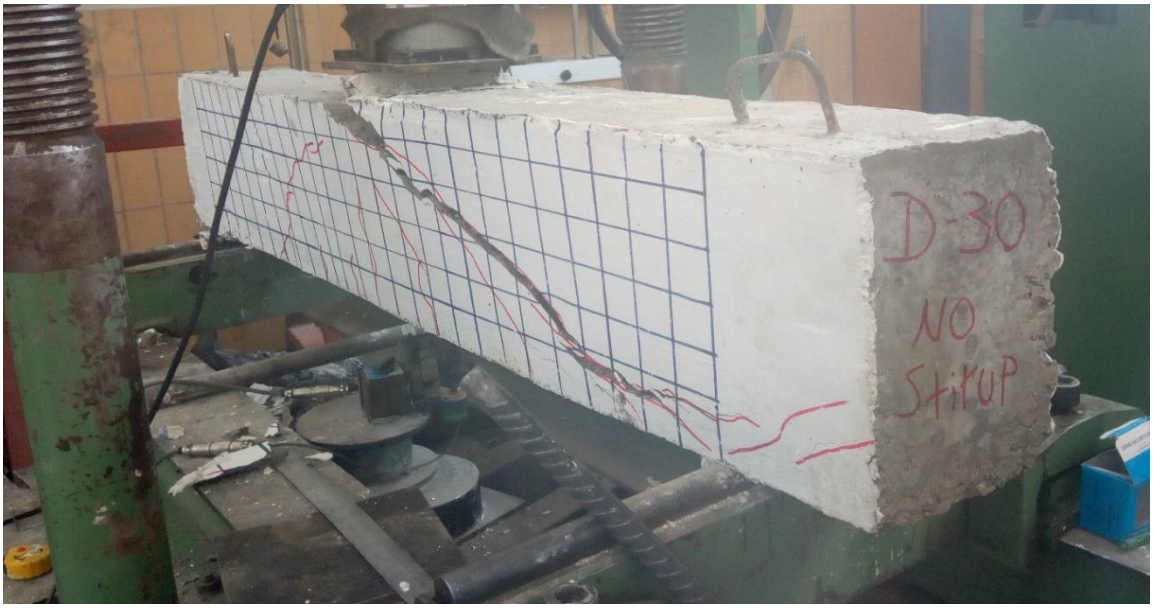

Figure 5-2: Specimen B30 beam without shear reinforcement after failure

5.2.1.3 Beam-3(B36)

First, the flexural cracks initiated in this specimen occurred at mid span location. As expected, a very brittle behavior was observed with failure happening without warning. The modes of failure for this specimen is Shear-Compression failure occurred after diagonal cracks propagated in the shear span causing high stresses to be developed in the compression zone above the tip of the cracks. It was noted that the ultimate shear capacity of this beam was only slightly higher than the load which caused diagonal cracking.

Figure 5-3: Specimen B36 beam without shear reinforcement after failure

5.2.1.4 Beam-4(BS24)

The letter S in this specimen stands for the presence of shear reinforcement on the shear span with ratio of 0.14% which is above minimum shear reinforcement recommended by both EC2 and ACI 318-14. Due to the presence of this shear reinforcement the flexural cracks developed very slowly and concentrated in a limited area under the mid-span load. This specimen failed in shear but it behaved in a relatively ductile manner as compared with the previous three beams without shear reinforcement. Unlike the previous beams the major diagonal failure crack occurred on the west side of the specimen. failure mode of this specimen is Diagonal Splitting failure occurred when the diagonal cracks propagated initially towards the load and then towards the support.

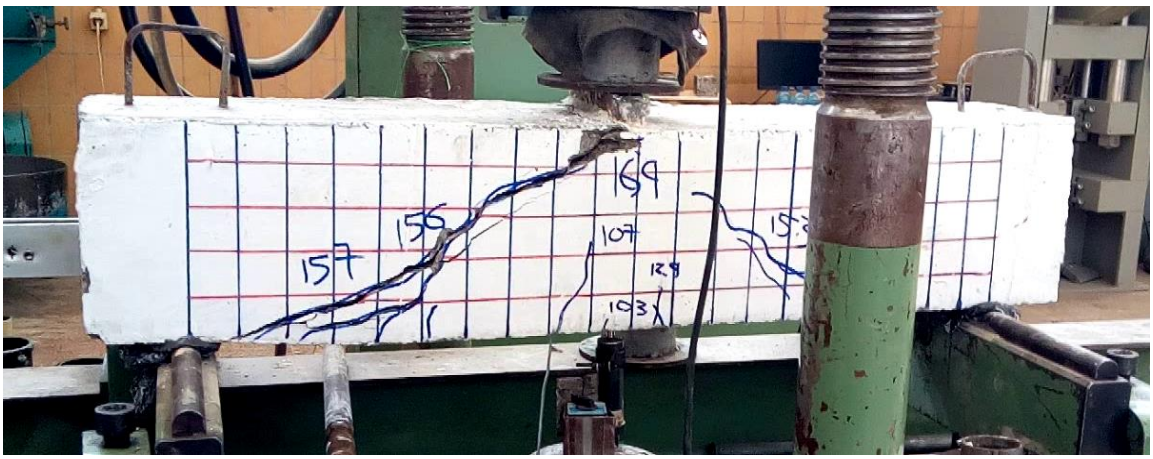

Figure 5-4: Specimen BS24 beam with shear reinforcement after failure

5.2.1.5 Beam-5(BS30)

Like the previous beam this beam has shear reinforcement that distribute diagonal crack on both sides and make the flexural cracks to develop very slowly. The failure mode of this specimen is Diagonal Splitting failure occurred when the diagonal cracks propagated initially towards the load and then towards the support. This type of failure was less brittle compared to the shear failure modes of other specimens without shear reinforcement. The major diagonal shear crack appeared on the west side of the beam.

Figure 5-5: Specimen BS30 beam with shear reinforcement after failure

5.2.1.6 Beam-6(BS36)

Just like the previous two beams it shows relatively ductile failure. Cracks begin to develop unsymmetrically with most of these cracks appearing in the west side of the beam. New cracks begin to develop on top of the older ones, particularly, one of the primary diagonal cracks which suddenly widened, showing a sign of shear failure. Cracks closer to the bottom edge of the beam are progressively developing, turning and go horizontally, forming splitting lines along the top level longitudinal rebars on west sides of the beam.

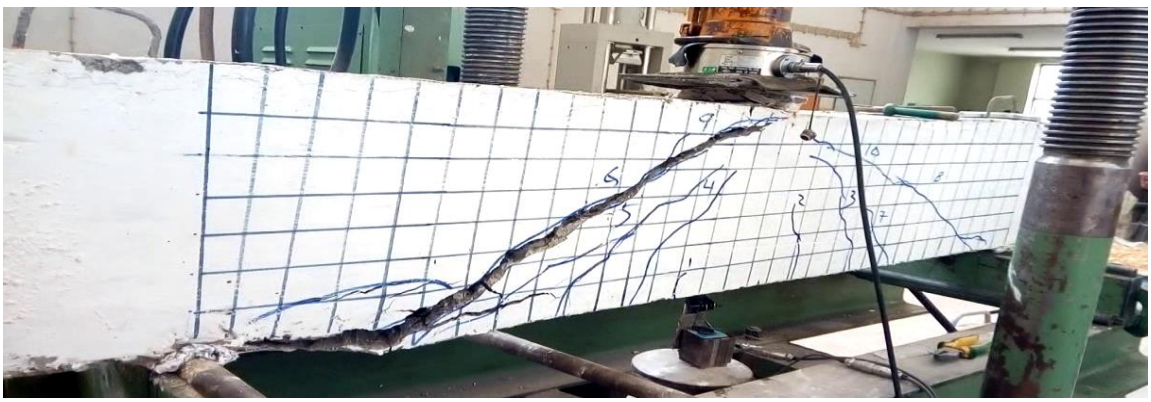

Figure 5-6: Specimen BS36 beam with shear reinforcement after failure

5.2.2 Load-Deflection Response

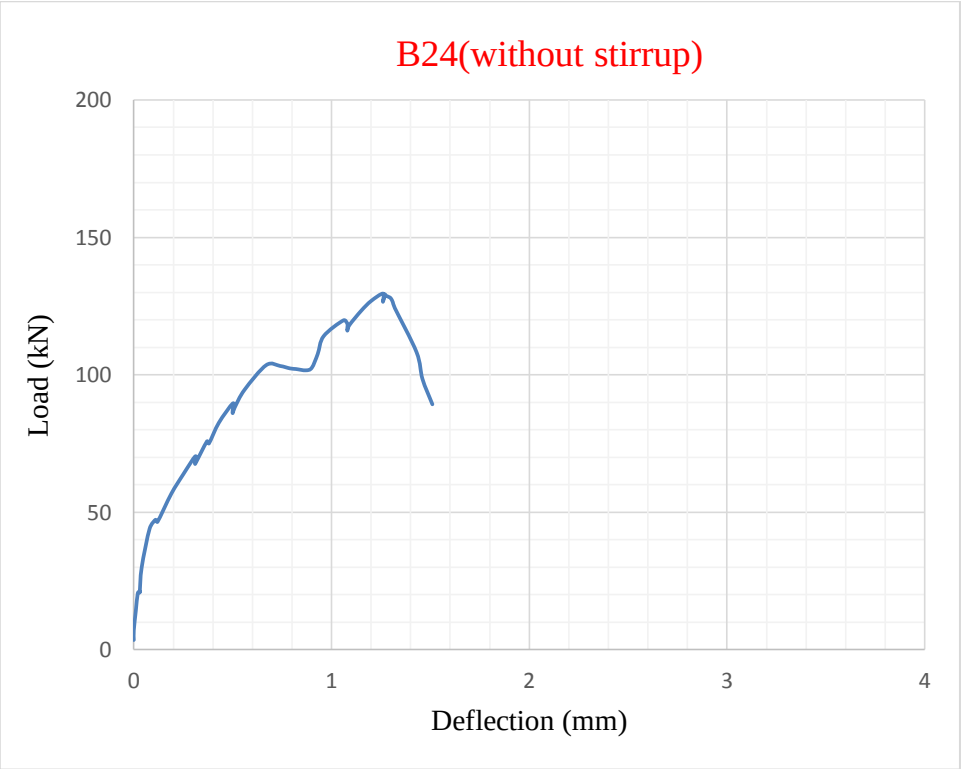

Figure 5-7: Load-Deflection response of B24 (without shear reinforcement)

Figure 5-8: Load-Deflection response of BS24 (with shear reinforcement)

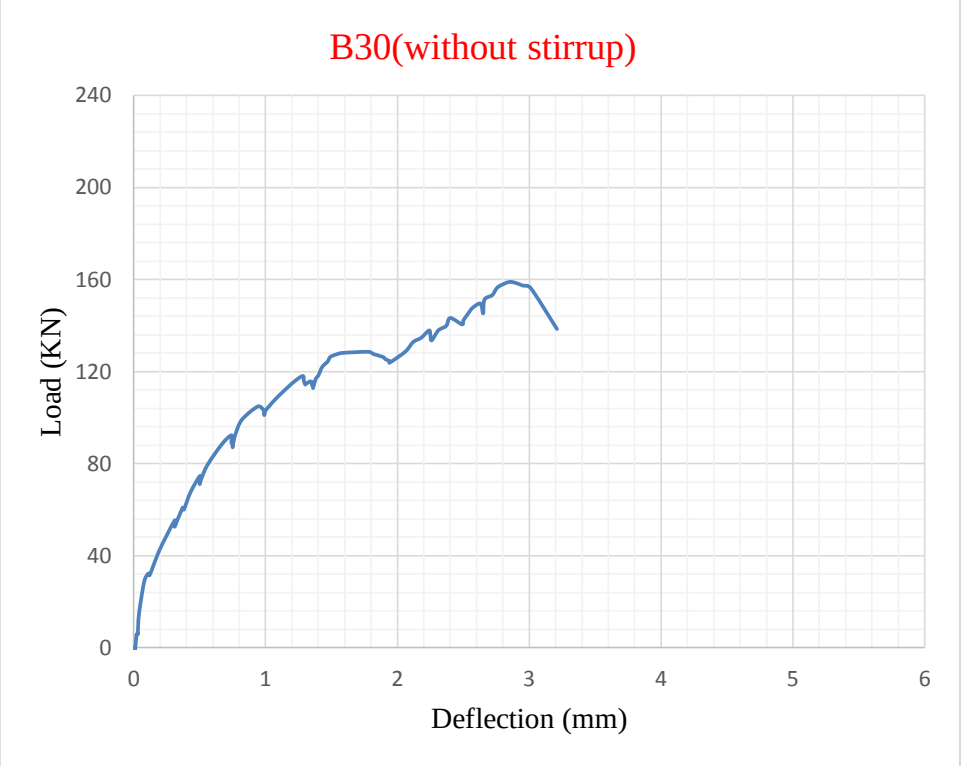

Figure 5-9: Load-Deflection response of B30 (without shear reinforcement)

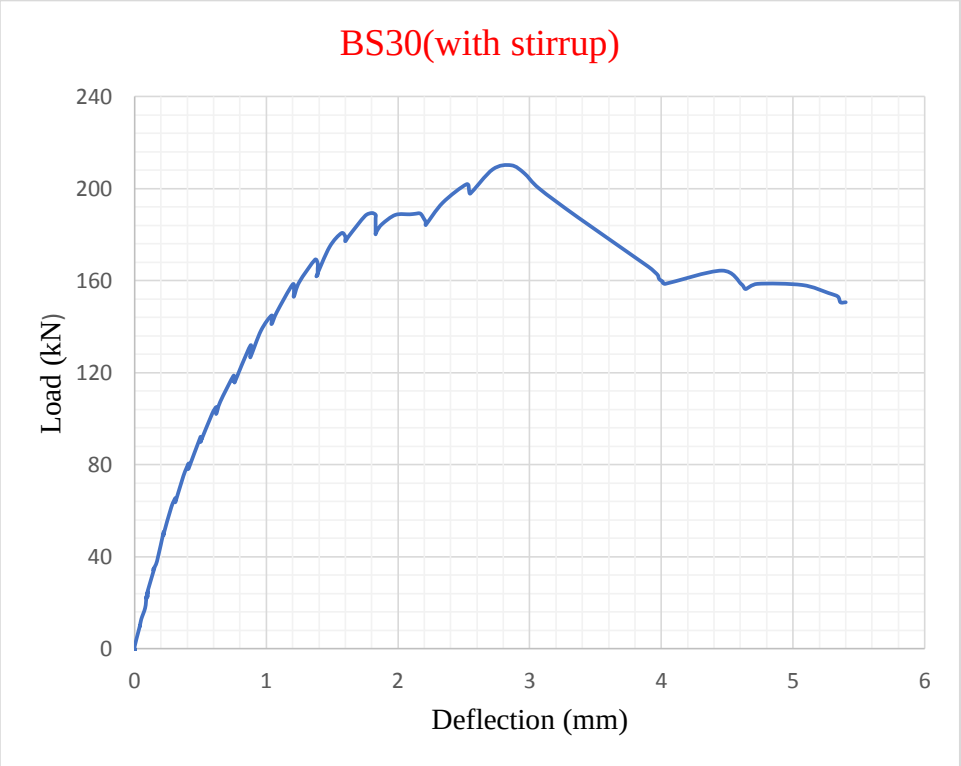

Figure 5-10: Load-Deflection response of BS30 (with shear reinforcement)

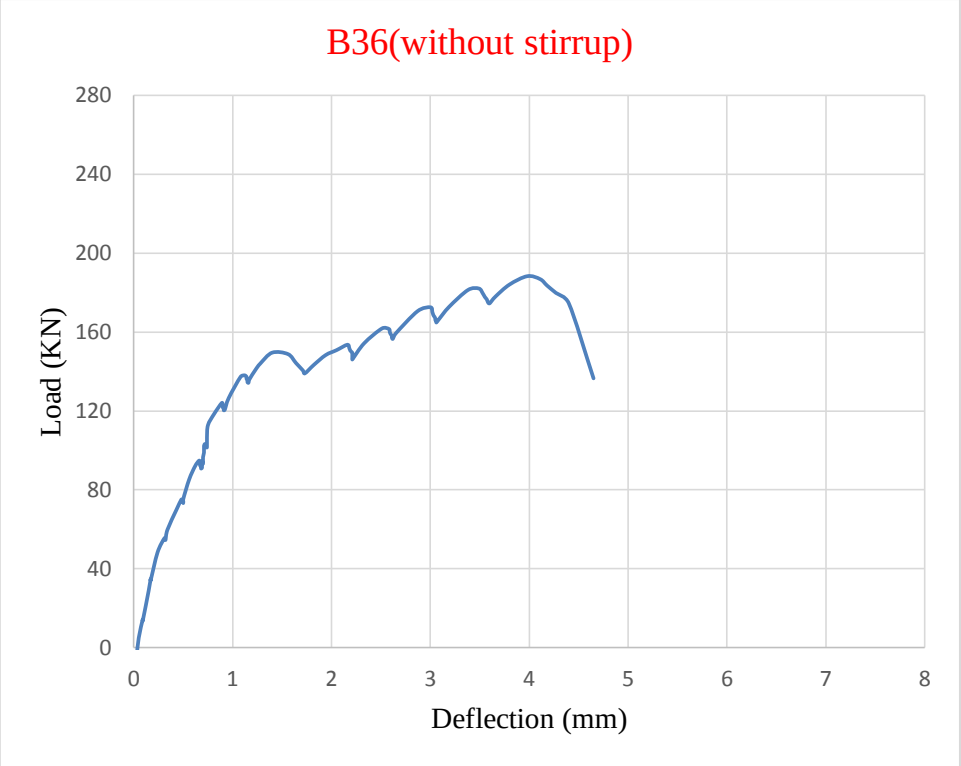

Figure 5-11: Load-Deflection response of B36 (without shear reinforcement)

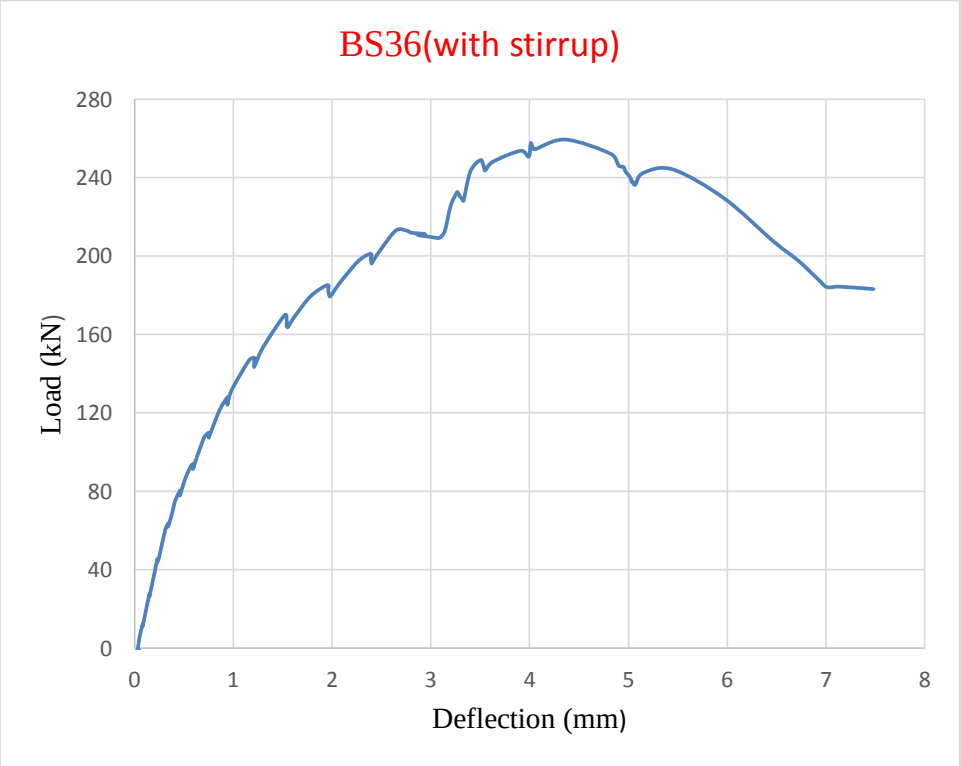

Figure 5-12: Load-Deflection response of BS36 (with shear reinforcement)

5.3 VecTor2 Analysis Results

A total of 12 reinforced concrete beams are analyzed. The loading is applied through prescribed displacement at the loading points to capture the failure load and post-peak response. As expected, all beam specimens failed in shear. The overall responses of the specimens with and without shear reinforcement are different. for beams without shear reinforcement the load deflection response shows that the beam stiffness reduces considerably after developing the first diagonal crack. This stiffness degradation decreases for beams with shear reinforcement.

Table 5-2: VecTor2 analyses result for beams of B series and BS series

Specimen	H (mm)	D (mm)	ρ_{shear} (%)	P_{crack} (KN)	V_{crack} (KN)	$P_{Ultmate}$ (KN)	$V_{Ultimate}$ (KN)	Deflection at failure Δ_{Ult} (mm)
B24	240	201	-	111.07	55.54	141.97	70.98	2.0
B30	300	259	-	138.52	66.32	178.16	89.08	2.49
B36	360	319	-	146.51	73.25	195.85	97.92	3.50
B60	600	557	-	226.10	113.05	293.88	146.94	5.99
B90	900	855	-	291.09	145.54	339.16	169.58	8.47
B120	1200	1153	-	311.48	155.74	340.55	170.275	10.74
BS24	240	201	0.14	159.16	79.58	195.36	97.68	2.24
BS30	300	259	0.14	184.61	92.30	236.56	118.28	2.99
BS36	360	319	0.14	221.12	110.56	290.43	145.22	4.0
BS60	600	557	0.14	337.67	168.84	421.09	210.54	6.75
BS90	900	855	0.14	423.01	211.51	536.06	268.03	9.74
BS120	1200	1153	0.14	480.69	240.34	573.50	286.75	12.48

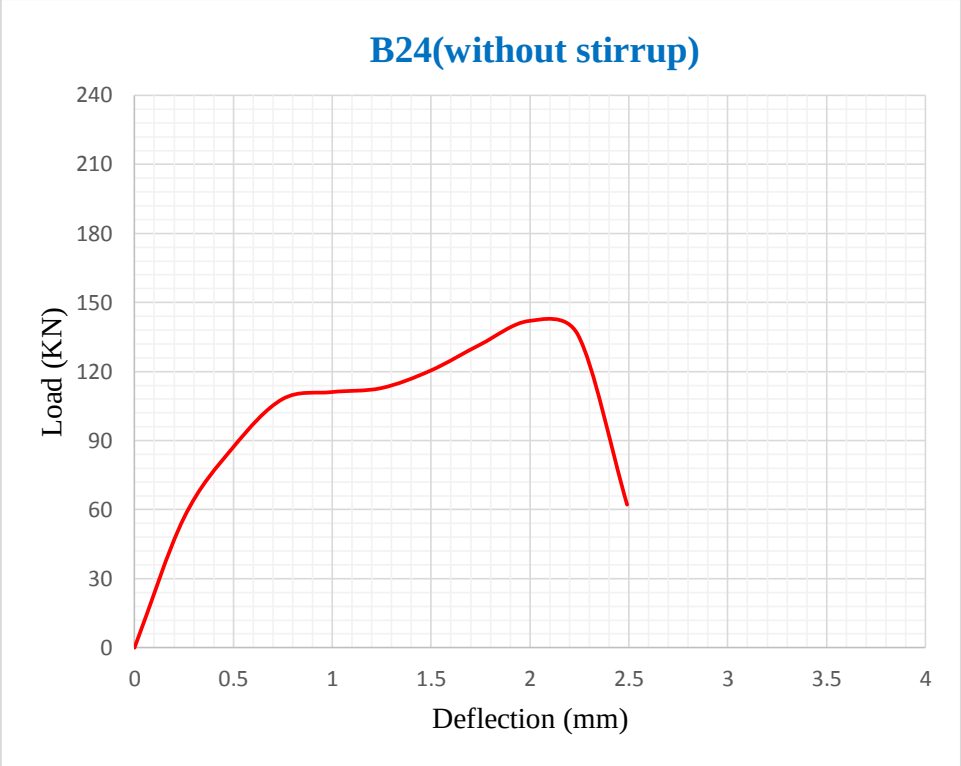

Figure 5-13: Load-Deflection response of B24 (without shear reinforcement)

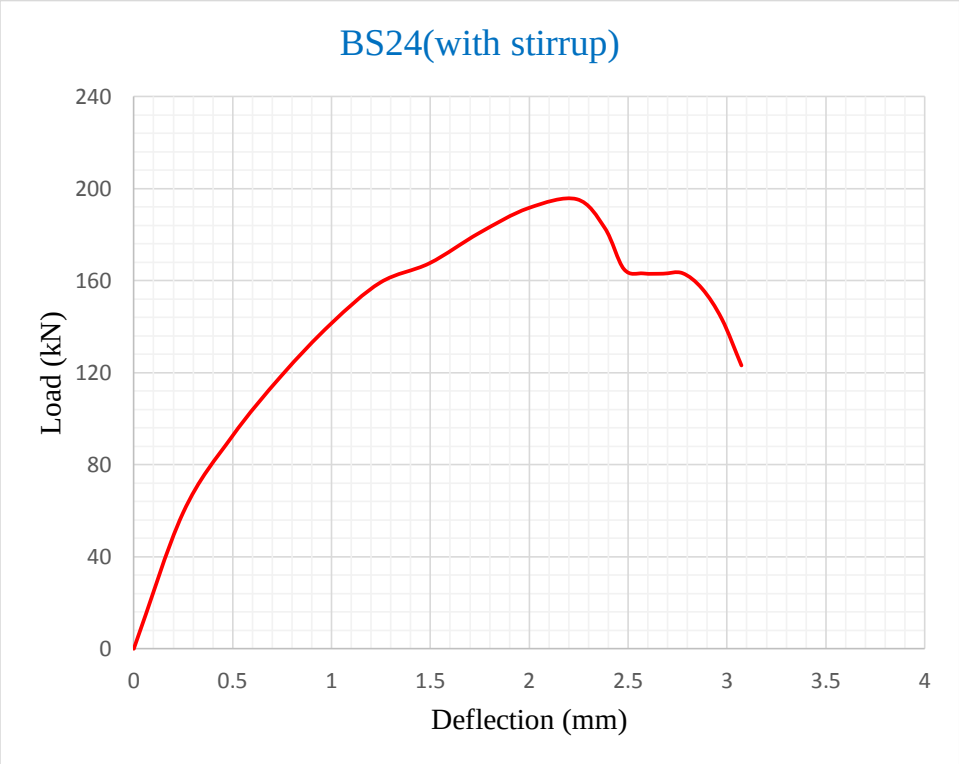

Figure 5-14: Load-Deflection response of BS24 (with shear reinforcement)

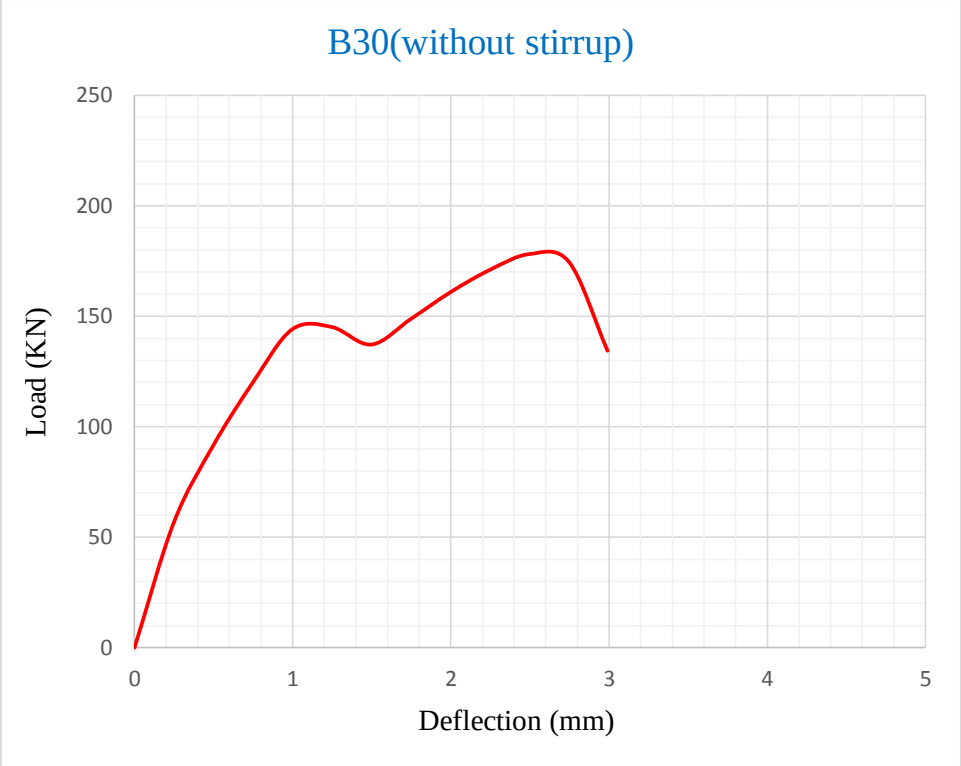

Figure 5-15: Load-Deflection response of B30 (without shear reinforcement)

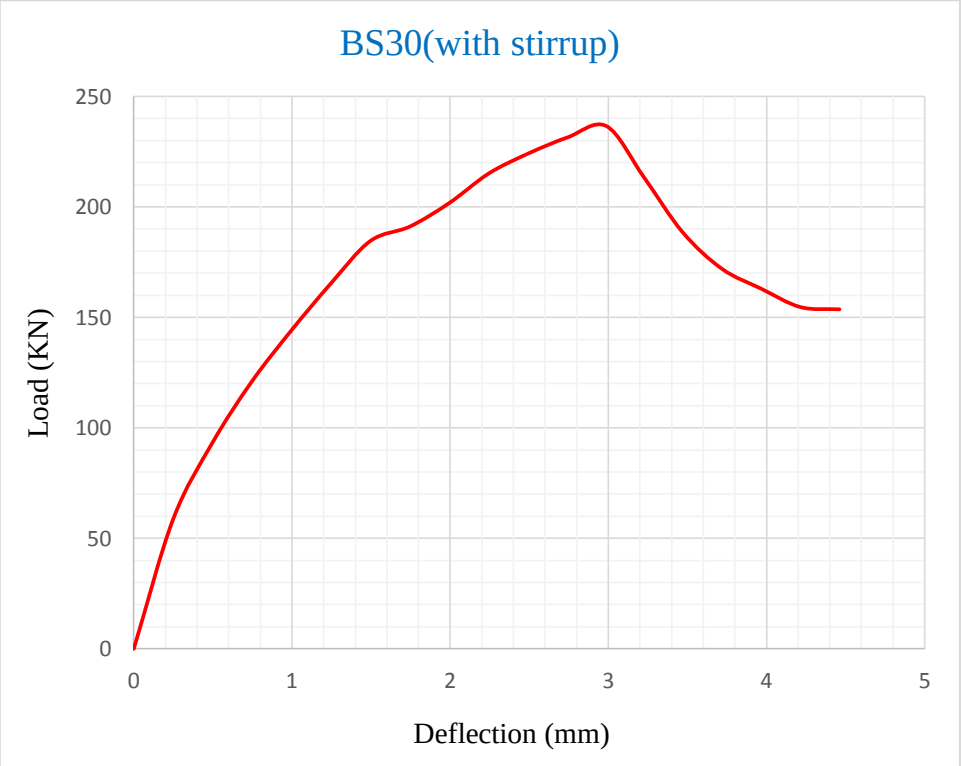

Figure 5-16: Load-Deflection response of BS30 (with shear reinforcement)

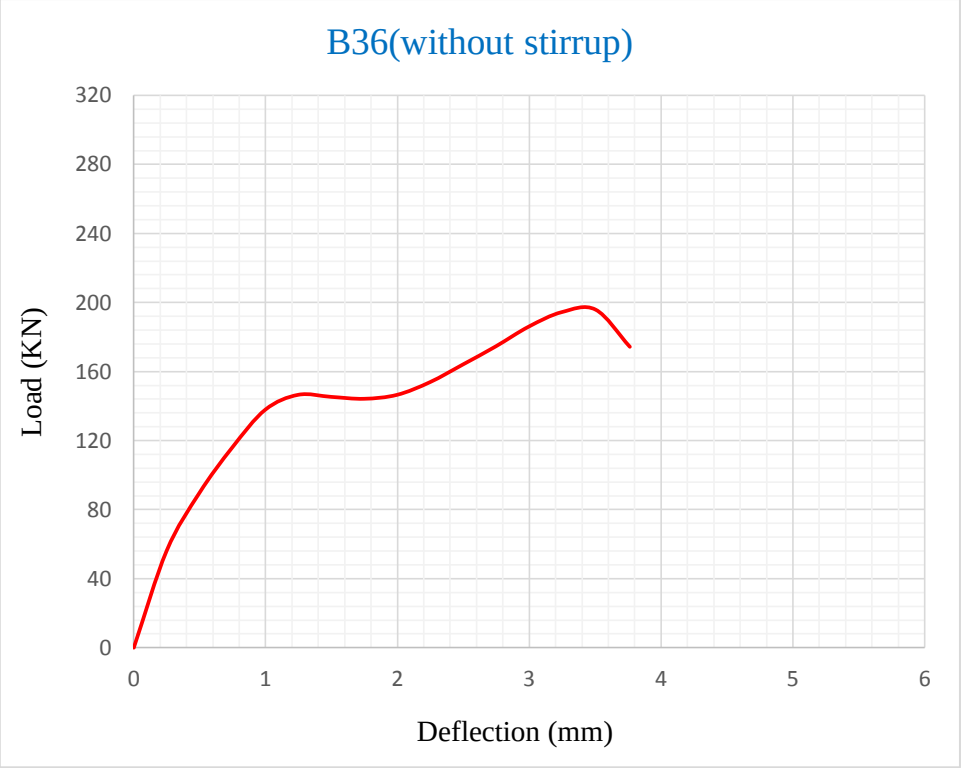

Figure 5-17: Load-Deflection response of B36 (without shear reinforcement)

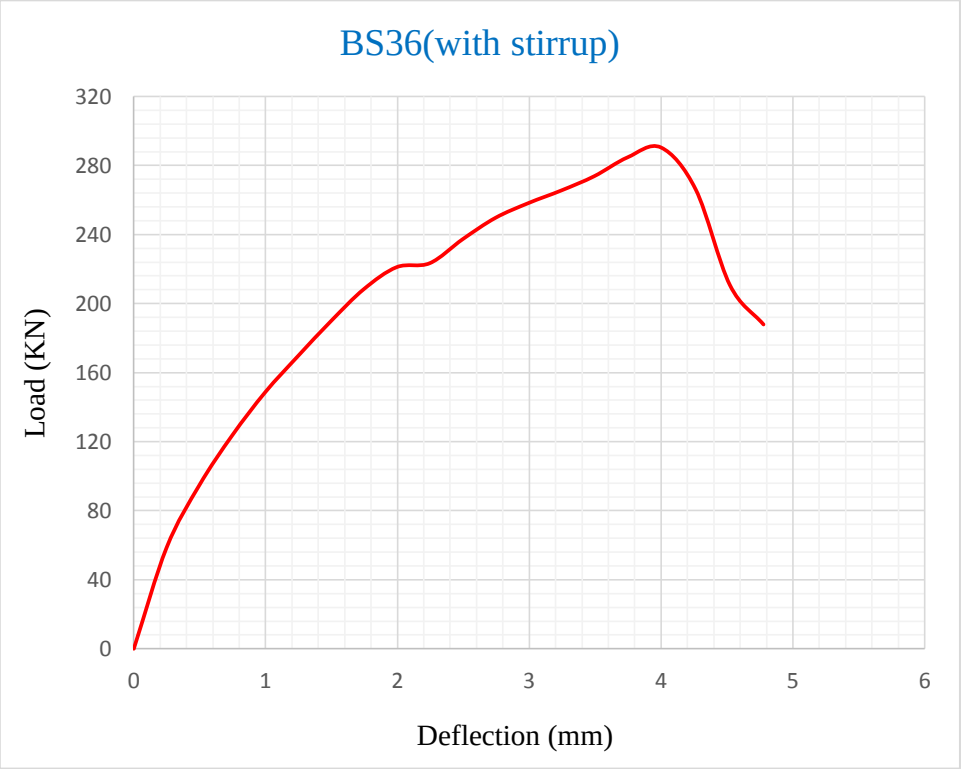

Figure 5-18: Load-Deflection response of BS36 (with shear reinforcement)

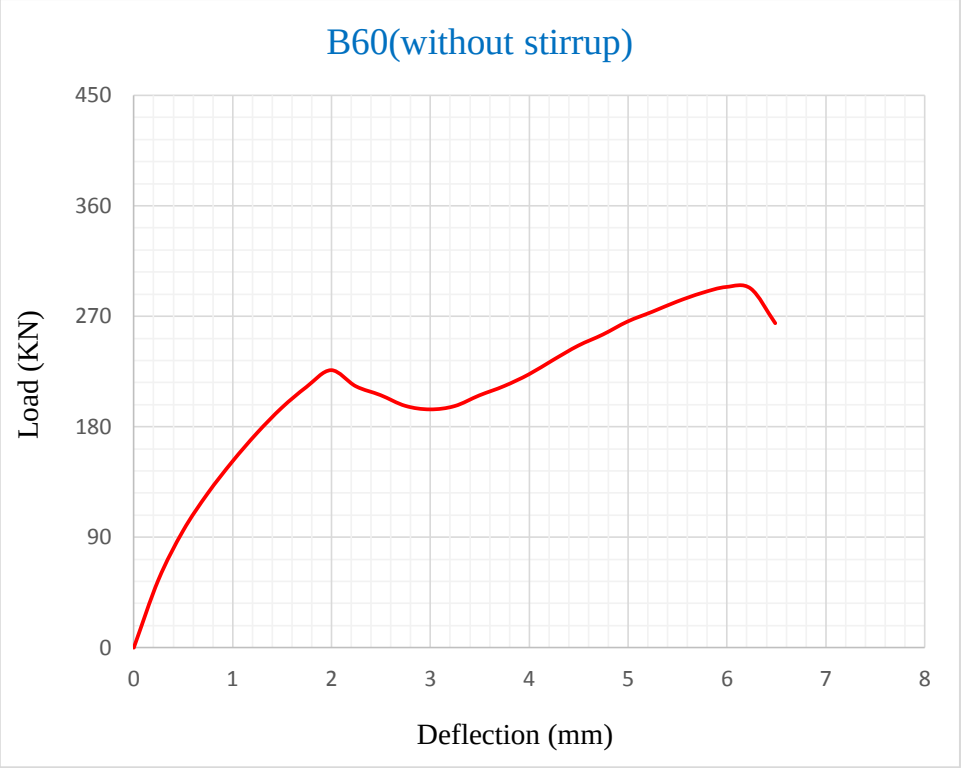

Figure 5-19: Load-Deflection response of B60 (without shear reinforcement)

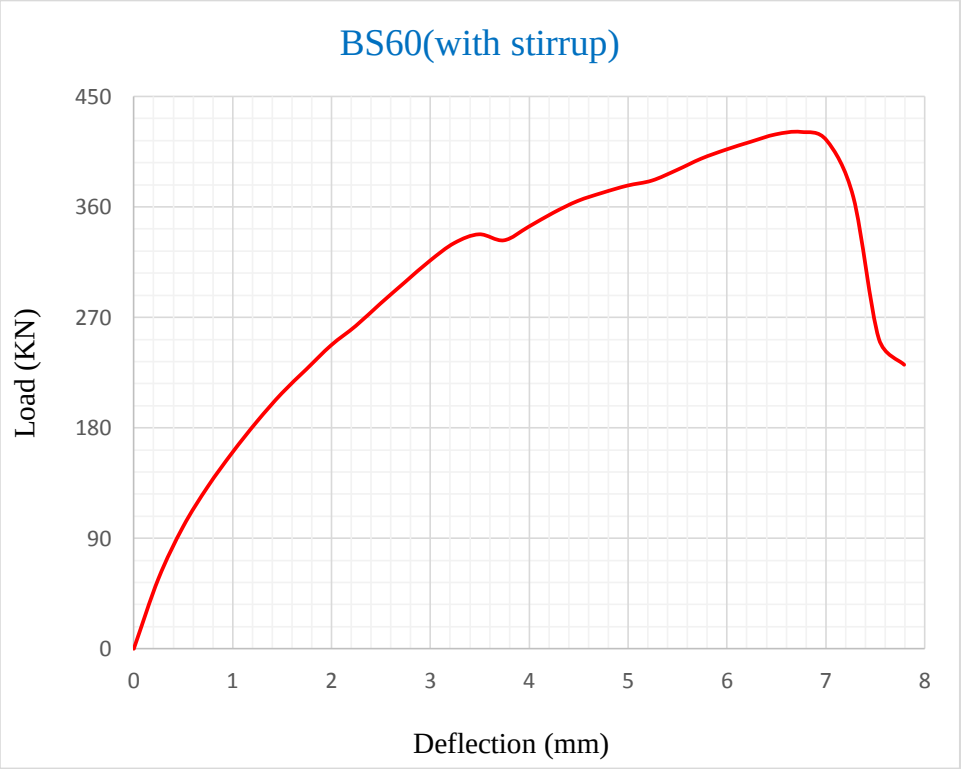

Figure 5-20: Load-Deflection response of BS60 (with shear reinforcement)

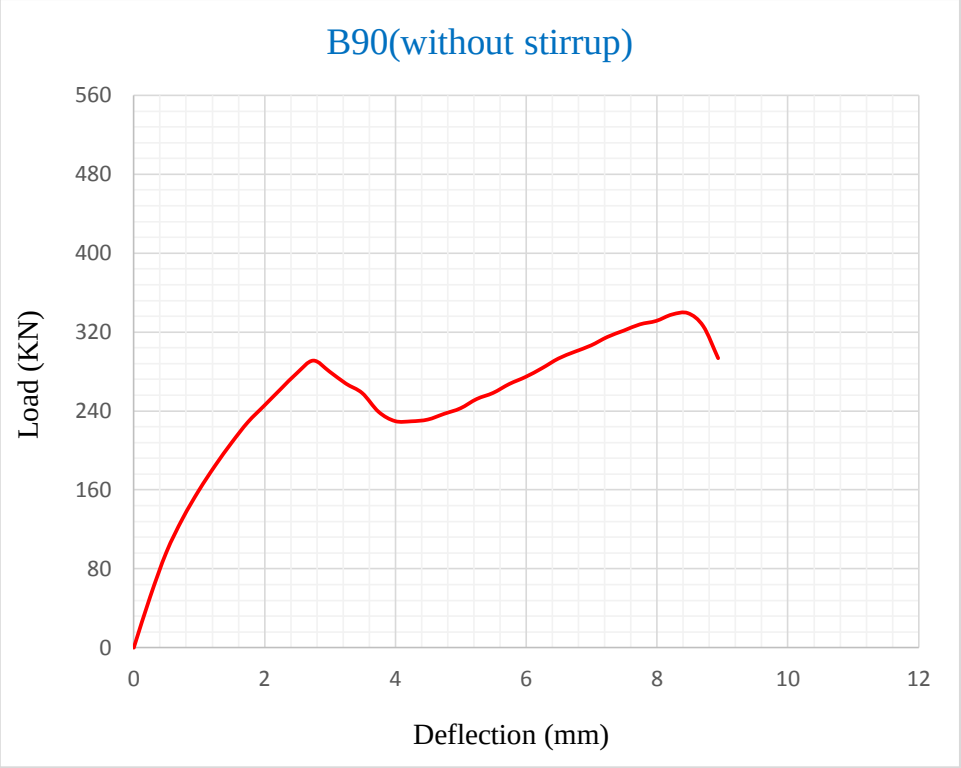

Figure 5-21: Load-Deflection response of B90 (without shear reinforcement)

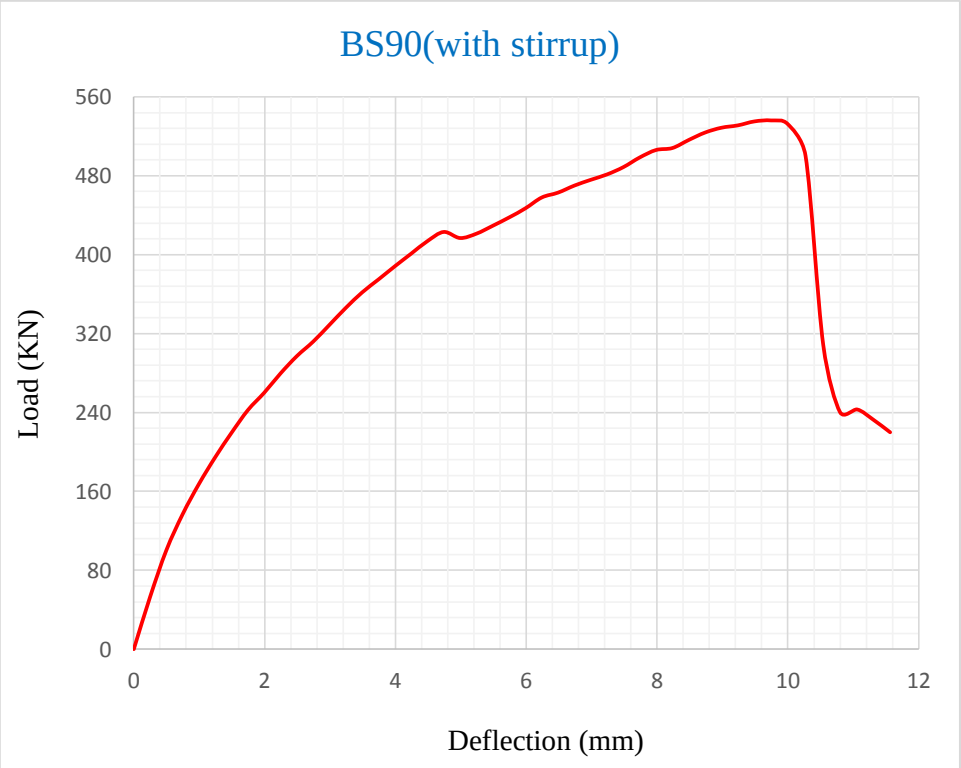

Figure 5-22: Load-Deflection response of BS90 (with shear reinforcement)

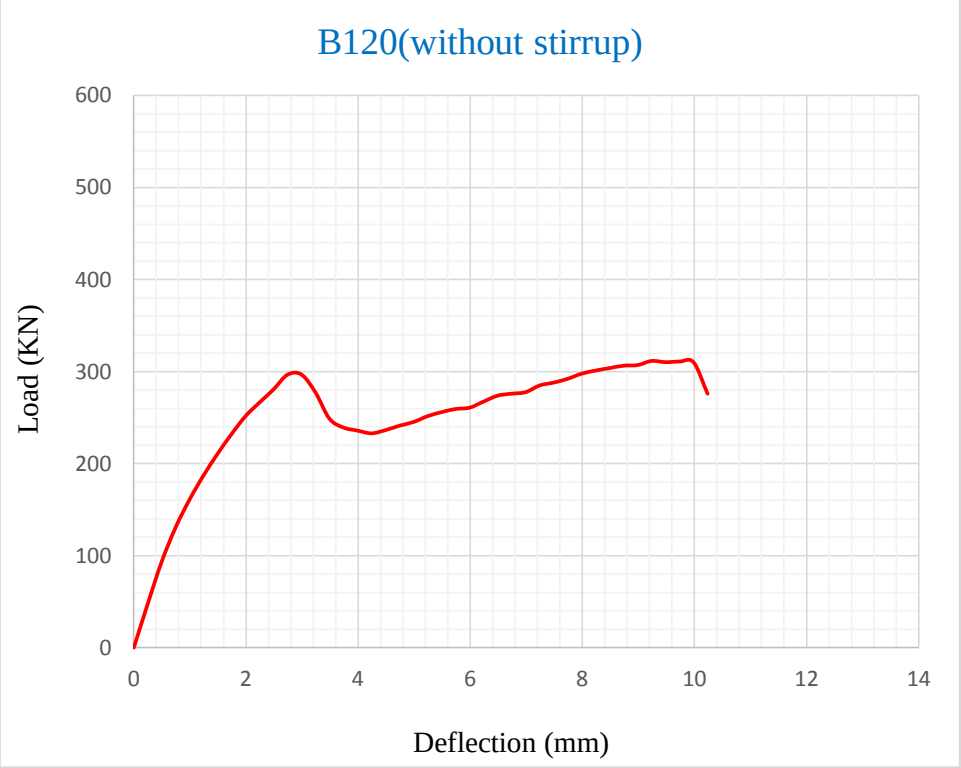

Figure 5-23: Load-Deflection response of B120 (without shear reinforcement)

Figure 5-24: Load-Deflection response of BS120 (with shear reinforcement)

5.4 VecTor2 Model Validation

Concrete and other quasi-brittle materials exhibit strain softening in the post-peak response in tension and compression. Due to this strain softening effect, finite element modeling results are sensitive to mesh size. Therefore, to minimize effect of element size, in finite element modeling, best mesh sizes should be chosen based the height of the specimens (Ismail, K.S. 2016).

To examine the effect of element size on global behavior, different element sizes were considered. It can be seen that for beam B24 and BS24, with an overall depth of 240mm, the element size on direction of y-axis is 8mm, for beam B30 and BS30, with an overall depth of 300mm, the element size on the direction of y-axis is 10mm, and for beam B36 and BS36, with an overall depth of 360mm, the element size on the direction of y-axis is 12mm, which is equal to 3.3% of the height of the specimens is in better agreement with the experimental results. The result from all six reinforced concrete beams showed that using an element size based the height of the specimens is in good agreement with the experimental results. In this study mesh sizes are 3.3 % of the height of the specimens.

Fairly accurate estimates were made by VecTor2 nonlinear finite element software for twelve beam specimens starting from 240mm up to 1200mm depth. The Figure below compares the load-deflection curve of six reinforced concrete beams obtained from the experimental test with the load-deflection curve analyzed by VecTor2. As can be seen, the results show an overall good agreement with the experimental data.

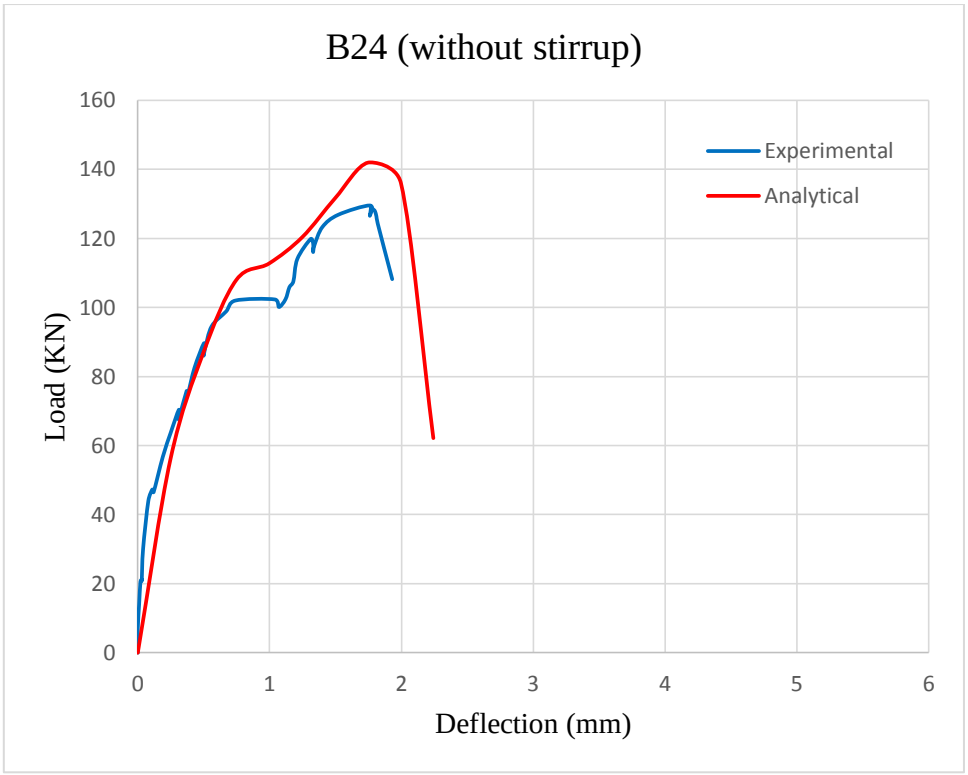

Figure 5-25: Experimental and Analytical Load-deflection comparison for B24

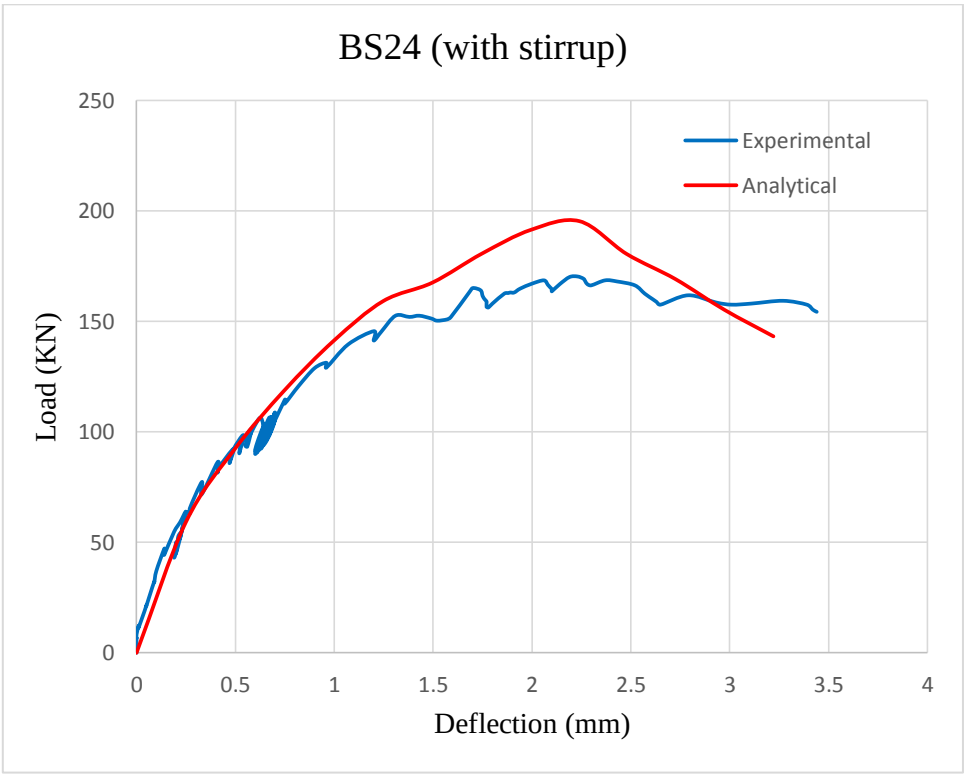

Figure 5-26: Experimental and Analytical Load-deflection comparison for BS24

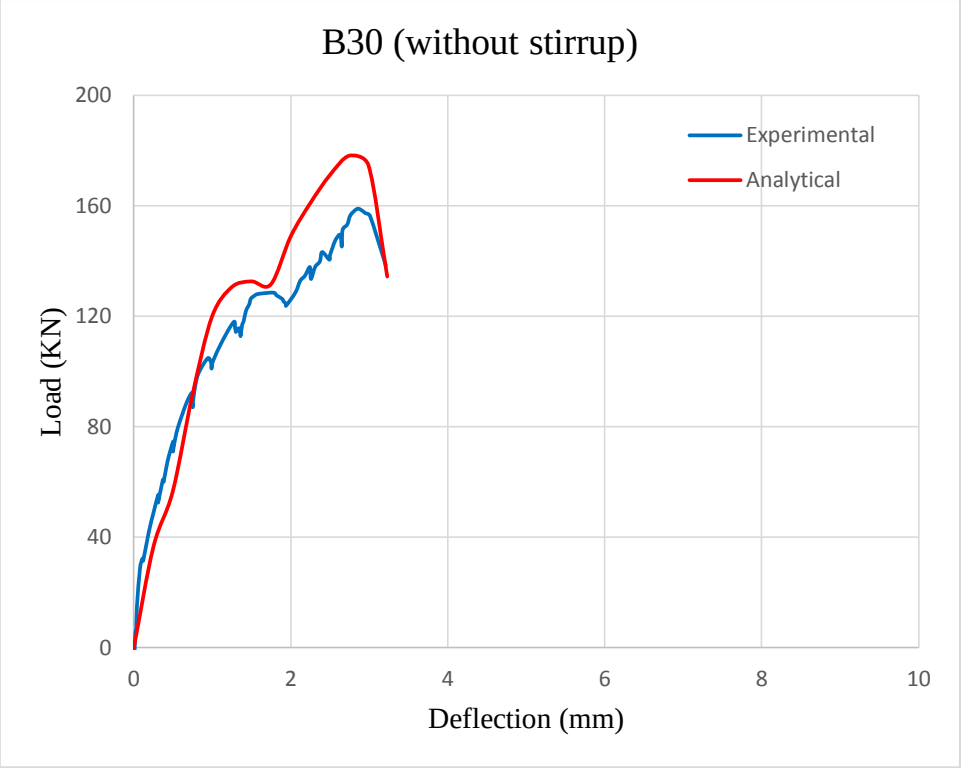

Figure 5-27: Experimental and Analytical Load-deflection comparison for B30

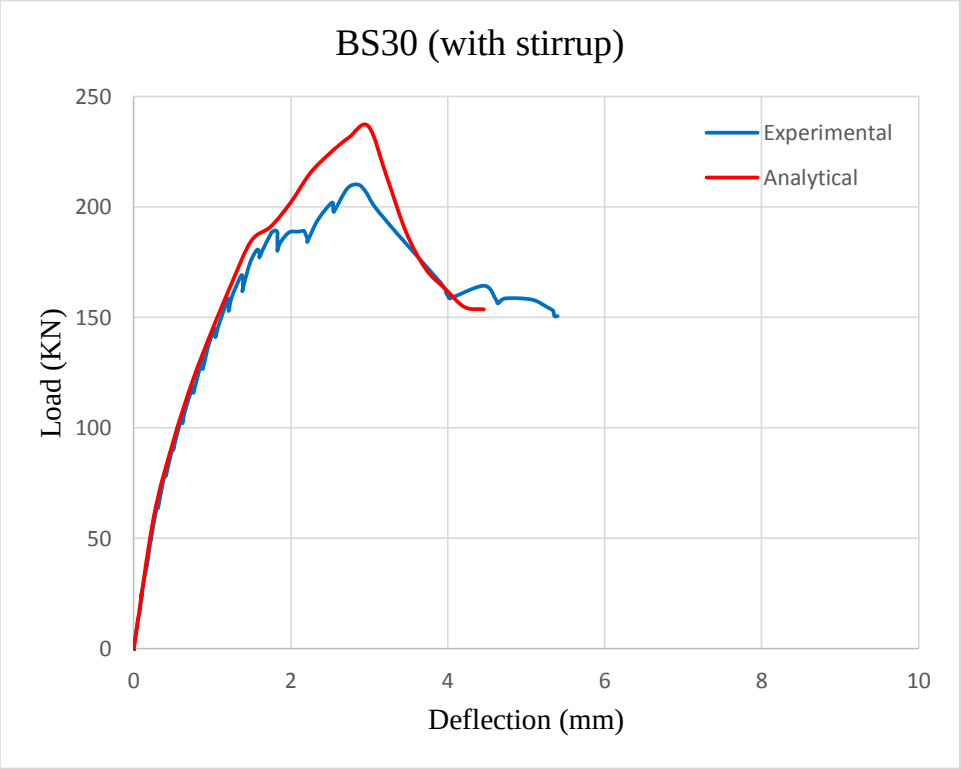

Figure 5-28: Experimental and Analytical Load-deflection comparison for BS30

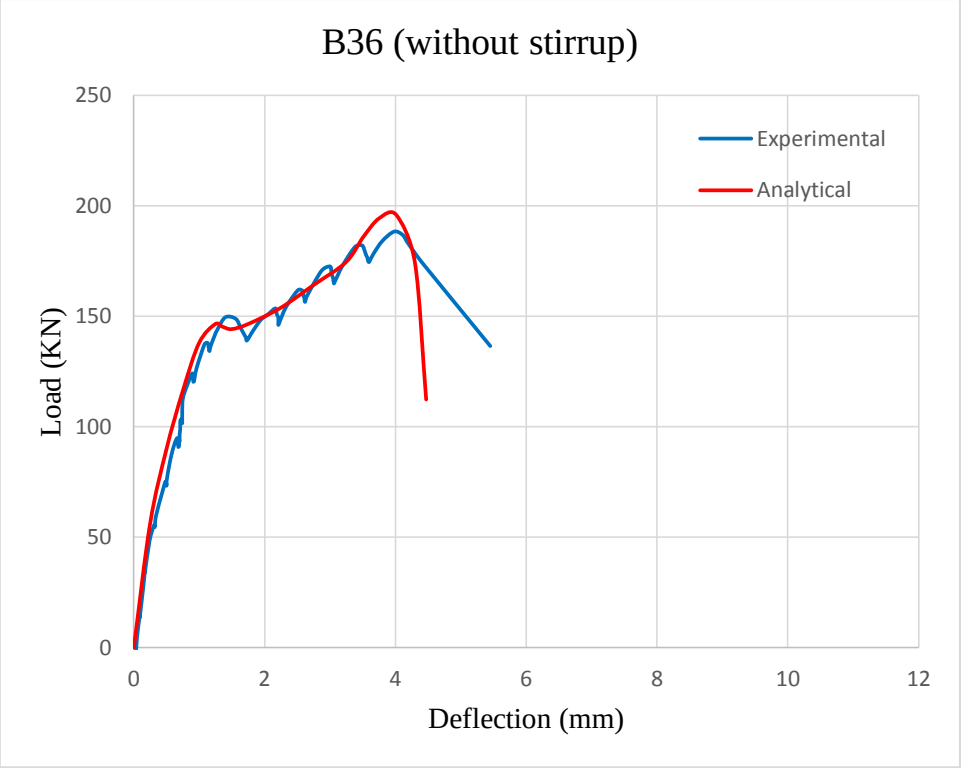

Figure 5-29: Experimental and Analytical Load-deflection comparison for B36

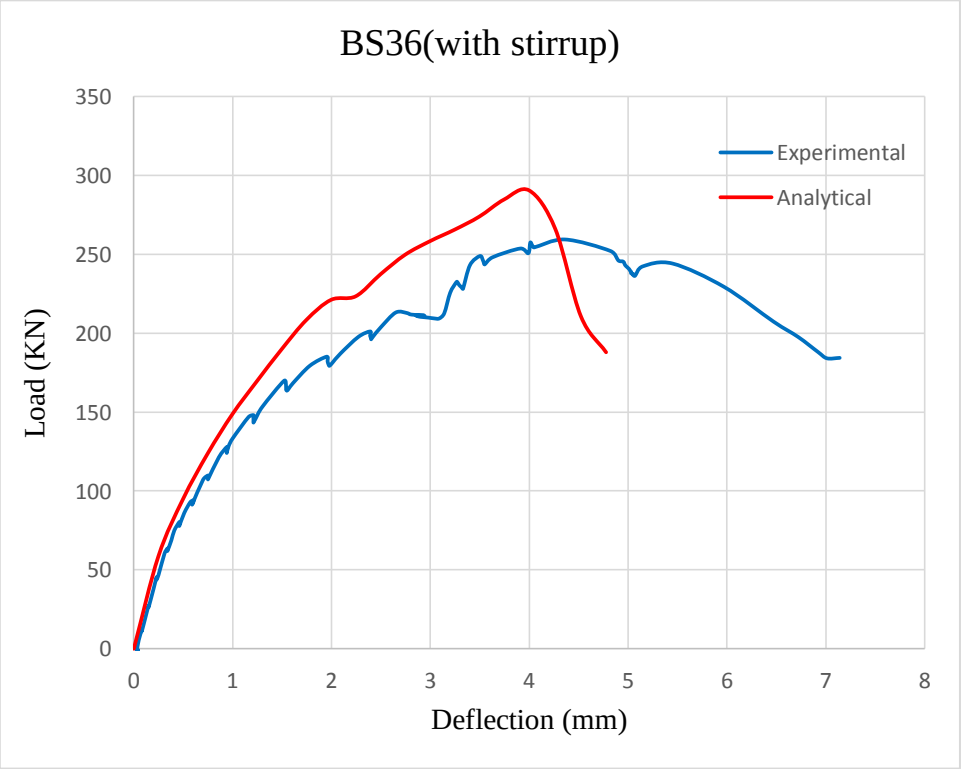

Figure 5-30: Experimental and Analytical Load-deflection comparison for BS36

The Figures below compare the load-deflection curve of large size beam obtained from the experimental test done by of Robert J. Frosch (2000) with the load-deflection curve analyzed by VecTor2. As can be seen, the results show an overall good agreement with the experimental data. An overall beam depth of 36 in. (914.4mm) was selected because ACI code requires face reinforcement for beams larger than 36 in. effective depth. **Conversion**s: 1 lb. = 4.45N, 1 in =25.4 mm, 1 psi = 0.00689 MPa

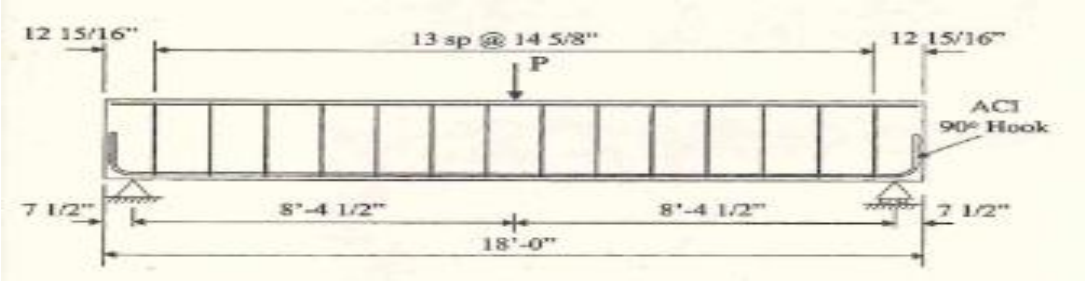

Figure 5-31: loading system of Robert J. Frosch (2000) specimen 2

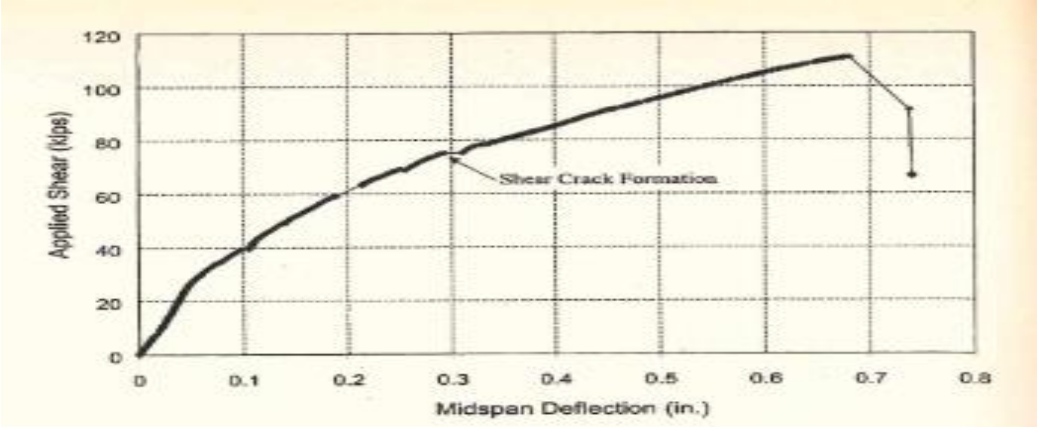

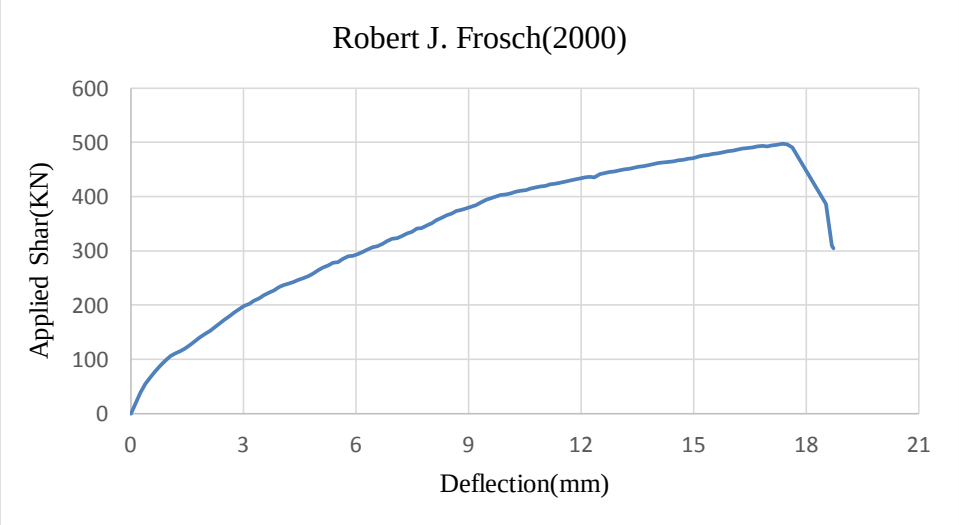

Figure 5-32: Robert J. Frosch (2000) specimen 2 load versus midspan deflection

5.5 Prediction of Beam's Shear Strength Using Design Codes

There are numerous building design codes in the world to predict the shear capacity of RC beams, too many to cover in this thesis. What is common at the end of the day they all rely on calibration against empirical data. The most used shear design procedures for RC members with and without shear reinforcement (Eurocode 2 (EC2), ACI 318-14 and ACI 318-19) are evaluated in this section to assess their effectiveness and identify their weaknesses in the discussion part later.

5.5.1 Eurocode 2 (2004)

5.5.1.1 Beams without Shear Reinforcement

Eurocode 2 provides an empirical equation to predict the ultimate shear strength of RC beams without shear reinforcement. This equation accounts for the effect of concrete compressive strength, flexural reinforcement and size effect.

$$V_{Rd,c} = [C_{Rd,c}k(100\rho_l f_{ck})^{1/3} + k_1\sigma_{cp}]b_w d \geq V_{Rd,c,min} \quad [KN] \qquad (5\text{-}2)$$

Table 5-3: Concrete shear capacity of beams without shear reinforcement

Specimen	$C_{Rd,c}$	K	ρ (%)	f_{cm} (Mpa)	b_w (mm)	d (mm)	$V_{Rd,c}$ (KN)
B24	0.12	1.997	2.00	26.55	200	201	36.21
B30	0.12	1.879	1.99	27.66	200	259	44.43
B36	0.12	1.792	1.97	27.81	200	319	52.11
B60	0.12	1.599	2.00	26.82	200	557	80.61
B90	0.12	1.484	2.00	26.82	200	855	114.84
B120	0.12	1.416	2.00	26.82	200	1153	147.77

5.5.1.2 Beams with Shear Reinforcement

The EC2 shear design procedure for the members with shear reinforcement is based on the plasticity theory and the truss model. This model accounts for the effect of transverse steel reinforcement and strut inclination with respect to the member's neutral axis.

$$V_{Rd} = V_{Rd,c} + V_{Rd,s} \quad [KN] \qquad (5\text{-}3)$$

$$V_{Rd,s} = \frac{A_{sw}}{s} z f_{ywd} (\cot\theta + \cot\alpha)\sin\alpha \quad [KN] \qquad (5\text{-}4)$$

For this thesis θ = 45º and α = 90º since shear reinforcement is perpendicular to bottom longitudinal tension reinforcement.

Table 5-4: Concrete shear capacity of beams with shear reinforcement

Specimen	$C_{Rd,c}$	B(mm)	D(mm)	K	A_{st}	ρ (%)	f_{cm} (Mpa)	$V_{Rd,c}$ (KN)
BS24	0.12	200	201	1.997	804.25	2.00	26.83	36.34
BS30	0.12	200	259	1.879	1030.44	1.99	25.64	43.32
BS36	0.12	200	319	1.792	1256.64	1.97	26.42	51.22
BS60	0.12	200	557	1.599	2228.00	2.00	26.82	80.61
BS90	0.12	200	855	1.484	3420.00	2.00	26.82	114.84
BS120	0.12	200	1153	1.416	4612.00	2.00	26.82	147.77

Table 5-5: Total shear capacity of beam specimens based on Eurocode 2

Specimens	A_v (mm^2)	Z=0.9d (mm)	f_{yd} (MPa)	S (mm)	V_s (KN)	V_c (KN)	$V=V_c+V_s$ (KN)
B24	-	180.9	-	-	-	36.21	36.21
B30	-	233.1	-	-	-	44.43	44.43
B36	-	287.1	-	-	-	52.11	52.11
B60	-	501.3	-	-	-	80.61	80.61
B90	-	769.5	-	-	-	114.84	114.84
B120	-	1037.7	-	-	-	147.77	147.77
BS24	56.55	180.9	366.29	200	18.73	36.34	55.07
BS30	56.55	233.1	366.29	200	24.14	43.32	67.46
BS36	56.55	287.1	366.29	200	29.73	51.22	80.95
BS60	56.55	501.3	366.29	200	51.91	80.61	132.52
BS90	56.55	769.5	366.29	200	79.69	114.84	194.53
BS120	56.55	1037.7	366.29	200	107.47	147.77	255.24

5.5.2 ACI 318-14 Code

ACI 318-14 provides simple equations to calculate the shear strength at first diagonal crack of reinforced concrete beams based on the concept of average shear stress acting on the full effective cross section.

$$Vn = Vc + Vs \quad \textbf{(5-5)}$$

In a member without shear reinforcement, the shear strength is carried by the concrete web of the member and can be calculated using:

$$\mathbf{V_c = (0.158\sqrt{f'_c} + 17.2\rho_w\frac{Vd}{M})b_w d \quad [KN]} \qquad \mathbf{(5\text{-}6)}$$

For the sake of simplicity, ACI 318-14 allows the replacement of the second term of the above equation with $0.01\sqrt{fc'}$ leading to simplified equation which only accounts for the effect of concrete compressive strength.

$$\mathbf{V_c = (0.17\sqrt{f'_c})b_w d \quad [KN]} \qquad \mathbf{(5\text{-}7)}$$

In a member with shear reinforcement a part of the applied shear force is carried by the concrete web and the remaining is carried by the shear reinforcement, which is based on the truss analogy, is used to calculate the contribution of shear reinforcement to the overall shear capacity of the RC members.

$$\mathbf{V_s = \frac{A_v f_{yt} d}{S} \quad [KN]} \qquad \mathbf{(5\text{-}8)}$$

Table 5-6: Total shear capacity of beam specimens based on ACI 318-14

Specimens	f'_C (MPa)	b_W (mm)	D (mm)	V_c (KN)	A_V (mm^2)	f_{yt} (Mpa)	V_S (KN)	$V= V_c+ V_S$ (KN)
B24	26.55	200	201	35.21	-	-	-	35.21
B30	27.66	200	259	46.31	-	-	-	46.31
B36	27.81	200	319	57.20	-	-	-	57.20
B60	26.82	200	557	98.08	-	-	-	98.08
B90	26.82	200	855	150.55	-	-	-	150.55
B120	26.82	200	1153	203.02	-	-	-	203.02
BS24	26.83	200	201	35.40	56.55	366.29	20.82	56.22
BS30	25.64	200	259	44.59	56.55	366.29	26.82	71.41
BS36	26.42	200	319	55.75	56.55	366.29	33.04	88.79
BS60	26.82	200	557	98.08	56.55	366.29	57.69	155.77
BS90	26.82	200	855	150.55	56.55	366.29	88.55	239.10
BS120	26.82	200	1153	203.02	56.55	366.29	119.41	322.43

5.5.3 ACI 318-19 Code

Relationship in ACI 318-14 for calculating the concrete contribution to shear resistance (Vc) in reinforced concrete members have been replaced in ACI 318-19 by one general relationship that considers the combined effects of member depth and percentage of longitudinal reinforcement (Daniel A. et.al 2019). This new relationship is:

$$\mathbf{V_c = [8\lambda_s\,\lambda(\rho_w)^{1/3}\sqrt{f'c} + \frac{N}{6Ag}]b_w d} \quad \textbf{(5-9)}$$

Since there is no axial force for this case N=0 the equation will reduce to

$$\mathbf{V_c = [8\lambda_s\,\lambda(\rho_w)^{1/3}\sqrt{f'c}\,]b_w d} \quad \textbf{(5-10)}$$

Notes: The above equation is in U.S. customary units: lb., inch and psi

Conversions: 1 lb. = 4.45N

1 in =25.4 mm

1 psi = 0.00689 MPa

Table 5-7: Concrete shear capacity of beams without shear reinforcement

Specimens	λ_s	ρ_w (%)	f_c(psi)	b_w(in)	d(in)	V_c(lb.)	V_c (KN)
B24	1.057	2.00	3853.41	7.87	7.91	8855.99	39.41
B30	0.995	1.99	4014.51	7.87	10.20	10971.66	48.82
B36	0.941	1.97	4036.28	7.87	12.56	12763.99	56.80
B60	0.791	2.00	3892.60	7.87	21.93	18465.63	82.17
B90	0.677	2.00	3892.60	7.87	33.66	24257.82	107.95
B120	0.601	2.00	3892.60	7.87	45.39	29039.13	129.22

Table 5-8: Concrete shear capacity of beams with shear reinforcement

Specimens	λ_s	ρ_w (%)	f_c(psi)	b_w(in)	d(in)	V_c(lb.)	V_c (KN)
BS24	1.057	2.00	3894.05	7.87	7.91	8901.64	39.61
BS30	0.995	1.99	3721.34	7.87	10.20	10563.00	47.00
BS36	0.941	1.97	3834.34	7.87	12.56	12440.52	55.36
BS60	0.791	2.00	3892.60	7.87	21.93	18465.63	82.17
BS90	0.677	2.00	3892.60	7.87	33.66	24257.82	107.95
BS120	0.601	2.00	3892.60	7.87	45.39	29039.13	129.22

$$Vn = Vc + Vs \quad \textbf{(5-11)}$$

$$\mathbf{V_s = \frac{A_v f_{yt} d}{s}} \quad \textbf{(5-12)}$$

Table 5-9: Total shear capacity of beam specimens based on ACI 318-19

Specimens	f'c (MPa)	Bw (mm)	D (mm)	Vc (KN)	Av (mm2)	*f*yt (Mpa)	Vs (KN)	V= Vc+ Vs (KN)
B24	26.55	200	201	39.41	-	-	-	39.41
B30	27.66	200	259	48.82	-	-	-	48.82
B36	27.81	200	319	56.80	-	-	-	56.80
B60	26.82	200	557	82.17	-	-	-	82.17
B90	26.82	200	855	107.95	-	-	-	107.95
B120	26.82	200	1153	129.22	-	-	-	129.22
BS24	26.83	200	201	39.61	56.55	366.29	20.82	60.43
BS30	25.64	200	259	47.00	56.55	366.29	26.82	73.82
BS36	26.42	200	319	55.36	56.55	366.29	33.04	88.40
BS60	26.82	200	557	82.17	56.55	366.29	57.69	139.86
BS90	26.82	200	855	107.95	56.55	366.29	88.55	196.50
BS120	26.82	200	1153	129.22	56.55	366.29	119.41	248.63

5.6 Discussion

5.6.1 Size Effect on Beam Shear Strength

5.6.1.1 B-series (without shear reinforcement)

Table 5-10 below summarizes the experimental and analytical results for reinforced concrete beam without shear reinforcement series giving effective depth, concrete compressive strength, longitudinal reinforcement ratio, ultimate shear force and ultimate shear stress capacity. Values given in this table include member self-weight.

Table 5-10: Failure shear stress for beams not containing shear reinforcement

Specimens	D (mm)	f'_C (MPa)	$\rho_{longitudinal}$ (%)	ρ_{shear} (%)	V_{exp} (KN)	$V_{VecTor2}$ (KN)	τ_{exp} (MPa)	$\tau_{VecTor2}$ (MPa)
B24	201	26.55	2.00	-	65.14	70.98	1.62	1.77
B30	259	27.66	1.99	-	79.66	89.08	1.54	1.72
B36	319	27.81	1.97	-	94.10	97.92	1.47	1.53
B60	557	26.82	2.00	-	-	146.94	-	1.32
B90	855	26.82	2.00	-	-	169.58	-	0.99
B120	1153	26.82	2.00	-	-	170.28	-	0.74

The ultimate shear capacities (V_{ult}) for the beams without shear reinforcement were normalized with respect to beam width and effective depth (bd). This relationship between the normalized shear capacity and the beam height is shown in figure 5-33 below. It shows that the size effect on shear strength of reinforced concrete beams without shear reinforcement is evident.

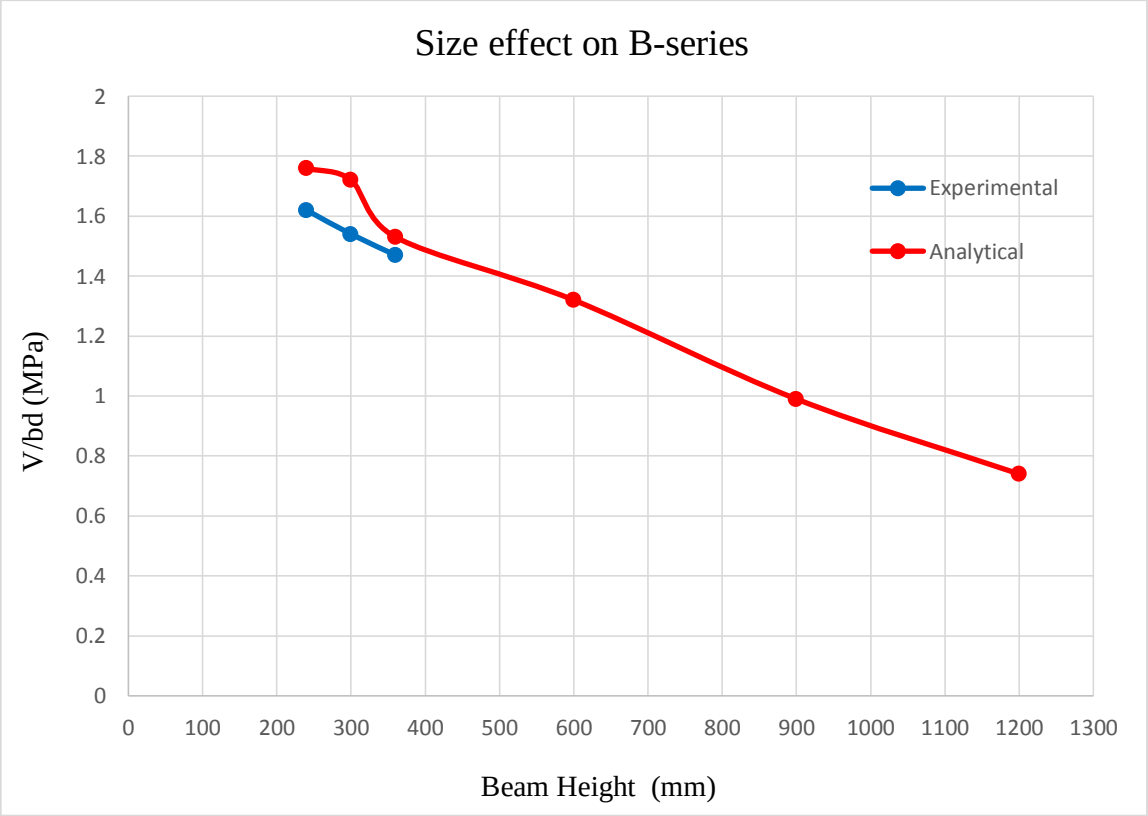

Figure 5-33: Shear stress capacity Vs effective depth of beams without stirrup

The above figure shows the experimental shear capacity result at failure for the three beam specimens and analytical shear stress result at failure for the six beam specimens in B-series (beams without shear reinforcement). It shows that the size effect occurred on both experimentally tested three specimens and numerically analyzed six specimens. Experimental result on table 5-10 indicate that the ultimate shear stress capacity decreased from τ = 1.62 MPa in B24 (H=240mm) and τ = 1.54 MPa in B30 (H=300mm) down to τ = 1.47 MPa in B36 (H=3600mm). As shown in figure 5-33 above experimental results showed that the shear stress capacity decreased by 9.3% when the beam depth scaled up from 240mm to 360mm it indicates that size effect is also exist in small beams.

Results from six reinforced concrete beams without stirrup analyzed by nonlinear finite element software showed that size effect is more significant on large size beams the ultimate shear stress capacity decreased from τ = 1.77 MPa in B24 (H=240mm) down to τ = 0.74 MPa in B120 (H=1200mm) as figure 5-33 shows ultimate shear stress capacity of 1200mm specimen decreased by 58.2% when compared to 240mm height specimen.

In both experimental and analytical results, the larger size beams had lower shear stress at failure than the smaller ones. Even if all specimens in this thesis contained about the same percentage of longitudinal reinforcement and similar material property. The results of beam specimens without shear reinforcement series clearly shows the significant decrease in shear stress at failure that occurs as member size increases.

5.6.1.2 BS-series (with shear reinforcement)

Table 5-11 below summarizes the experimental and analytical results for reinforced concrete beam with shear reinforcement series giving effective depth, concrete compressive strength, longitudinal reinforcement ratio, ultimate shear force and ultimate shear stress capacity. Values given in this table include member self-weight.

Table 5-11: Failure shear stress for beams containing shear reinforcement

Specimens	D (mm)	f'_C (MPa)	$\rho_{longitudinal}$ (%)	ρ_{shear} (%)	V_{exp} (KN)	$V_{VecTor2}$ (KN)	τ_{exp} (MPa)	$\tau_{VecTor2}$ (MPa)
BS24	201	26.55	2.00	0.14	85.03	97.68	2.12	2.43
BS30	259	27.66	1.99	0.14	105.58	118.28	2.03	2.28
BS36	319	27.81	1.97	0.14	130.48	145.22	2.04	2.28
BS60	557	26.82	2.00	0.14	-	210.54	-	1.89
BS90	855	26.82	2.00	0.14	-	268.03	-	1.57
BS120	1153	26.82	2.00	0.14	-	286.75	-	1.24

Experimental result on table 5-11 indicate that the ultimate shear stress capacity decreased from τ = 2.12 MPa in BS24 (H=240mm) and τ = 2.03 MPa in BS30 (H=300mm) down to τ = 2.04 MPa in BS36 (H=3600mm) for beam specimens with shear reinforcement. Analytical result also indicate that the shear stress capacity decreased from τ = 2.43 MPa in BS24 (H=240mm) down to τ = 1.24 MPa in BS120 (H=1200mm) for beam specimens with shear reinforcement.

Figure 5-34 shows the relationship between the ultimate shear capacity of beam specimens with shear reinforcement and the beam height.

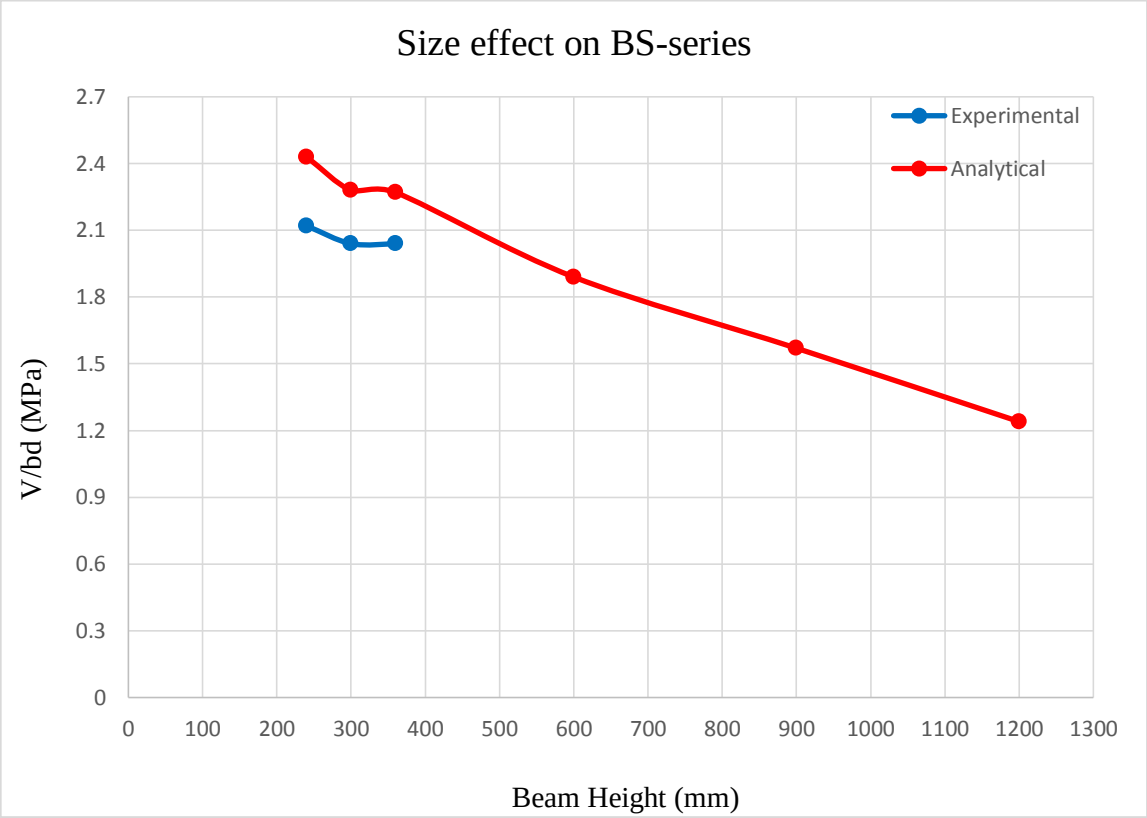

Figure 5-34: Shear stress capacity Vs effective depth of beams with stirrup

Figure 5-35 shows that experimental shear stress result at failure for the three specimens and analytical shear stress result at failure for the six specimens in BS-series. It can be seen from the figure that reinforced concrete beam series with 0.14% shear reinforcement ratio also affected by size effect. Experimental results showed that the shear stress at failure of 360mm depth beam decreased by 3.8% when compared to 240mm depth beam. Analytical result showed that as the depth of the beam raised from 240 mm to 1200mm the corresponding shear stress decreased by 48.9% meaning that a size effect is also present in reinforced concrete beams with shear reinforcement.

The results of beam specimens with shear reinforcement series also show decrease on the failure shear stress but not the same decrease as shown in beam specimens without shear reinforcement series. The specimens in this thesis all contained about the same percentage of longitudinal reinforcement and their concrete strengths were also very similar. The results show that size effect is visible in both reinforced concrete beams with and without shear reinforcement.

5.6.2 Effect of Using Shear Reinforcement to Mitigate Size Effect

Figure 5-34 shows the failure shear stress versus specimen height for both reinforced concrete beam with and without shear reinforcement series. In this figure it can be seen that the size effect is very evident in both reinforced concrete beams with and without shear reinforcement series. The shallower specimens on both series were consistently able to resist higher shear stresses than the larger ones. However, for largest specimens beams without shear reinforcement has a smaller failure shear stress than the same type of beam with shear reinforcement that means size effect is more significant on reinforced concrete beams without shear reinforcement than beams with shear reinforcement.

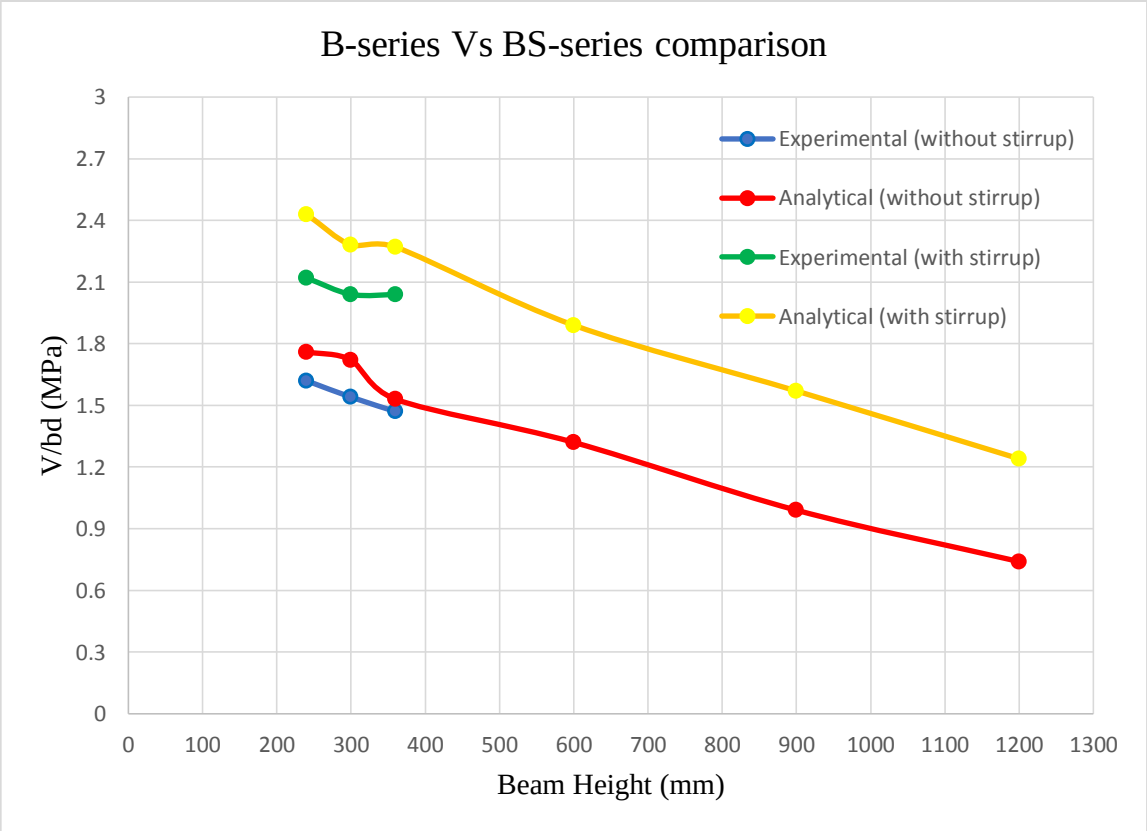

Figure 5-35: Failure shear stress Vs depth of all beams with and without stirrup

Figure 5-34 also showed that the line decreased significantly with increasing depth for both beam series but the rate of decrease was lower for beam series with shear reinforcement. The experimental result showed that there is 9.3% decrease in shear stress capacity for reinforced concrete beams without shear reinforcement when the specimen depth scaled up from B24 (H=240mm) to B36 (H=360mm) but for beam series with shear reinforcement only 3.8% decrease on the shear capacity shown when the size scaled up from BS24 to BS36.

Analytical result also shown for beams without shear reinforcement a 58.2% decrease in shear stress capacity when the specimen depth raised from 240mm to 1200mm, on the other hand for beams having shear reinforcement with ratio of 0.14% there was 48.9% decrease shown when the specimen depth raised from 240mm to 1200mm.

The above figure indicates that the presence of shear reinforcement with ratio of 0.14% minimize the size effect in shear capacity. it can be concluded that the presence of shear reinforcement did not completely avoid the size effect. even if using shear reinforcement mitigate the size effect on the shear strength of reinforced concrete beams, they cannot eliminate it completely.

5.6.3 Effect of Using Shear Reinforcement on Shear Capacity

Experimental results show that addition of shear reinforcement improves the shear capacity and ductility of all specimens especially for large specimens. Midspan deflections at failure for the specimens with shear reinforcement were larger than those for the specimen without shear reinforcement. In experimentally tested beam specimens, the presence of shear reinforcement increased the beams shear capacity by 30.5% for BS24 (H=240mm) and 38.7% for BS36 (H=360mm) when compared to the same type of specimens without shear reinforcement.

Analytical result showed that the increase in shear capacity due to the presence of shear reinforcement varied from 37.6% to 68.4% depending on the depth of the specimens. As the beam depth was 240mm shear capacity of beam with shear reinforcement increased by 37% when compared to the same size beam without shear reinforcement. For largest size beam as the beam depth was 1200mm shear capacity of beam with shear reinforcement increased by 68.4% when compare to same size specimen without shear reinforcement. The increase in beams shear capacity due to the presence of shear reinforcement was much higher for large size beam specimens.

Figure 5-35 compare the load versus midspan deflection relationships of all six reinforced concrete beams without shear reinforcement. Figures 5-36 compare the load versus midspan deflection for the beams containing shear reinforcement with ratio of 0.14%. Both Figure 5-35 and 5-36 shows that al1 of the specimens with shear reinforcement gained a significant increase in shear capacity and ductility (midspan deflection) when compared to specimens without shear reinforcement.

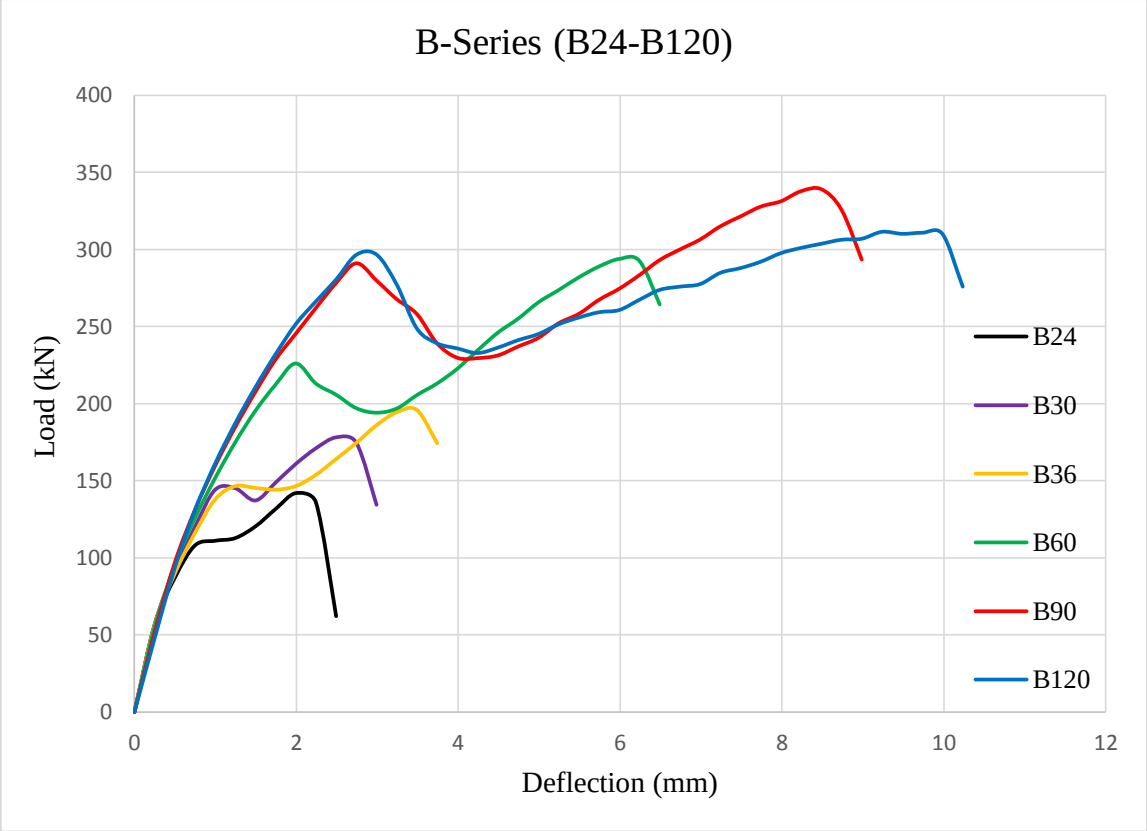

Figure 5-36: load-deflection comparison of all B-series specimens (without stirrup)

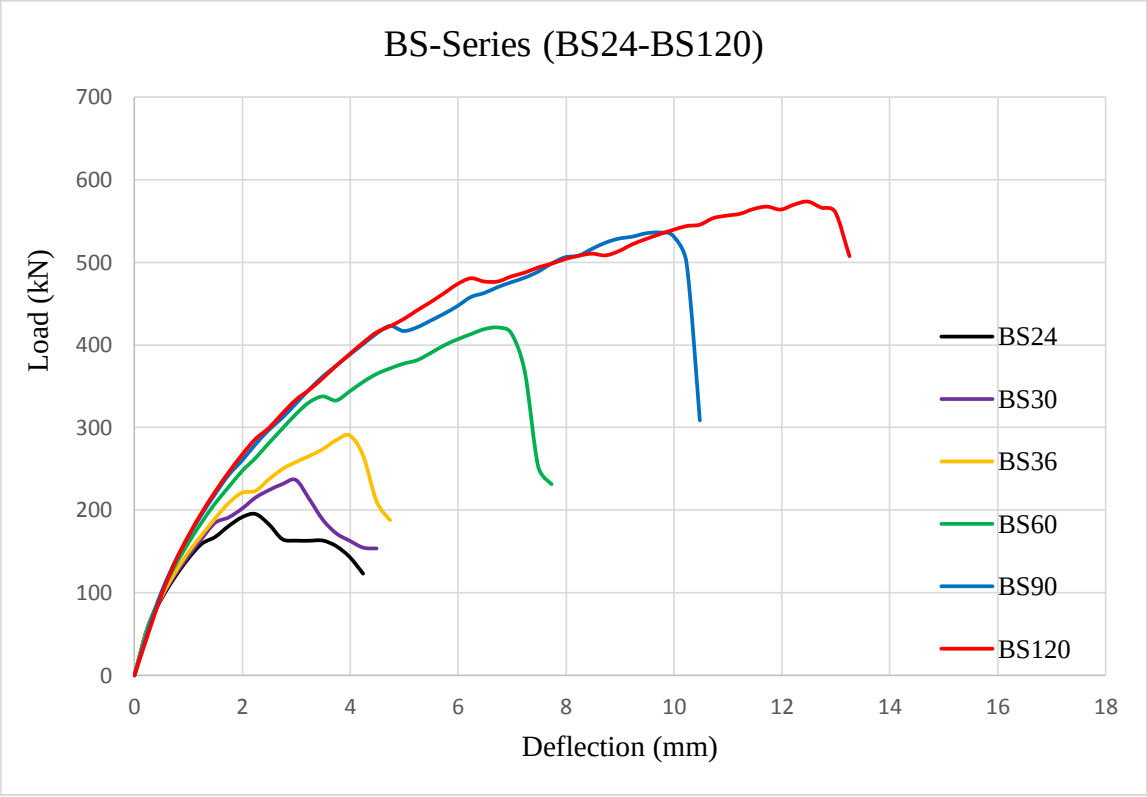

Figure 5-37: load-deflection comparison of all BS-series specimens (with stirrup)

5.6.4 Comparison of Experimental, Code-based and Analytical Predictions

In this section, a comparison among the experimental results, analytical prediction and predictions using some design codes are made. Table 5-12 below shows the analytical results by VecTor2 and estimation using AC13 18-14, AC13 18-19, and Eurocode2.

Table 5-12: Comparison between tested shear capacity and calculated shear capacity

specimens	EC2		ACI 318-14		ACI 318-19		VecTor2	
	V (KN)	V/bd (MPa)	V (KN)	V/bd (MPa)	V (KN)	V/bd (MPa)	V (KN)	V/bd (MPa)
B24	36.21	0.90	35.21	0.88	39.41	0.98	55.54	1.38
B30	44.43	0.86	46.31	0.89	48.82	0.94	66.32	1.28
B36	52.11	0.82	57.20	0.90	56.80	0.89	73.25	1.15
B60	80.61	0.72	98.08	0.88	82.17	0.74	113.05	1.01
B90	114.84	0.67	150.55	0.88	107.95	0.63	145.54	0.85
B120	147.77	0.64	203.02	0.88	129.22	0.56	155.74	0.67
BS24	55.07	1.37	56.22	1.40	60.43	1.50	79.58	1.98
BS30	67.46	1.30	71.41	1.38	73.82	1.42	92.30	1.78
BS36	80.95	1.27	88.79	1.39	88.40	1.38	110.56	1.73
BS60	132.52	1.19	155.77	1.40	139.86	1.26	168.84	1.52
BS90	194.53	1.14	239.10	1.40	196.50	1.15	211.51	1.24
BS120	255.24	1.11	322.43	1.40	248.63	1.08	240.34	1.04

Figure 5-38 and 5-39 shows experimental, analytical and predicted shear strength by Eurocode2, ACI 318-14 and ACI318-19 shear provisions versus beam height for reinforced concrete beam series without and with shear reinforcement respectively. It can be seen that with increasing beam size, all experimental, analytical and calculated shear stress capacity (V/bd) by codes of practice decreased except ACI 318-14.

Experimentally tested six reinforced concrete beam specimens exhibit shear stress reduction when the beam depth increase but the rate of decrease was higher on specimens without shear reinforcement when compared to specimens with shear reinforcement. Analytical results of twelve reinforced concrete beams also showed a decrease on shear stress capacity when the beam depth increase but the decreasing rate was higher for reinforced concrete beam specimens without shear reinforcement when compared to specimens with shear reinforcement.

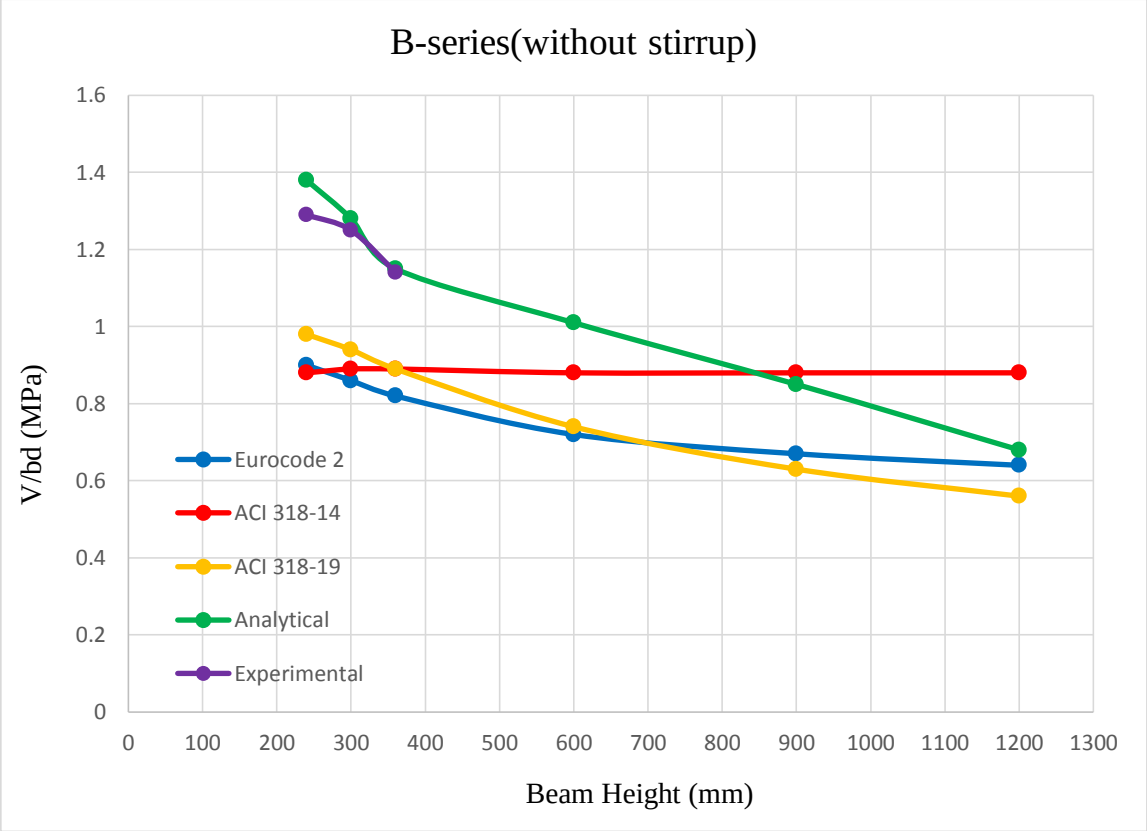

Figure 5-38: Code shear provisions comparison for beams without stirrup (BS-series)

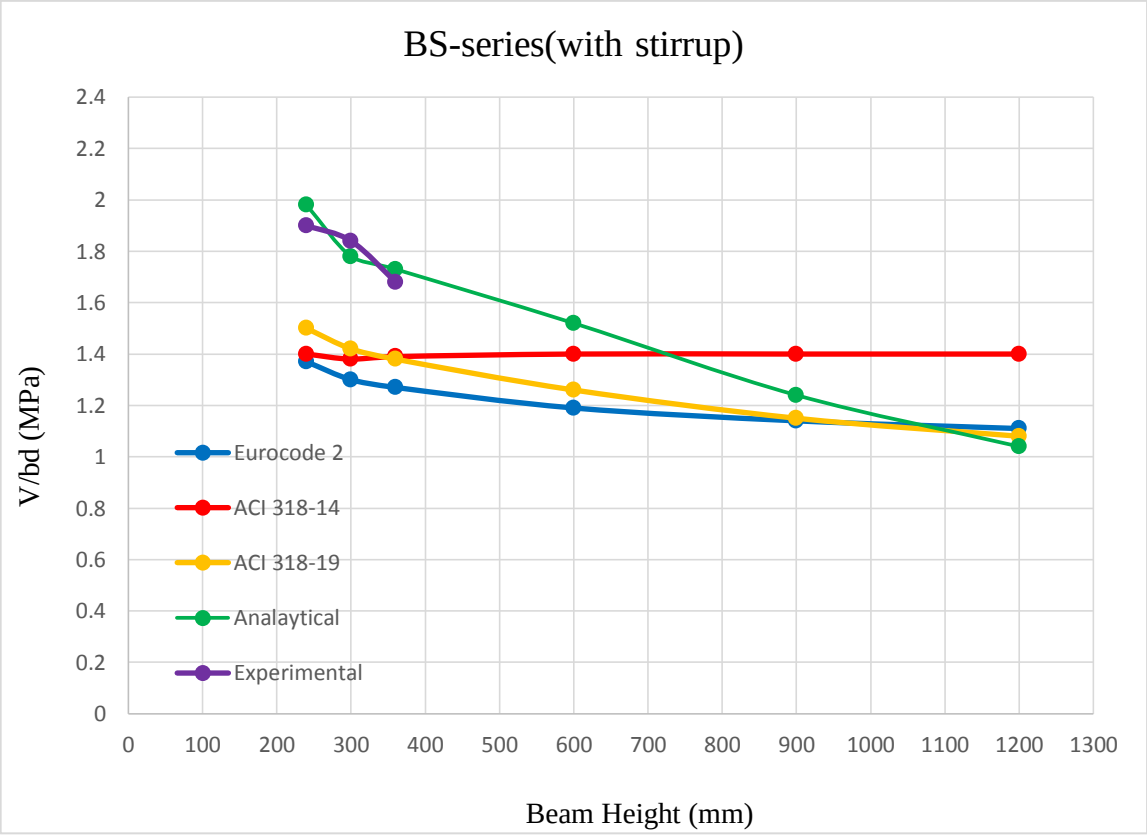

Figure 5-39: Code shear provisions comparison for beams with stirrup (BS -series)

The AC13 18-14 code predicts well the shear capacity for the specimens with relatively small depths. However, Specimens B90 (d=855mm) and B120 (d=1153mm) had much smaller shear strength than the ones the ACI 318-14 code predicts. Therefore, the shear design according to the AC1 318-14 code possibly leads to very unconservative design for large depth members. The unconservative aspect of the predictions seems to increase as the member depth increases. The largest gap between the analytical result and ACI 318-14 occurred in large size beams

The AC13 18-19, and Eurocode2, on the other hand, yields conservative predictions for the beam series without shear reinforcement and Eurocode2 gives a close but somewhat unconservative estimate for the failed load of Specimen B120. Size effect factor added in the AC13 18-19 shear provision help to provide more accurate predictions for the shear strength of larger beam specimens.

From the results of this study and figures shown above it can be concluded that replacing of ACI 318-14 shear provision for calculating the concrete contribution to shear resistance in reinforced concrete beams by ACI 318-19 shear provision which considers size effect is a good decision.

A comparison of the analytical results for the shear capacity of reinforced concrete beams with values predicted by Eurocode2, ACI 318-14 and ACI 318-19 is summarized in table 5-13 shown below.

Table 5-13: Ratio of code provisions to VecTor2 analyzed shear capacity

Specimens	EC2 / Analytical	ACI 318-14 / Analytical	ACI 318-19 / Analytical
B24	0.65	0.63	0.71
B30	0.64	0.67	0.70
B36	0.71	0.78	0.77
B60	0.71	0.87	0.73
B90	0.79	1.03	0.74
B120	0.95	1.30	0.83

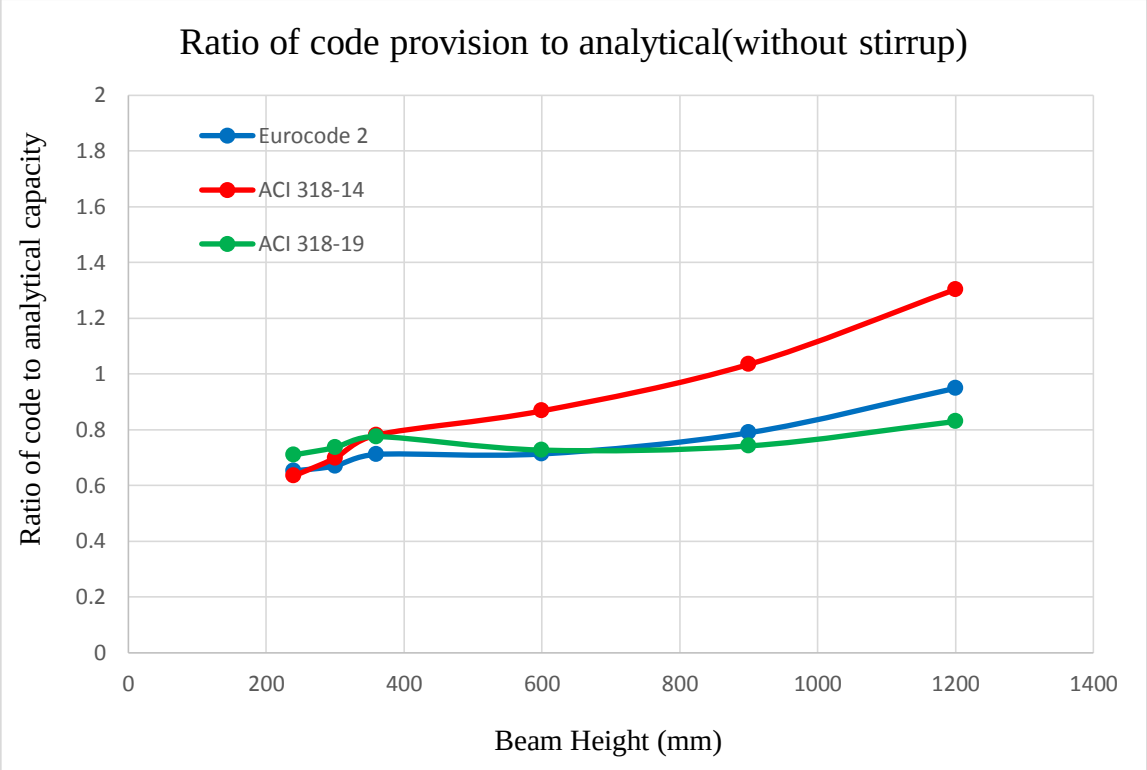

Figure 5-40: Ratio between calculated shear capacity and VT2 for B-series

Figure 5-39 shows that the comparison between analytical result and predicted shear capacity according to Eurocode 2, ACI 318-14 and ACI 318-19 codes for reinforced concrete beams without shear reinforcement. The prediction of ACI 318-14 are conservative for beams with depth less than 800mm for beam without shear reinforcement. However, with increasing depth they become unconservative. This is because ACI 318-14 neglect size effect parameter in its shear provision. On the other hand, the Eurocode 2 and ACI 318-19 shear provisions account size effect as a result they give more accurate and conservative predictions.

From the results shown in table 5-13, figure 5-39 it can be concluded that shear capacity of all specimens is well predicted by Eurocode 2 and ACI 318-19 because they directly account effect of beam depth on their shear provisions. On the other hand, ACI 318-14 overestimate the shear capacity of large size specimens such as B90 (H=900mm) and B120 (1200mm).

CHAPTER 6 CONCLUSIONS AND RECCOMENDATIONS

6.1 Conclusions

Based on the experimental investigation and numerical simulation results, the following conclusion were made:

1. Experimentally tested six reinforced concrete beams with varying depth showed that the failure shear stress decreases with increased beam depth for both non shear reinforced and shear reinforced beam series, for beams without shear reinforcement shear stress decreased by 9.3% and for beams with shear reinforcement the failure shear stress decreased by only 3.8% when the beam height raised from 240mm to 360mm.
2. All of the tested beams carried more load in the laboratory than calculated with the Eurocode 2 shear provisions. It indicates that there is a safety margin present in the shear design formulas for reinforced concrete beams.
3. The size effect is very evident in both reinforced concrete beams with and without shear reinforcement series. For beams without shear reinforcement a 58.2% decrease in shear stress capacity shown when the specimen depth raised from 240mm to 1200mm, on the other hand for beams having shear reinforcement with ratio of 0.14% there was 48.9% decrease shown when the specimen depth raised from 240mm to 1200mm.
4. The results of this thesis showed that even if using shear reinforcement mitigate the size effect on the shear strength of reinforced concrete beams, they cannot eliminate it completely.
5. Eurocode 2 and ACI 318-19 shear provisions, are quite conservative in their predictions for al1 beam specimens and they give generally good estimates of shear failure for al1 of the specimens the reason for that is they consider the size effect parameter in their shear provisions.
6. The ACI 318-14 shear provision do not consider size effect and it is highly unconservative for the large size beams with depth greater than 800mm deep, so that the decision made to replace it by ACI 318-19 which consider effect of member depth is correct.

6.2 Recommendations

Based on work conducted as part of this thesis program the following recommendations for future work are reported:

1. More experimental work is needed on large size beam specimens to investigate other major parameters which have significant effect on the shear capacity of reinforced concrete beams, such as concrete strength, longitudinal reinforcement ratio and shear span to depth ratio.
2. Since not only amount of shear reinforcement has a significant effect on the shear crack distribution of reinforced concrete beams, tests should be conducted to also investigated the effect of shear reinforcement spacing on the size effect of large reinforced concrete beams.
3. The VecTor2 finite element model needs to be further validated against experimental results, especially for reinforced concrete beams without shear reinforcement as the shear resisting mechanisms are different from reinforced concrete beams with shear reinforcement.
4. More experimental research is required to examine the current shear provisions of EC2 and ACI-318-19 for reinforced concrete beams with and without shear reinforcement and to assess the possible contribution of concrete to the total shear resistance.

REFERENCES

Abebe Dinku (2002), "Construction Materials Laboratory Manual", Department of Civil Engineering, Faculty of Technology, AAU, 2002.

ACI Committee 318, ACI 318-14 Building Code Requirements for Structural Concrete and Commentary, Farmington Hills, Michigan: American Concrete Institute (ACI), 2014.

Axel Althin and M˚arten Lippe, "Size Effects in Shear Force Design of Concrete Beams" [Master Thesis] Division of Structural Engineering, Faculty of Engineering, LTH Lunds University, Sweden, 2018.

Dino Angelakos, The influence of concrete strength and longitudinal reinforcement ratio on the shear strength of large-size reinforced concrete beams with, and without, transverse reinforcement [M.A.Sc. Thesis], Toronto: University of Toronto, Department of Civil Engineering, 1999.

EN 1992-1-1: Eurocode 2: Design of Concrete Structures - Part 1-1: General rules and rules for buildings, Brussels: European Committee for Standardization, 2004.

ES EN2 Design of Concrete Structures (EBCS EN 1992-1- 1:2015). Addis Ababa, Ethiopia: Ministry of Urban Development & Construction, 2015.

Hadi Nasir Ghadhban, Effect of Beam Size on Shear Strength of Reinforced Concrete Normal Beams, Journal of Engineering and Development, Vol. 11, No. 1, March (2007)

Ismail, K. S., "Shear Behavior of Reinforced Concrete Deep Beams". PhD thesis, University of Sheffield, 2016.

J. K. Wight and J. G. MacGregor, Reinforced concrete: mechanics and design, 6th ed., vol. 27, no. 6. New Jersey, USA: Pearson Education, INC, 2012.

Kani, G.N.J., How safe are our large reinforced concrete beams? ACI journal, 1967. 64(3): p. 128-141.

M. P. Collins and D. Kuchma, "How Safe Are Our Large, Lightly Reinforced Concrete Beams, Slabs, and Footings?" ACI Structural Journal, vol. 96, no. 4, pp. 482-490, 1999.

Mekdes Tadesse, "Effects of Spacing and Configuration of Web Reinforcement on Shear Behavior of Reinforced Concrete Beams" [M.Sc. Thesis], Addis Ababa Institute of Technology, School of Civil and Environmental Engineering, 2015.

Netsanet Bezu, "Parametric Study of Shear Strength of Reinforced Concrete Beams" [M.Sc. Thesis], Addis Ababa Institute of Technology, School of Civil and Environmental Engineering, 2018.

Phillip T. Quach, Understanding and Safely Predicting the Shear Response of Large-Scale Reinforced Concrete Structures [M.A.Sc. Thesis], Toronto: University of Toronto, Department of Civil Engineering, 2016.

P. S. Wong, H. Trommels and F. J. Vecchio, VecTor2 & Formworks User's Manual, Toronto: VecTor Analysis Group, 2013.

Qiang Yu and Zdeněk P. Bažant, "Can Stirrups Suppress Size Effect on Shear Strength of RC Beams? Journal of Structural Engineering © American Society of Civil Engineers (ASCE), 2011.

Robert J. Frosch, "Behavior of Large-Scale Reinforced Concrete Beams with Minimum Shear Reinforcement. ACI Structural Journal, vol. 97, no. 6, pp. 814-821, 2000.

Sadik Muzeyin, "Effect of Aggregate Size and Type on Shear Capacity of Normal Strength Reinforced Concrete Beams" [M.Sc. Thesis], Addis Ababa Institute of Technology, School of Civil and Environmental Engineering, 2016.

S. Cao, Size Effect and the Influence of Longitudinal Reinforcement on the Shear Response of Large Reinforced Concrete Members [M.A.Sc. Thesis], Toronto: University of Toronto, Department of Civil Engineering, 2001.

Tsigereda Getachew, Fatigue behavior of shear-critical Reinforced Concrete beams" [M.Sc. Thesis], Addis Ababa Institute of Technology, School of Civil and Environmental Engineering, 2018.

W.M Ghannoum, Size effect on shear strength of reinforced concrete beams. [M.A.Sc. Thesis], Toronto: University of Toronto, Department of Civil Engineering, 1998.

Y. Yoshida, Shear Reinforcement for Large Lightly Reinforced Concrete Members [M.A.Sc. Thesis], Toronto: University of Toronto, Department of Civil Engineering, 2000.

Appendix A

1. Estimation of beam shear capacity using Eurocode 2

Sample calculation for specimen BS24

Concrete Strength: fc= 26.83 MPa

Yield Strength of Transverse Rebar: f_{wy}=366MPa

Area of a Transverse Rebar: A_{sw}=56.52mm^2

Spacing of Transverse Rebars: S=200mm

Beam width: b=200mm

Effective depth: d=201mm

$$\mathbf{V_{Rd}=V_{Rd,\,c}+V_{Rd,s}} \quad \mathbf{[KN]}$$

$V_{Rd,c} = [C_{Rd,c}k(100\rho_l f_{ck})^{1/3} + k_1\sigma_{cp}]b_w d \geq V_{Rd,c,min}$ [KN]

$C_{Rd} = \frac{0.18}{\gamma_c} = \frac{0.18}{1.5} = 0.12$

$k = 1+ \sqrt{\frac{200}{201}} = 1.997$

$\rho = \frac{A_{sw}}{bd} = \frac{804}{(0.2)(0.201)} = 0.02$

$\sigma_{cp} = 0$

$V_{Rd,c} = [0.12(1.997)(100*0.02*26.83k)^{1/3} + k_1(0)](0.02)(0.0201)$

$= \underline{36.34 \text{ kN}}$

$V_{Rd,s} = \frac{A_{sw}}{s} z f_{ywd}(\cot\theta + \cot\alpha)\sin\alpha$ [KN]

$\theta=45^o \quad \alpha=90^o \quad z=0.9d= 0.9(201) =180.9mm$

$V_{Rd,s} = \frac{56.52}{200}(180.9)(366)(\cot 45 + \cot 90)\sin 90$

$V_{Rd,s} = \underline{18.73 \text{ kN}}$

$V_{Rd} = V_{Rd,\,c} + V_{Rd,s}$

$= 36.34 + 18.73$

$= \underline{55.07 \text{ kN}}$

2. Estimation of beam shear capacity using ACI 318-14

Sample Calculation for Specimen BS24

Concrete Strength: fc= 26.83 MPa

Yield Strength of Transverse Rebar: f_{wy}=366MPa

Area of a Transverse Rebar: A_{sw}=56.52mm^2

Spacing of Transverse Rebars: S=200mm

Beam width: b=200mm

Effective depth: d=201mm

$$Vn = Vc + Vs$$

Concrete contribution on shear capacity

$V_c = (0.17\sqrt{f'_c})b_w d$ [KN]

$= (0.17\sqrt{26.83})0.02*0.0201$

$= \underline{35.40 \text{ KN}}$

Shear reinforcement contribution on shear capacity

$$V_s = \frac{A_v f_{yt} d}{S}$$

$$= \frac{56.52*366*201}{200}$$

$= \underline{20.82 \text{ KN}}$

Total shear resistance capacity of BS24 specimen

$V_n = V_c + V_s$

$= 35.40 + 20.82$

$= \underline{56.22 \text{ KN}}$

3. Estimation of beam shear capacity using ACI 318-19

Sample Calculation for Specimen BS24

Concrete Strength: fc= 26.83 MPa

Yield Strength of Transverse Rebar: f_{wy}=366MPa

Area of a Transverse Rebar: A_{sw}=56.52mm2

Spacing of Transverse Rebars: S=200mm

Beam width: b=200mm

Effective depth: d=201mm

$$Vn = Vc + Vs$$

Concrete contribution to shear capacity

$$V_c = [8\lambda_s \lambda(\rho_w)^{1/3}\sqrt{f'c} + \frac{N}{6Ag}]b_w d$$

$\lambda = 1$, $N = 0$, $\lambda_s = \sqrt{\frac{2}{1+\frac{d}{10}}} = 1.057$

$$V_c = [8(1.057)\ (1)\ (0.02)^{1/3}\sqrt{3888.4} + \frac{0}{6Ag}](7.87in)\ (7.91)$$

=8901.64lb =39.61 KN

Shear reinforcement contribution on shear capacity

$$V_s = \frac{A_v f_{yt} d}{S}$$

$$= \frac{56.52*366*201}{200}$$

= 20.82 KN

Total shear resistance capacity of BS24 specimen

$$V_n = V_c + V_s$$

= 39.61 + 20.82

= 60.43 KN

Conversions: 1 lb. = 4.45N

1 in =25.4 mm

1 psi = 0.00689 MPa

Table A1: Shear capacity prediction based on Eurocode 2, ACI 318-14 and ACI 318-19

Beam	EC2			ACI 318-14			ACI 318-19		
	V_c (KN)	V_s (KN)	V_{Total} (KN)	V_c (KN)	V_s (KN)	V_{Total} (KN)	V_c (KN)	V_s (KN)	V_{Total} (KN)
B24	36.21	-	36.21	35.21	-	35.21	39.41	-	39.41
B30	44.43	-	44.43	46.31	-	46.31	48.82	-	48.82
B36	52.11	-	52.11	57.20	-	57.20	56.80	-	56.80
B60	80.61	-	80.61	98.08	-	98.08	82.17	-	82.17
B90	114.84	-	114.84	150.55	-	150.55	107.95	-	107.95
B120	147.77	-	147.77	203.02	-	203.02	129.22	-	129.22
BS24	36.34	18.73	55.07	35.40	20.82	56.22	39.61	20.82	60.43
BS30	43.32	24.14	67.46	44.59	26.82	71.41	47.00	26.82	73.82
BS36	51.22	29.73	80.95	55.75	33.04	88.79	55.36	33.04	88.40
BS60	80.61	51.91	132.52	98.08	57.69	155.78	82.17	57.69	139.86
BS90	114.84	79.69	194.53	150.55	88.55	239.10	107.95	88.55	196.50
BS120	147.77	107.5	255.27	203.02	119.4	322.42	129.22	119.4	248.62

Appendix B

Analytical Modelling and Results for sample Specimen BS36

Structure Data

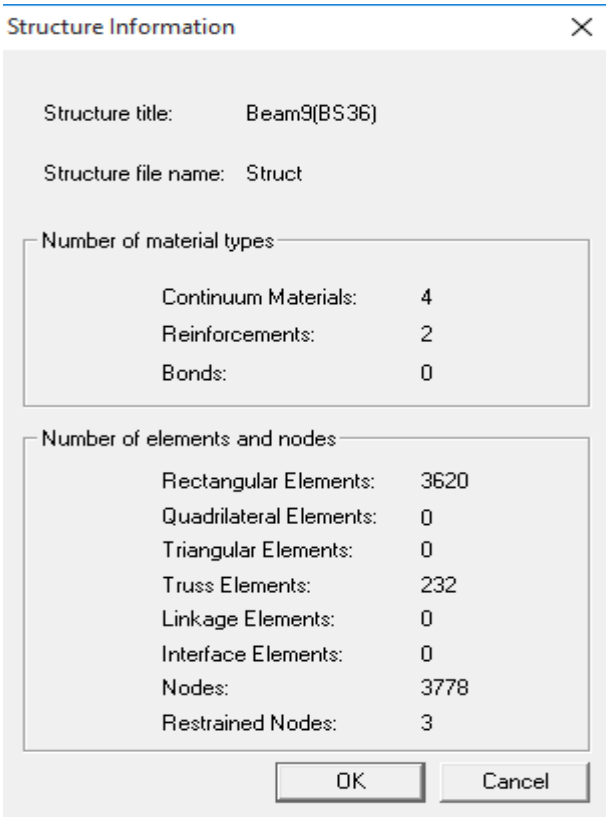

Material specifications

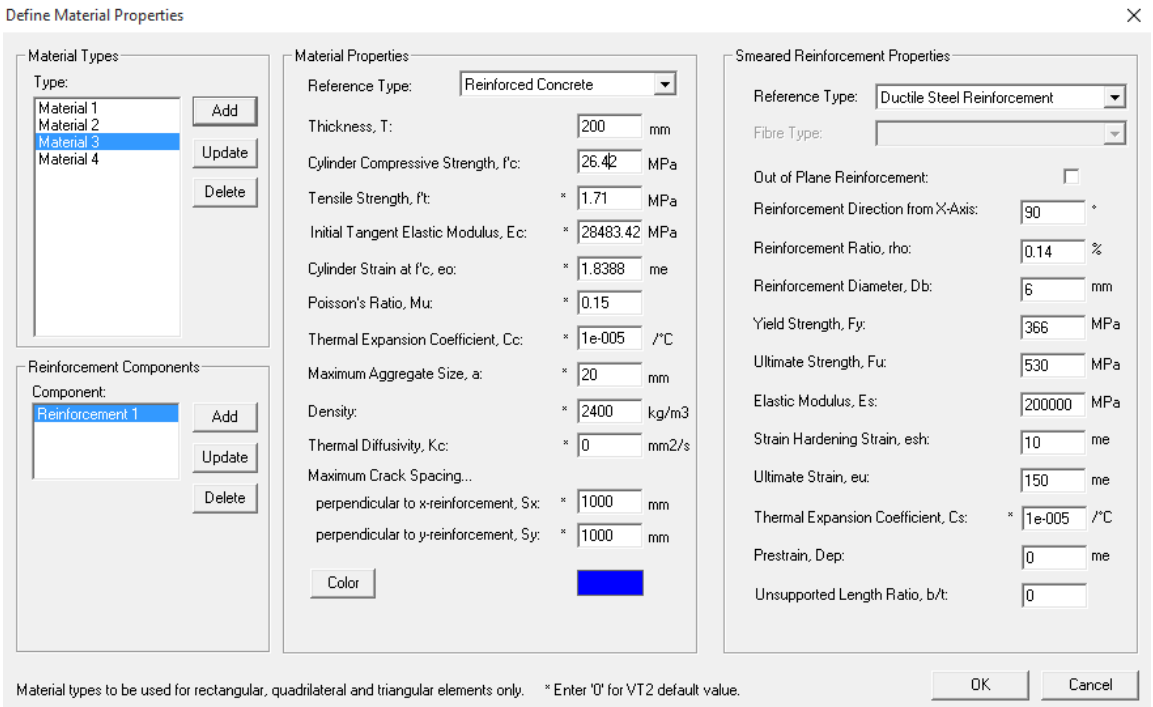

Longitudinal Reinforcement properties

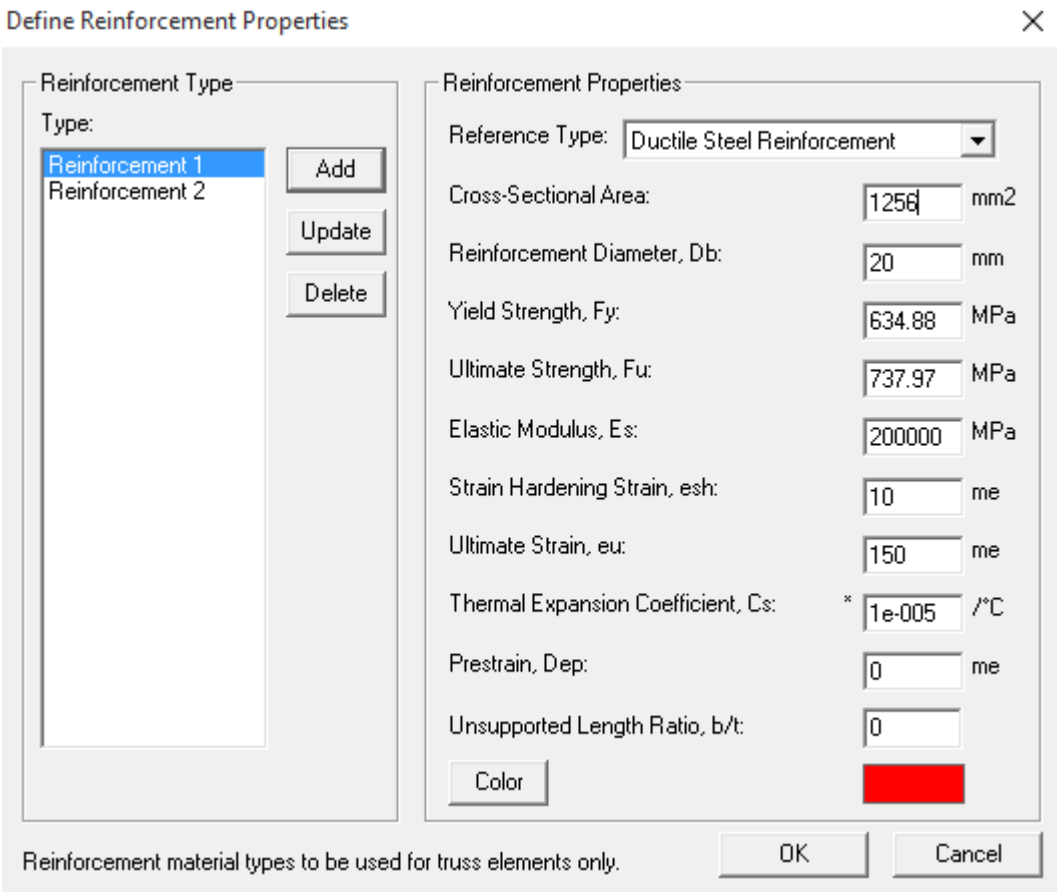

Geometric Properties

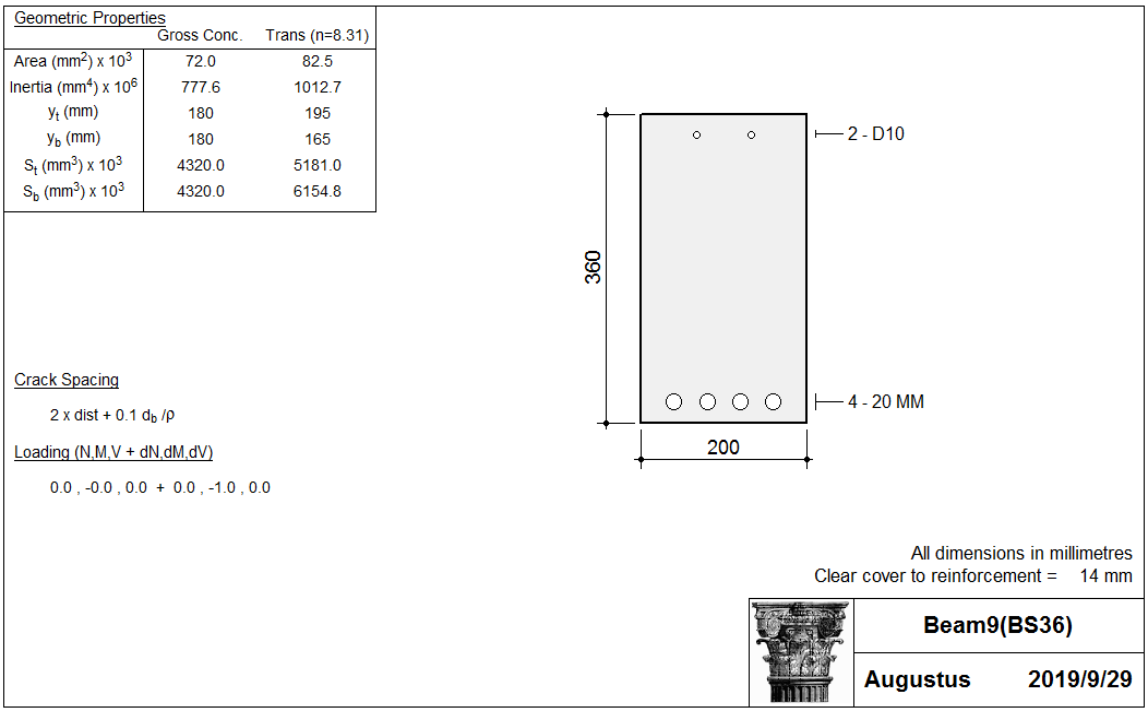

Results for sample specimen BS36

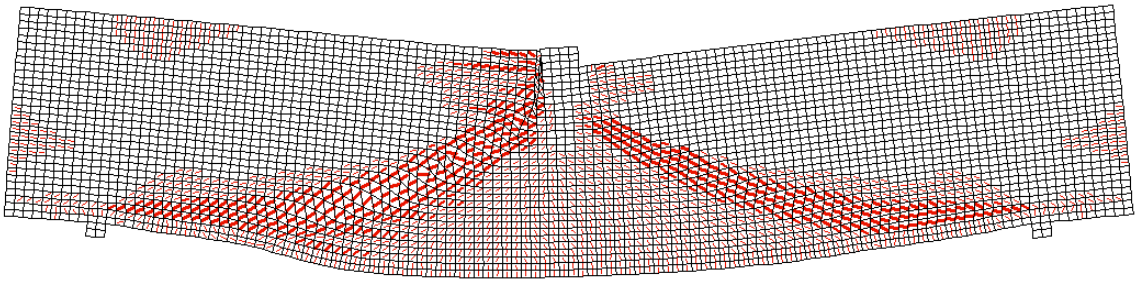

Crack Width w_{cr}

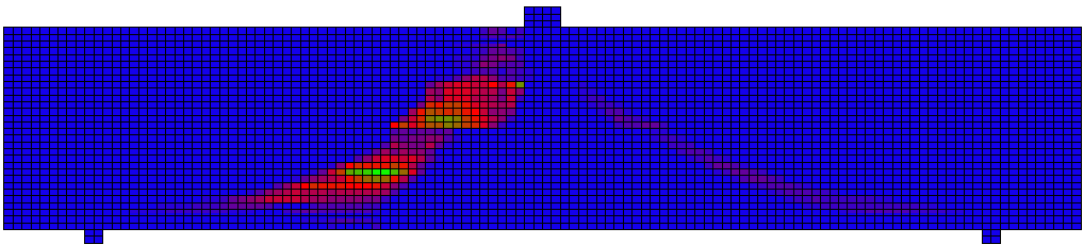

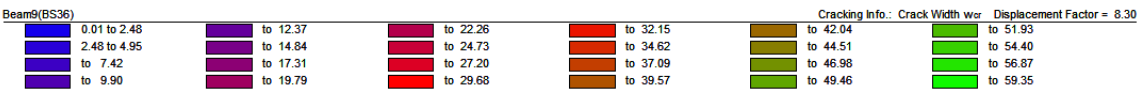

Crack Spacing $s\theta$

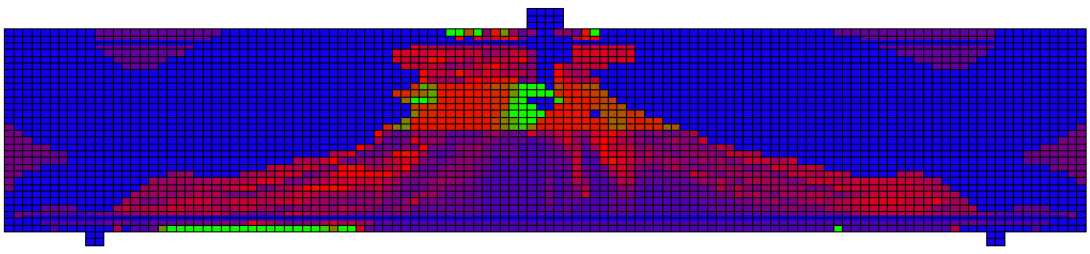

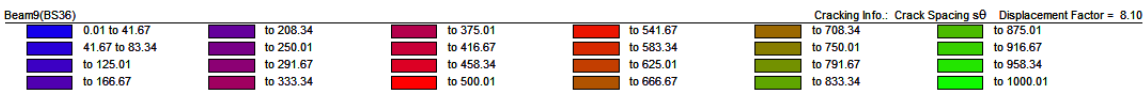

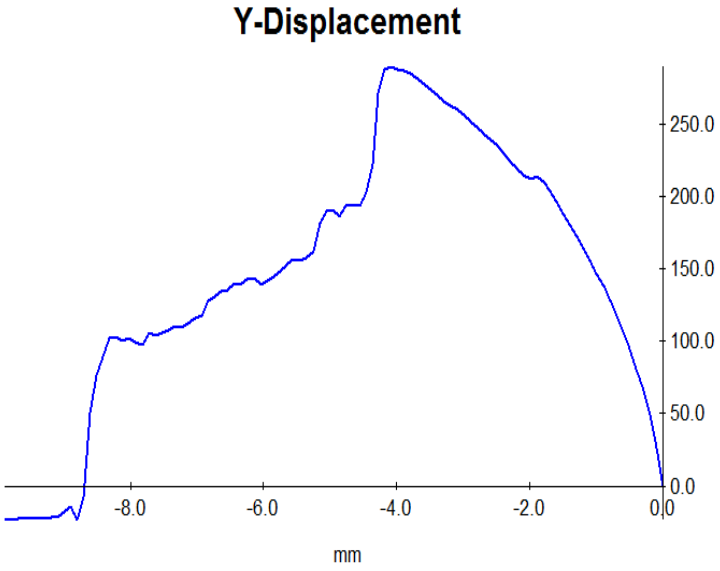

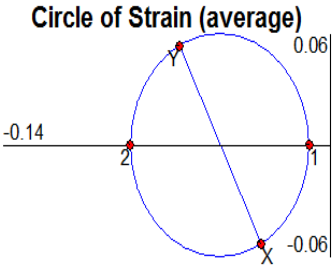

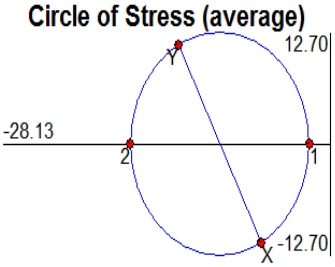

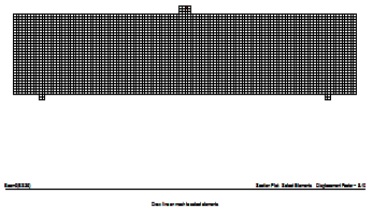

ε_x: -0.05 mm/m	f_{cx}: -9.58 MPa
ε_y: -0.11 mm/m	f_{cy}: -21.29 MPa
γ_{xy}: 0.11 mm/m	v_{xy}: 11.28 MPa
ε_1: -0.01 mm/m	f_1: -2.74 MPa
ε_2: -0.14 mm/m	f_2: -28.1 MPa
θ: 58.7 deg.	f_{2max}: -0.0 MPa
f_{sx}: -0.0 MPa	f_{sxcr}: -0.0 MPa
f_{sy}: -0.0 MPa	f_{sycr}: -0.0 MPa
$s_{m-\theta}$: 0 mm	w: 0.00 mm
v_{ci}: 0.00 MPa	v_{cimax}: -0.03 MPa